

**Proceeding
Of
7th International Conference on Instrumentation,
Electrical And Electronics Engineering (ICIEEE 2015)
&
7th International Conference on Production, Mechanical
And Automobile Engineering (ICPMAE-2015)**

**Date: 28th June 2015
Raipur**

**Editor-in-Chief
I.Hameem Shanavas,
Assistant HOD, Department of ECE,
M.V.J College of Engineering, Bangalore**

Organized by:



**TECHNICAL RESEARCH ORGANISATION INDIA
Website: www.troindia.in**

ISBN: 978-93-85225-36-9

About Conference

Technical Research Organisation India (TROINDIA) is pleased to organize the 7th International Conference on Instrumentation, Electrical And Electronics Engineering (ICIEEE 2015) & 7th International Conference on Production, Mechanical And Automobile Engineering (ICPMAE-2015)

ICIEEE is a comprehensive conference covering all the various topics of Electrical And Electronics Engineering. The aim of the ICIEEE is to gather scholars from all over the world to present advances in the aforementioned fields and to foster an environment conducive to exchanging ideas and information. This ICPMAE conference will also provide a golden opportunity to develop new collaborations and meet experts on the fundamentals, applications, and products of Production, Mechanical and Automobile Engineering. We believe inclusive and wide-ranging conferences such as ICPMAE can have significant impacts by bringing together experts from the different and often separated fields of Production, Mechanical and Automobile Engineering.

Topics of interest for submission include, but are not limited to:

- Electrical Engineering
- Energy Sources
- Power Systems
- Power Electronics
- Electrical Drives
- Electromagnetic Design
- Smart Grids
- Electronics Engineering
- Instrumentation Engineering
- Mechanical Engineering
- Acoustics and Noise Control
- Aerodynamics
- Applied Mechanics
- Automation, Mechatronics and Robotics
- Automobiles
- Automotive Engineering
- Ballistics
- Biomechanics
- Production Engineering
- CAD/CAM/CIM
- CFD
- And many more.....

Organizing Committee

Programme Chair

I.Hameem Shanavas,

Assistant HOD, Department of ECE,
M.V.J College of Engineering, Bangalore

Programme Committee Members:

Prof. S. V. Viraktamath

Dept. of E&CE S.D.M. College of Engg. & Technology
Dhavalagiri, Dharwad

Dr. A. Lakshmi Devi,

Professor,
Department of Electrical Engineering,
SVU College of Engineering, Sri Venkateswara University, Tirupati,
Email: energylak123@yahoo.com

Prof. Dr. MIRZA MOHAMMED SAJID RUB

Asst. Professor & Head Of the of the department
Department of Electronics & Telecommunication Engineering
BIET, Bhadrak – 756100Odisha
Email: mirza.iit@gmail.com

DR. BHASKER GUPTA

Assistant Professor. Jaypee University of Information Technology, Himachal Pradesh

Dr. D.J. Ravi

Professor & HOD
Department of ECE, Gokulam 3rd stageVVCE, Mysore

Prof. SHRAVANI BADIGANCHALA

Assistant professor, Shiridi sai institute of science and engineering

IIT KHARAGPUR

Prof. Rajakumar R. V.

DEAN Academic, rkumar @ ece.iitkgp.ernet.in

Prof. Datta D., ddatta @ ece.iitkgp.ernet.in

Prof. Pathak S S,r,ssp @ ece.iitkgp.ernet.in

XIMB,BHUBANESWAR

Prof Dr. Subhajyoti Ray.M-Stat, (ISI); Fellow, IIM(A),
Dean academic,XIMB-subhajyoti@ximb.ac.in ,

AMIT R. Wasnik

Assistant Professor in Mechanical Engineering,
Sinhgad Institute of Technology, Lonavala, Pune Maharashtra

PROF. (DR.) Arjun Pralhad Ghatule,

Sinhgad Institute of Computer Sciences (SICS), Korti

Prof.Subzar Ahmed Bhat

,Assistant Professor, GLA UNIVERSITY

Dr. G.SURESH BABU,

Professor, Dept. of EEE, CBIT, Hyderabad, Andhra Pradesh

Tejinder Singh Saggu,

Assistant Professor, Dept. of Electrical Engineering, PEC University of University,
Chandigarh

Sanjith J,

Assistant Professor & P.G. Co-ordinator, Department of Civil Engineering,
Adhichunchanagiri Institute of Technology, Karnataka

Manpreet Singh Manna,

Director, AICTE, New Delhi

Prof (Dr) Punyaban patel,

Department of Computer science and engineering, Chhatrapati shivaji institute of
technology, Durg

Prof. Dipak S.Bajaj,

Asst. Professor, Department of Mechanical Engineering,
Amrutvahini College of Engineering, Sangamner

Dr. Rajeev Agrawal,

Assistant Professor, department of Production engineering, Birla Institute of Technology
(Deemed University), Ranchi, Jharkhand

Prof O. V. Krishnaiah Chetty,

Dean, Mechanical Engineering, Sri Venkateswara College of Engineering and Technology,
Tirupati

Prof. Balwant singh Bisht

Asst. Prof. K.J. college of Engg and Management Research
PUNE

TABLE OF CONTENTS

SL NO	TOPIC	PAGE NO
Editor-in-Chief		
I.Hameem Shanavas		
1.	SMART GRID IN POWER SYSTEM - ¹ Deependra Rathore, ² Dr.Sushil Kumar	01-04
2.	INTELLIGENT AUTONOMOUS FARMING ROBOT WITH PLANT HEALTH INDICATION & CARING USING IMAGE PROCESSING - Shrikant Borate ¹ , Prof. P. V. Mulmule ²	05-10
3.	LOW VOLTAGE DC BUS MICRO-GRID PROTECTION SYSTEM - ¹ Pate Pawan V., ² Kamal Sandeep K., ³ Pate Poonam V.	11-20
4.	ANALYSIS OF SMART METER DATA USING HADOOP - ¹ Balaji K. Bodkhe, ² Dr. Sanjay P. Sood	21-25
5.	AN EXPERIMENTAL WORK ON MULTI-ROLLER BURNISHING PROCESS ON ALUMINUM ALLOY - Kundan Kumar D ¹ , Dr. K. Eshwara Prasad ²	26-30
6.	OPTIMIZATION OF PARAMETERS TO MINIMIZE THE SKIN FRICTION COEFFICIENT IN ABRASIVE WATER SUSPENSION JET MACHINING THROUGH TLBO - Rakesh Kumar Sahu ¹ , Saurabh Verma ² , Santosh Kumar Mishra ³	31-39
7.	A REBROADCAST ROUTE DISCOVERY IN MANET FOR REDUCING ROUTING OVERHEAD - ¹ Mr. Prasad R. Patil, ² Prof. R.S.Nipanikar	40-44
8.	BACKGROUND AND RESIDUAL NOISE REDUCTION FOR SPEECH ENHANCEMENT: SPECTRAL SUBTRACTION AND MEDIAN FILTER APPROACH - ¹ Disha Desai	45-49
9.	WATERMARKING FOR VIDEO AUTHENTICATION - ¹ Pathak Utsav A	50-59

- 10. WIRELESS SENSOR NETWORK LOCALIZATION USING SOCP RELAXATION**
- ¹Pragnesh S Patel, ²Niteen B.Patel 60-67
- 11. COMPARATIVE ANALYSIS OF DIFFERENT APPROACHES FOR HYPERSPECTRAL UNMIXING**
- ¹Chirag Hirpara, ²Vankar Jyoti P. 68-75
- 12. DENOISING USING FRAMELET TRANSFORM**
- Swati D. Khandare¹, Vandana Shah² 76-81
- 13. MACHINE TRANSLATION SYSTEM IN INDIAN PERSPECTIVE**
- ¹Dr. Sushil Kumar, ²Kiran Soni 82-85
- 14. AUTOMATED WHEELCHAIR**
- Rupali Deshmukh¹, Y. V. Chavan² 86-90
- 15. INCREASING EFFICIENCY OF TRANSMISSION LINES BY SIMULTANEOUS AC-DC POWER TRANSMISSION SCHEME AND THEIR PERFORMANCE AT FAULT OPERATION**
- ¹Dr. Sushil Kumar, ²Kiran Soni, ³Prakash Soni 91-97

Editorial

The conference is designed to stimulate the young minds including Research Scholars, Academicians, and Practitioners to contribute their ideas, thoughts and nobility in these two integrated disciplines. Even a fraction of active participation deeply influences the magnanimity of this international event. I must acknowledge your response to this conference. I ought to convey that this conference is only a little step towards knowledge, network and relationship.

The conference is first of its kind and gets granted with lot of blessings. I wish all success to the paper presenters.

I congratulate the participants for getting selected at this conference. I extend heart full thanks to members of faculty from different institutions, research scholars, delegates, TROI Family members, members of the technical and organizing committee. Above all I note the salutation towards the almighty.

Editor-in-Chief

I.Hameem Shanavas,

Assistant HOD, Department of ECE,

M.V.J College of Engineering, Bangalore



SMART GRID IN POWER SYSTEM

¹Deependra Rathore, ²Dr.Sushil Kumar

Research scholar, Dr. C.V. Raman university, Bilaspur (C.G.)India

Principal, Pragati college of engineering and management,Raipur (C.G) India

Email:¹deependrarathore75@gmail.com, ²Sk1_bit@rediffmail.com

Abstract— Improving energy efficiency and conservation are essential to achieving Environmental sustainability. They are the simplest ways to reduce energy consumption by good energy management starts with energy audit. The smart grid has dual effect environmental protection as well as energy consumption. Smart grid is a type of electrical network that can smartly handle the entire user which connected to the particular station. A smart grid system is a real time operating system which automatic control the system with the help of power electronic equipment and daily useful devices. One major method to manage electrical network with the increase in demand of power, we have to apply smart grid technique such as load shifting, intelligent load management (ILM), load balancing, power factor improvement device, comparative study of load in power station .The demand of power increasing now day by day as population increasing at the same time we have decreasing the sources of energy which would help to produce electrical power. The smart grid is another option which would help to energy consumption as well as environmental protection. For handling the power we have to move towards the hybridization of electrical power rural area as well as urban area. Hybridization is an part of smart grid where we can handle the electrical power according to our daily power requirement. This paper gives an idea how we handle the power smartly whether it

is electrical power generation, power distribution, electrical power transmission and electrical power handling.

Keywords— Smart Grid, Demand response, Future Challenges, Smart stations, Power quality, Power restoration.

I. INTRODUCTION

Improving energy efficiency and conservation are essential to achieving environmental sustainability. Energy is the basic need for the economic development of an country. Energy exists in a different form in a nature but the most important is a electrical energy. The greater the per capita consumption of energy in a country, the higher is the standard of living of its people so that there is a close relationship between the energy used per person and his standard of living. The present day advancement in science and technology has made it to possible to convert electrical energy into any desired form. Smart grid is new technique and is also known as Advance Metering Infrastructure, whose technology helpful electricity use with high accuracy in demand side as well as particular consumer through a distribution process. For smart grid power system we have to prepare priority value of each type of load and then calculate consumption of load any particular station.

In recent study of paper we analyse that different method for improving the energy efficiency by a Intelligent Load Management (ILM), Demand Side Management (DSM),

Building Management System (BMS) and Advanced Metering Infrastructure (AMI).

Smart grid system contain four measure parts after the analysis of this part the smart grid system is applied (1) Energy Auditing - It require the analysis of energy demand and losses of station after the analysis we suggest for a smart grid system, (2) Intelligent Energy Metering - Advanced energy metering is require to calculate the correct energy consumption with minimum losses. (3) Goal oriented smart grid-improving the efficiency and more reliable power station.

This paper give an idea about how smart grid work. Smart grid increasing the utilization factor of energy consumption and also give new idea for new circuit development with minimum losses.

II. ENERGY AUDIT

Electrical power system is not a single unit but an integration of multiple electrical power generation and substation where the operator communicate with the system by varying the load according to is requirement. An important part of energy auditing is a collect energy requirement data of a particular station by regular analysis. In the energy auditing process we first note down the peak demand period time and base demand period time and minimum demand period time. After the energy auditing we improve 10% efficiency of a particular station as shown in figure 1.

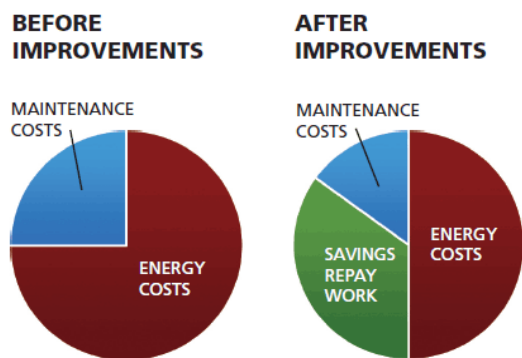


Fig.1. Energy Audit Process...

The fig. 1 shows after energy audit process we decrease the maintenance cost and reduce the energy cost. Energy audit is very helpful for smart grid system after the analysis we know which area is to be focused for improvement the energy data of a particular station.

III. TECHNOLOGY USED IN SMART GRID

Smart grid technology may be combination of three words: Intelligence, compatibility and assimilation. In the smart grid system our main focus is reliability power provide to all consumer without interruption of power supply with least value. The power quality is also part of our grid system. The future power system consist power switching and protecting device, advanced metering scheme at the distribution end and consumer ends, controlling of wastage of electrical power. In the future in the smart grid, we also include whether detector device which controlled with GPS technology where we protect our instrument according to the situation of whether. The Table 1 shows the comparison between with smart grid and conventional grid.

TABLE 1
COMPARISON BETWEEN SMART AND CONVENTIONAL GRID

S.N.	Conventional Grid	Smart grid
1	Manual Repairing	Self Repairing
2	Limited Control	Persistent Control
3	Manual Checking	Remote Checking
4	Self Monitored	Manually
5	Sensor Controlled	Not many sensor
6	Manual metering	Auto metering
7	Distributed Network	Centralized
8	One way control	Two way control
9	Mostly electro-Mechanical device	More digitalized device
10	More time for correction	Less time for correction
11	Fault locating problem	Fault locating very rare
12	None	Information about fault
13	Operating voltage is high	Operating voltage is very low
14	Less Reliable	More reliable

The smart technology comes in every field but the electrical power system is very behind in terms of smart technology. There for we have to focus for improvement in technology in electrical power system. Main object of our paper is the we have to suggest new technology which works smartly without increments in cost.

IV. HYBRIDIZATION OF ELECTRICAL POWER

In the rural area of an India does not have electricity, lots of rural are does not connected with main power substation therefore we can produce the electrical power in rural area the sources present in these areas like a wind, bio-materials and solar system. In the rural areas we provide power of electricity is the part of smart grid. Hybridisation means of combination of electrical sources according to situation we can handle electrical power smartly. In the hybridized electrical power system we are using renewable energy sources because of the chances of pollution is zero. Today’s uses natural sources of power is increasing day by day because of their bad effect on environment therefore we have find alternate sources of an energy which produce electricity. We have recent power analysis of electricity which produces in India as shown in Table 2.

TABLE 2
PRODUCTION OF POWER

Types of Power plant	MW/Hr/Yr
Thermal Power Plant	4500 approx.
Hydro Power Plant	150 approx.
PV array	5 approx.
Wind	2.5approx.
Other sources	8 approx.
Total	4665.5 approx.

Rural areas of an India is not so develop there for we have to move for the develop our rural area which are not connected with main power grid substation because of their geographical not suited. The smart grid technology in hybrid power station as shown in figure 2.

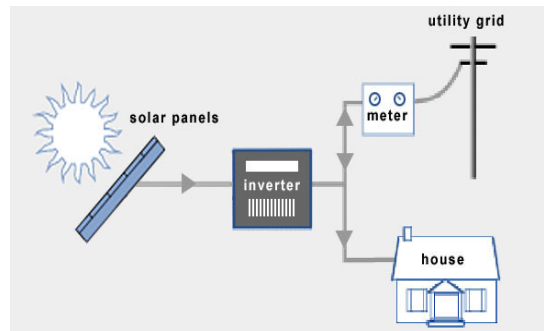


Fig.2. Simple Hybrid power System

V. SMART GRID IN INDIA

Smart Grid vision of India is “Transform the Indian power sector into a secure, adaptive, sustainable and digitally enabled ecosystem that provide reliable and quality energy for all with active participation of stakeholders”

In order to achieve the goal of smart grid in India, we have to make some formula, policies and program according to the power sources available conventional and non-conventional.

A) Improvement in distribution

1. To supply nonstop electricity including peak hour time and electrification of 100% house in India, and improve the quality of power with minimising loss.
2. Completion of ongoing program which will base of smart grid for example consumer indexing ,advance metering ,RAPDRP(Restructured-accelerated Power Development and Program)
3. Modernisation of distribution substation and conversion of substation in all urban areas.
4. Development of Micro-grids, storage option, Virtual Power Plant (VPP), Building to Grid (B2G), Photovoltaic to Grid (PV2G) technology to improve our substation efficiency during peak hour time and base load time.
5. Improvement in load balancing mechanism to minimize the distribution losses.

B) Improvement in Transmission

1. Development of more consistent, safety supported by strong structure which is used for electrical power communication from one end to another
2. Development of large area controlling system with power factor controlling

unit to provide good quality of power every consumer.

3. Development of substation which include all the electrical power which generating from conventional and nonconventional energy sources
4. Development of communication system which transfer bulky electrical power (in GW).

C) Other ideas

1. Active participation of consumer in smart grid system
2. Make a road map for development of power grid system in India
3. Make a policy which is supported to the consumer as well as distributor.
4. Create an platform where the idea can share consumer as well as distributor for high quality of electrical power transmission

In this idea are suggested by the paper by analysis the recent situation of power in now days. In India there are many places where smart grid project are running shown by the figure 3.

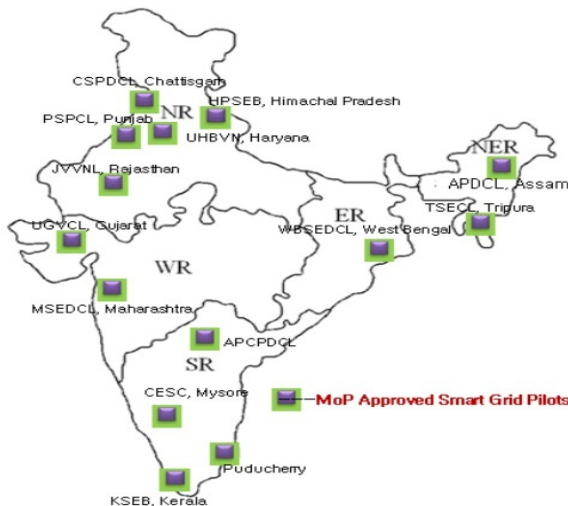


Fig.3. Smart grid project in India

VI. CONCLUSION

One organization should be made for running smart grid power system which work on the according to road map. In the development countries smart grid power project are very useful for environmental and consumer purpose. Smart grid power system minimizing the power loss and also improves the power factor for improving voltage fluctuation. Existing institutions related to smart grid are the India

Smart Grid Task Force (ISGTF) and India Smart Grid Forum (ISGF). Both these bodies currently lack the organizational and financial strength to take-up the above responsibilities, and also lack authority. To begin with, ISGTF can be supported by induction of permanent, independent staffs who are experts in their respective areas who will work exclusively for smart grids. ISGTF can assign some tasks on selective basis to ISGF which could leverage the vast knowledge base of its members. ISGTF should have broader powers in taking decisions in matters related to smart grid developments. Independent, strengthened and empowered ISGTF may be accomplished by end 2013.

REFERENCES

- [1] PETER ASMUS, "INCHING OUR WAY TO A SMARTER POWER GRID", THE ELECTRICITY JOURNAL, VOLUME 19, ISSUE 4, MAY 2006, PP.52-55.
- [2] W. FREI, WHAT IF...? UTILITY VISION 2020, ENERGY POLICY 36 (2008), PP. 640-3645.
- [3] AMY POH AI LING, MUKAIDONO MASAO, "GRID INFORMATION SECURITY FUNCTIONAL REQUIREMENT FULFILLING INFORMATION SECURITY OF A SMART GRID SYSTEM", INTERNATIONAL JOURNAL OF GRID COMPUTING & APPLICATIONS (IJGCA), VOL. 2, No. 2, JUNE 2011, PP. 1-19.
- [4] WENYE WANG, YI XU, MOHIT KHANNA, "A SURVEY ON THE COMMUNICATION ARCHITECTURES IN SMART GRID", W. WANG ET AL., A SURVEY ON THE COMMUNICATION ARCHITECTURES IN SMART GRID, COMPUT. NETW. (2011).
- [5] FOLEY MF. THE DANGERS OF METER DATA (PART 1). AVAILABLE FROM: [HTTP://WWW.SMARTGRIDNEWS.COM/ARTMAN/PUBLISH/INDUSTR/THE_DANGERS_OF_METER_DATA_PART_1.HTML](http://www.smartgridnews.com/artman/publish/INDUSTR/THE_DANGERS_OF_METER_DATA_PART_1.HTML).
- [6] JINGCHENG GAO, YANG XIAO, JING LIU, WEI LIANG, C.L. PHILIP CHEN, "A SURVEY OF COMMUNICATION/NETWORKING IN SMART GRIDS", FUTURE GENERATION COMPUTER SYSTEMS, IN PRESS, CORRECTED PROOF, AVAILABLE ONLINE 10 MAY 2011.
- [7] J.A. MOMOH, SMART GRID DESIGN FOR EFFICIENT AND FLEXIBLE POWER NETWORKS OPERATION AND CONTROL, IN: POWER SYSTEMS CONFERENCE AND EXPOSITION, 2009, PSCE '09. IEEE/PES, 2009, PP. 1-8.



INTELLIGENT AUTONOMOUS FARMING ROBOT WITH PLANT HEALTH INDICATION & CARING USING IMAGE PROCESSING

Shrikant Borate¹, Prof. P. V. Mulmule²

^[1] PG Scholar, E&TC Engineering, PVPIT Pune, Savitribai Phule Pune University, Pune, India.

^[2] Asst. Prof E&TC Engineering ,PVPIT Pune, Savitribai Phule Pune University , Pune ,India

Email: shrikantborate2389@gmail.com, pvmulmule@yahoo.com

Abstract – In agriculture field there are various diseases, specially leaf diseases are the most popular diseases where spots occurs on the leaves. If this spots are not detected on time cause several losses. Insects are also affecting the leaves. If not treated on time caused severe loss. Excessive use of pesticides for plant treatment increases the cost and environmental pollution so their use must be minimized. Many farmers are still using traditional methods for spraying fertilizers. These methods are more time and money consuming it requires large man power. By using traditional methods for spraying fertilizers may cause different effects on farmers health and it does not give accurate results. The solution for the mentioned problem is to design autonomous robot for performing different farming work like detect the diseases on crop, suggest the pesticide for that disease, spray the fertilizer on crop. By using autonomous farming robot save the excessive use of pesticide, consume the labor cost and protect farmer health from pesticide.

Index Terms – Raspberry Pi, PIC microcontroller, Agriculture image processing, crop leaf.

I. INTRODUCTION

Leaf diseases on plant are the most predominant diseases which appear as spots on the leaves. In case of severe infection, the leaf becomes totally covered with spots. The various types of leaf diseases on plant determine the quality, quantity, and stability of yield.



Fig 1: Leaf miner disease

Leaf miners are the larval stage of an insect family that feeds between the upper and lower surfaces of leaves. On heavily infested plants it is not uncommon to find 6 or more maggots per leaf. Although damage can restrict plant growth, resulting in reduced yields and loss of vigor, healthy plants can tolerate considerable injury.



Fig 2: Yellow spot disease

The diseases in plant not only reduce the yield but also deteriorate of the variety and its withdrawal from cultivation. Excessive uses of pesticide for plant diseases treatment increases the danger of toxic residue level on agricultural products and has been identified as a major contributor to ground water contamination also pesticides are among the highest components in the production cost their use must be minimized. This can be achieved by estimating severity of disease and target the diseases places, with the appropriate quantity and concentration of pesticide. The naked eye observation method is generally used to decide diseases severity in the production practice but results are subjective and it is not possible to measure the disease extent precisely.

As one of the trends of development on automation and intelligence of agricultural machinery in the 21st century, all kinds of agricultural robots have been researched and developed to implement a number of agricultural production in many countries, such as picking, harvesting, weeding, pruning, planting, grafting, agricultural classification, etc.[4]. And they gradually appear advantages in agricultural production to increase productivity, improve application accuracy and enhance handling safety.

For disease detection and fertilizer spray develop a autonomous farming robot, this robot take images of crop and by using image processing in raspberry pi find out the disease is present or not on crop leaf. After that robot shows the name of the disease the suitable

fertilizer for that disease, and finally spray the fertilizer on crop by using robot.

II. LITRETURE REVIEW STAGE

A deep and profound literature survey is backbone of any successful project. Extensively search has been carried out for past and related work in this field. Internet tool is used as source of information for carrying out this literature survey.

(1) "Autonomous Agricultural Robot and Its Row Guidance" XUE Jinlin, XU Liming, IEEE2010

A vision-based row guidance method is presented to guide a robot platform which is designed independently to drive through the row crops in a field according to the design concept of open architecture, then offset and heading angle of the robot platform are detected in real time to guide the platform on the basis of recognition of a crop row using machine vision. And the control scheme of the platform is proposed to carry out row guidance[4].

(2) "Leaf Disease Severity Measurement Using Image Processing" Sanjay B. Patil et al. / International Journal of Engineering and Technology Vol.3 (5), 2011, 297-301

For leaf disease detection Simple threshold and Triangle thresholding methods are used to segment the leaf area and lesion region area respectively[5].

(3) Autonomous Robots for Agricultural Tasks and Farm Assignment and Future Trends in Agro Robots" Sajjad Yaghoubi, Negar Ali Akbarzadeh, Shadi Sadeghi Bazargani, International Journal of Mechanical & Mechatronics Engineering IJMME-IJENS-june2013

This paper give brief review of research in agricultural vehicle guidance technologies is presented. Application of new popular robotic technologies will augment the realization of agricultural vehicle in future[6].

III. PROPOSED SYSTEM

For autonomous farming robot it required all system on robot, for that raspberry pi and PIC controller are used to perform robotic operation.

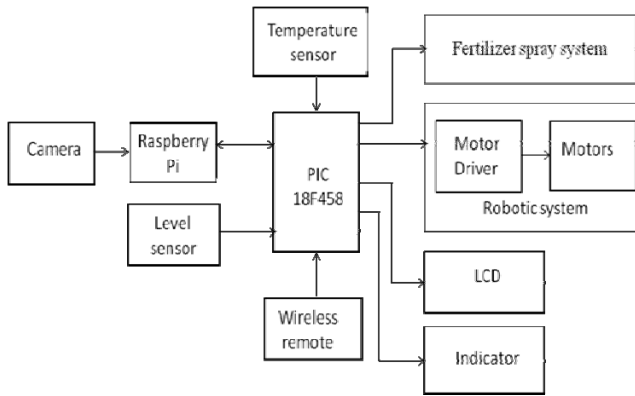


Fig 3: “Block Diagram of Autonomous Farming Robot system”

A. Block Diagram Description

a. Camera

It is used for take a image of crops, it is directly connected to the raspberry Pi. There are two ways to connect camera to raspberry Pi first one is USB camera and second is camera module of raspberry Pi.

b. Temperature Sensor

Temperature sensor are used to sense the environment temperature. We have used a Temperature sensor called LM35. This temperature sensor can sense the temperature of the atmosphere around it and gives the reading of the temperature. The LM35 series are precision integrated-circuit temperature sensors, whose output voltage is linearly proportional to the Celsius (Centigrade) temperature. Temperature sensor is an analog sensor and gives the output into form of analog signal. This signal is feed to ADC which will convert it into digital form. Once converted into digital form, the microcontroller can process the digital temperature signal as per the application.

c. LCD Display

Lampex,16*2, Backlit facility LCD is used in a project to visualize the output of the application. We have used 16x2 LCD which indicates 16 columns and 2 rows. So, total 32 characters we can display on 16x2 LCD. It can also used in a project to display the pesticide name to be spray on the crops. Thus LCD plays a vital role in a project to see the output and it also display the status of fertilizer tank that is tank is empty or not.

d. Motor Diver

A L293d motor driver IC is used to control motors in autonomous robotics. Motor driver act as an interface between controller and the motors in the robotics. Motor driver are primarily used in autonomous robotics only. Also the controller operate at low voltages and require a small amount of current to operate while the motors require a relative higher voltages and current. Thus current cannot be supplied to the motors from the controller. This is the primary need for the motor driver.

e. Fertilizer Spraying system

Fertilizer spraying system are used to spray the fertilizer on crop. By using this system we cover large area in less fertilizer. When the fertilizer tank is empty then this system activate the indicator and also show the status of tank on display.

f. Raspberry Pi

Raspberry Pi is used for image processing. Camera is connected to the raspberry pi, raspberry pi take image through that camera. After taking image of crop image processing is start on that image and finally we get the result of image processing. By using image processing we detect the disease on leaf. The Raspberry Pi is a credit card-sized single-board computer developed in the UK by the Raspberry Pi Foundation with the intention of promoting the teaching of basic computer science in schools.

The Raspberry Pi has a Broadcom BCM2835 system on a chip (SoC), which includes an ARM1176JZF-S 700 MHz processor, VideoCore IV GPU, and was originally shipped with 256 megabytes of RAM, later upgraded (Model B & Model B+) to 512 MB. It does not include a built-in hard disk or solid-state drive, but it uses an SD card for booting and persistent storage, with the Model B+ using a MicroSD.

g. PIC18f458 Microcontroller

PIC controller are used for control the all robotic operation, it give command to raspberry pi for image capturing and image processing. Autonomous robot system required more input and output pins for that PIC18f458 controller are

selected. It has 40 pin controller out of that 33 pins are input output pins. It has 10bit ADC.

h. Wireless Remote

A wireless radio frequency (RF) transmitter and receiver can be easily made using HT12D Decoder, HT12E Encoder and ASK RF Module. Wireless transmission can be done by using 433Mhz or 315MHz ASK RF Transmitter and Receiver modules. In these modules digital data is represented by different amplitudes of the carrier wave, hence this modulation is known as Amplitude Shift Keying (ASK). Radio Frequency (RF) transmission is more strong and reliable than Infrared (IR) transmission due to following reasons :

- Radio Frequency signals can travel longer distances than Infrared.
- Only line of sight communication is possible through Infrared while radio frequency signals can be transmitted even when there is obstacles.
- Infrared signals will get interfered by other IR sources but signals on one frequency band in RF will not interfered by other frequency RF signals.

B. System Flow Chart

a. Disease Detection

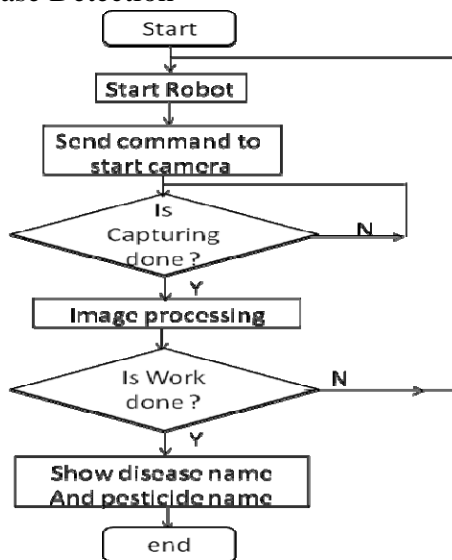


Fig 4: Disease detection

b. Fertilizer Spraying System

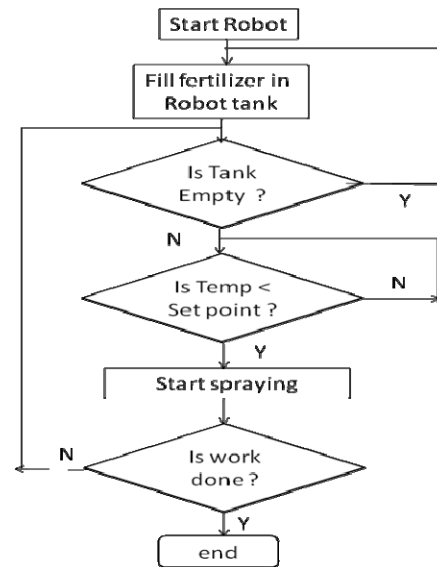


Fig 5: Fertilizer spray system

Fig 4 shows the flow chart for disease detection and fertilizer suggestion. First take the image of crop then make image processing on that image, after that check work done signal if it is high then show the disease name and fertilizer name on display else repeat the process of image capturing and image processing.

Fig 5 shows the flow chart for fertilizer spraying system, first fill the fertilizer in robot tank after that check the status of temperature sensor if it is above set point then spraying system is stop else continue the spraying.

IV WORKING MODEL

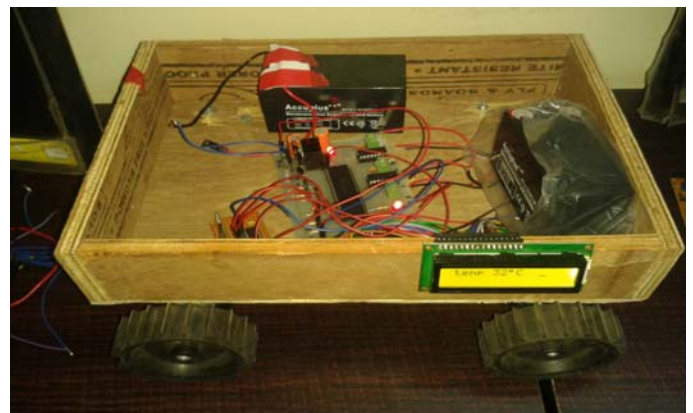


Fig 6: Autonomous farming robot

Fig 6 show the physical structure of autonomous farming robot, robot structure is divided in to

three section first is embedded section second is battery section and third is fertilizer tank section. Operation of robot is controlled by using PIC18f458 microcontroller, DC motors are used for robotic operation and that motors are drive through L293d IC. PIC give the signal to the L293d, according to that signal L293d IC give signal to the DC motor. 12v battery are used for provide the supply voltage to the PIC controller, raspberry pi and DC motors.

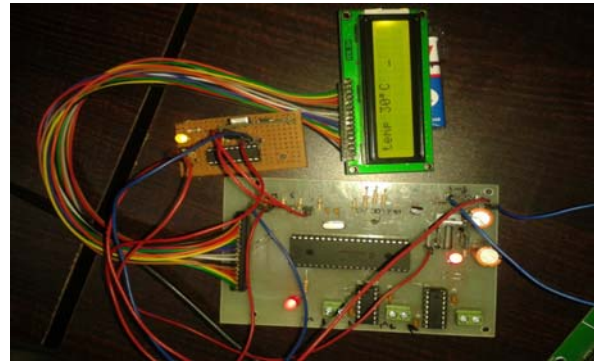


Fig 9: Environment temperature



Fig 7: Image capturing system with raspberry pi

Fig 7 shows the required component for capture the images of crops, for that raspberry pi, camera are used. Raspberry pi require 5v DC supply for operation that supply is provided through the battery which is mounted on robot. Camera is connected to the USB port of raspberry pi.

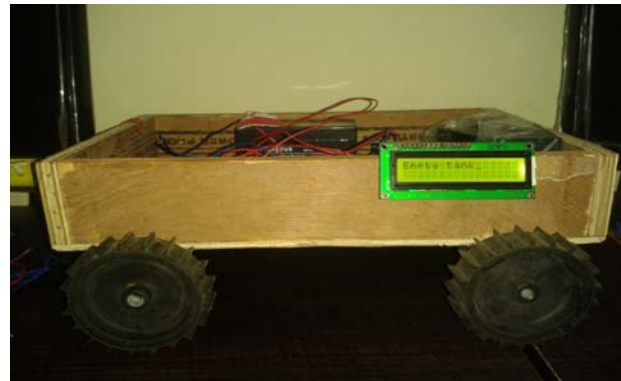


Fig 10: Status of fertilizer tank

V Test Result

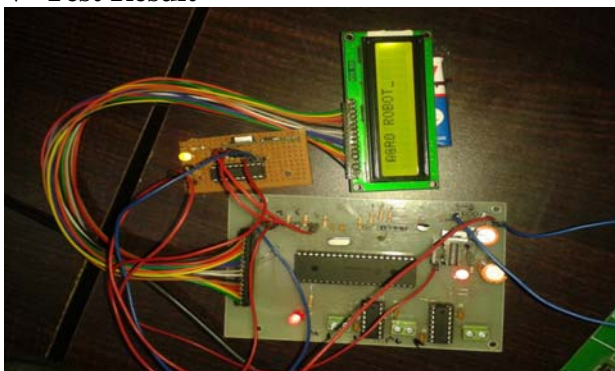


FIG 8: STARTUP MESSAGE SHOWN BY SYSTEM

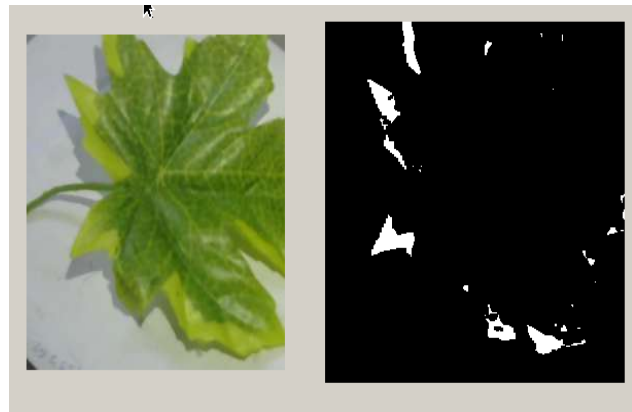


Fig 11: Yellow spot disease detected

VI CONCLUSION

Leaf diseases in plant are the most predominant diseases which appear as spots on the leaves. Although leaf disease can restrict plant growth, resulting in reduced yields and loss of vigor, healthy plants can tolerate considerable injury.

By using image processing find out the type of disease and according to that disease spraying the fertilizer on crop through autonomous farming robot. By using farming robot we give the accurate treatment to the crop and maintain the crop healthy and increase the production. Main advantage of farming robot is to save the pesticide cost, labor cost and avoid the direct contact of farmer with pesticide.

VII ACKNOWLEDGMENT

I would like to acknowledge all the people who have been of the help and assist me throughout my analysis of project work. It gives me a great pleasure in bringing out the project work entitled, INTELLIGENT AUTONOMOUS FARMING ROBOT WITH PLANT HEALTH INDICATION & CARING USING IMAGE PROCESSING. It is observed outcome of the exciting work, done under the inspiring guidance of my guide Prof. P. V. Mulmule.

VIII REFERENCES

- [1] “Vision Based Guidance for Robot Navigation in Agriculture” Andrew English, Patrick Ross, David Ball, Member, IEEE, Peter Corke, Fellow, IEEE-2014
- [2] “Zigbee-assisted Mobile Robot Gardener” Chung L. Chang, Senior Member, IEEE, and Jia H. Jhu IEEE -2013
- [3] Applications of Perceptual Hash Algorithm in Agriculture Images, Xin Liu, Qian Zhang*, RuPeng Luan, Feng Yu, 2013 IEEE.
- [4] “Autonomous Agricultural Robot and Its Row Guidance ” XUE Jinlin, XU Liming, IEEE 2010.
- [5] “Leaf Disease Severity Measurement Using Image Processing” Sanjay B. Patil et al. / International Journal of Engineering and Technology Vol.3 (5), 2011, 297-301
- [6] “Autonomous Robots for Agricultural Tasks and Farm Assignment and Future Trends in Agro Robots” Sajjad Yaghoubi, Negar Ali Akbarzadeh, Shadi Sadeghi Bazargani, International Journal of Mechanical & Mechatronics Engineering IJMME-IJENS-june2013.
- [7] “Agricultural Robots – Applications and Economic Perspectives” Pedersen S. M, Fountas S and Blackmore S, University of Copenhagen, Institute of Food and Resource Economics.
- [8] “Object detection combining recognition and segmentation” liming wang, Jianbo shi, Gang song and I-fan shen, Fudan university shanghai.



LOW VOLTAGE DC BUS MICRO-GRID PROTECTION SYSTEM

¹Pate Pawan V., ²Kamal Sandeep K., ³Pate Poonam V.

¹VDF school of Engineering Latur, ²Zeal institute DCOER, Pune,

³Sinhagad Academy of Engg., pune.

Email: ¹pawanpate1913@gmail.com, ²kamalsundeep@gmail.com, ³p.poonam095@gmail.com

Abstract—Use of DC Microgrid can lead to more efficient integration of distributed generation, but the protection of DC Microgrid is a quite challenging task. The conventional protection scheme for DC Microgrid uses circuit breaker on AC side, on occurrence of fault AC circuit breaker opens and this cause's complete shutdown of DC link and introduces a forced outage in the system. A new protection scheme for DC micro-grid against line to line fault is presented in this paper. It avoids the complete shutdown of the DC link and continuity of supply is maintained through other buses, as ring type distribution is considered. The current sensors placed at both end of transmission line continuously check the current at both side. When fault occur in line, current difference occurs at both end of line. Controller detects the current difference and opens the power switches which placed at both ends. To satisfy the requirement of fast interrupting time and high short circuit current withstanding capability, IGBTs used as power switches, the proposed scheme is verified through MATLAB Simulink.

Index Terms— DC system, DC bus micro-grid, Distributed generation, DC distribution, Fault protection,

I. INTRODUCTION

The ever increasing demand of power puts pressure on generation system and distribution

system, this increase in demand causes imbalance between supply and demand.

Nowadays there is a large gap between supply and demand of power, and also there is large scarcity of non-renewable sources. To cope up with this, there is need to increase the generation from renewable energy resources like wind energy conversion systems and solar energy systems etc. Power generate from distributed generation, is transferred through the AC or DC grid. When this power is supplied to the isolated area, there is large scope for DC micro-grid instead of AC system [1]. The main advantage of DC microgrid is reduced losses so higher efficiency than AC. Due to change in energy generation patterns from non-renewable to renewable it is convenient to use DC link, as most of them generate power in DC form.

Conventional protection techniques in DC microgrid completely de-energies the DC link. Because such protection scheme the area under healthy condition also goes to dark, this causes forced outage in the system. The main objective of this work is to find out the effective method for protection of DC grid which isolate only the faulty section and avoid complete shutdown of DC grid. So healthy sections are operated without any disturbance and supply continuity is maintained through other buses.

II. DIRECT CURRENT SYSTEM

A. Advantages of D.C System

DC system having number of advantages such as

- a. More power can be transmitted per

conductor per circuit: For the same insulation, the direct voltage V_d is equal to the peak value ($\sqrt{2}$ x rms value) of the alternating voltage V_a .

b. Use of Ground Return Possible:

In the case of HVDC transmission, ground return (especially submarine crossing) may be used, as in the case of a mono polar DC link.

c. Smaller Tower Size:

The DC insulation level for the same power transmission is likely to be lower than the corresponding AC level.

d. No skin effect:

Skin effect under conditions of smooth DC is completely absent and hence there is a uniform current in the conductor, and the conductor metal is better utilized.

e. Less corona and radio interference:

Since corona loss increases with frequency, there is much lower corona loss and hence more importantly less radio interference with DC.

f. No Stability Problem:

The DC link is an asynchronous link and hence any AC supplied through converters or DC generations do not have to be synchronized with the link. Hence the length of DC link is not governed by stability.

g. Asynchronous interconnection possible:

For different frequency interconnections both converters can be confined to the same station.

h. Tie line power is easily controlled:

With DC tie lines, the control is easily accomplished through grid control.

There are also inherent problems associated with DC such as, Expensive converters, Generation of harmonics, Difficulty of circuit breaking, Difficulty of voltage transformation, Difficulty of high power generation, Absence of overload capacity

B. Configuration of DC Grid

DC grid can be configured in many ways on the basis of cost, flexibility, and operational requirements.

1.Monopolar Link

In this system, one of the terminals of the rectifier is connected to earth ground. The other

terminal, at a potential high above ground, is connected to a transmission line.

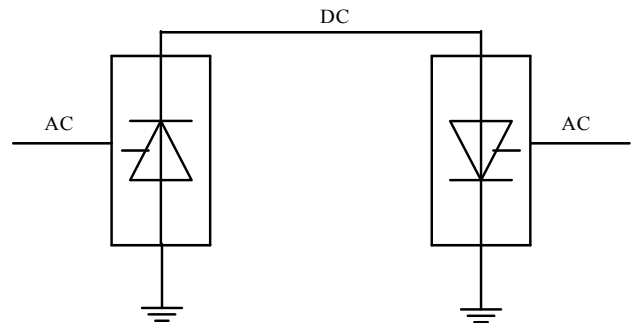


Fig.1 Monopolar link.

The earthed terminal may be connected to the corresponding connection at the inverting station by means of a second conductor. Monopolar link is depicted in Fig.1.

2.Bipolar Link

This system consists of a pair of conductors, each at high potential with respect to ground. These conductors are opposite in polarity i.e. one is of positive and other is of negative polarity. Fig. 2 shows bipolar DC link. Since these conductors must be insulated for the full voltage, transmission line cost is higher than a monopole with a return conductor. However, there are a number of advantages to bipolar transmission which can make it an attractive option.

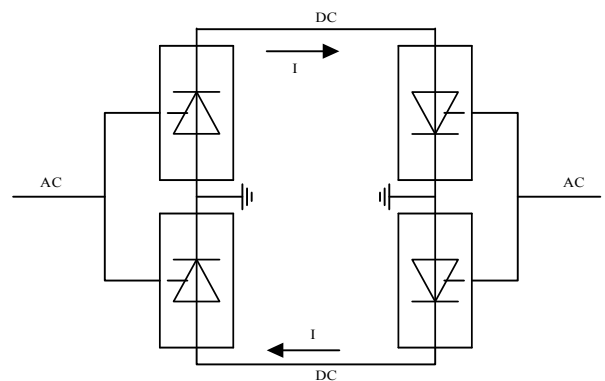


Fig.2 Bipolar link.

3.Homopolar Link

Homopolar link has two or more conductors all having the same polarity (usually negative) and always operated with ground or metallic return. Fig.3 shows configuration of homopolar link Homopolar link has the advantage of reduced insulation costs. But the disadvantages of earth return outweigh the advantages.

4. Back to Back Connection

A back-to-back station (or B2B for short) is a plant in which both converters are in the same area, usually in the same building. The length of the direct current line is kept as short as possible.

5. Multi terminal system

The most common configuration of an HVDC link consists of two converter stations connected by an overhead power line or undersea cable. Multi-terminal HVDC links, connecting more than two points. Fig.4 shows a multi terminal connection system.

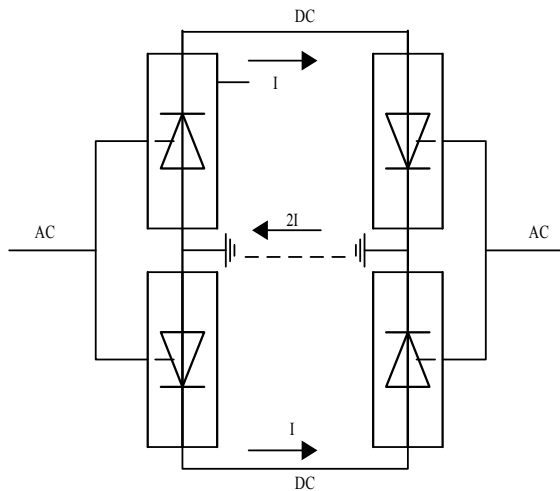


Fig.3. Homopolar Link

The configuration of multiple terminals can be series, parallel, or hybrid. Parallel configuration tends to be used for large capacity stations, and series for lower capacity stations. Multi-terminal systems are difficult to realize using line commutated converters because reversals of power are effected by reversing the polarity of DC voltage, which affects all converters connected to the system.

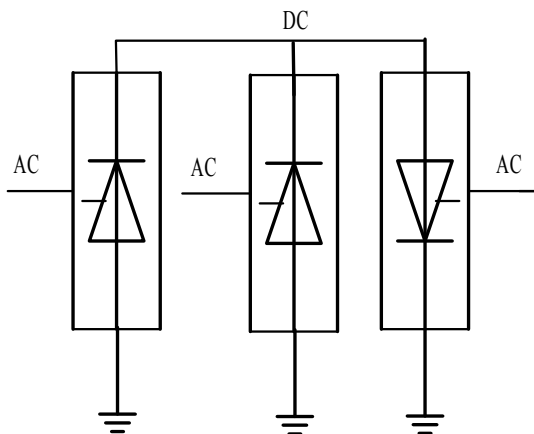


Fig.4 Multi terminal system.

There are three types of DC grids: a) High voltage DC grids (HVDC): $V_{dc} > 30$ kV; b) Medium voltage DC grids (MVDC) : 1500 V $< V_{dc} < 30$ kV; c) Low voltage DC grids (LVDC) : $V_{dc} < 1500$ V

III. LOW VOLTAGE DC (LVDC) MICROGRID

Low voltage DC grid (LVDC) is emerging concept in distribution system. The microgrid system is a small-scale distributed power system consisting of distributed energy sources and loads, and it can be readily integrated with the renewable energy sources [4]–[6]. Due to the distributed nature of the micro- grid approach, the connection to the central dispatch can be removed or minimized, It can be operated in the grid-connected mode, operation in the autonomous (islanded) mode, and ride-through between the two modes [7], [8]. There is simple and easy control and large development in the protection technology of AC system as compared to DC system. But it faces the problem like skin effect, proximity effect, and reactive power control; also losses are more in AC grid. On the other hand DC micro-grid having less loses, and DC system can deliver 1.41 times more power as compared to AC system with the same cable cross section [8], [9].

The schematic diagrams of a LVDC micro-grid is shown on Fig. 5 As the figure indicates, AC loads are interfaced to the grid through power converters. All DER require power converters. General DC loads may require power converters if the voltage rating is not the same as the rated grid voltage. Power converters are used for adjusting generator and load voltages to the standard grid voltage, if required [7].

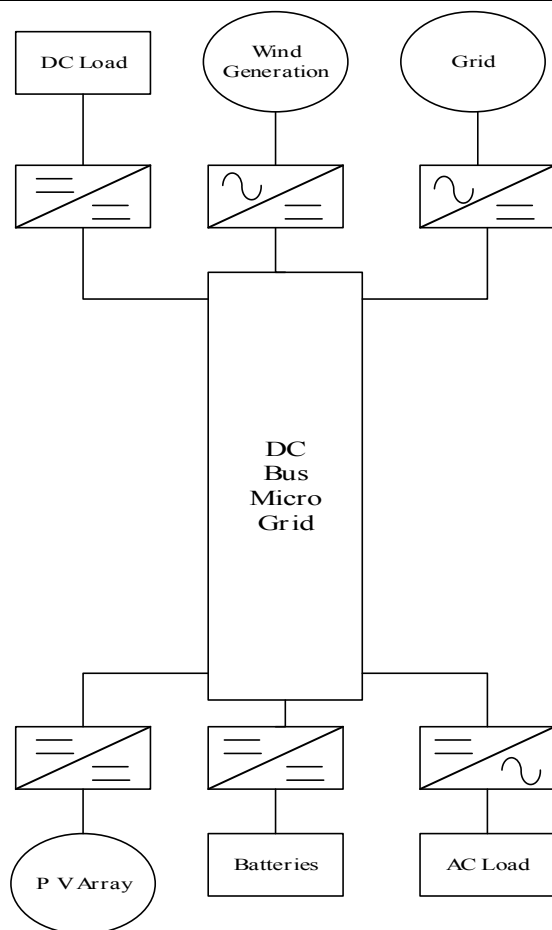


Fig.5 DC Bus Microgrid.

The LVDC is well suited for the system such as offices with computer loads or rural power system [10]. A DC micro-grid is also suited for integrate a range of DER units, such as internal combustion engines, gas turbines, micro-turbines, photovoltaic panels, fuel cells, and wind-power. Most of these sources are not well suited to operate with fixed frequency, or fixed DC voltage, so they require power converters to interface with either DC or AC electrical distribution systems. The LVDC have many advantages as compared to AC distribution system. Power electronics converters are used for connection of load to either AC or DC bus for power conversion. When load connected to bus is DC such as computers, fluorescent lamp, TV sets; DC bus requires fewer power conversion stages [10]-[11]. Since power conversion stages is less, losses in conversion also reduced. Most of the resistive load can be connected to either AC or DC bus. But the AC load cannot connect

directly to DC micro-grid [8].

IV. POSSIBLE FAULTS IN DC GRIDS

For DC system two types of faults exist, line-to-line and line-to-ground. A line-to-line fault occurs when a path between the positive and negative line is created, shorting the two together. A line-to-ground fault occurs when a path between the positive or negative pole and ground is created. A line-to-ground fault is the most common type of fault.

a. Line to Ground fault

A line to ground fault (ground fault) occurs when the positive or negative line is shorted to ground. In overhead lines faults may occur when lightning strikes the line. This may cause the line to break, fall to the ground and create fault. In this situation the fault is always permanent and the line must be isolated for repair. Ground faults may also occur by objects falling onto the line, such as trees, providing a path to ground. In some cases when an object causes the ground fault it may fall away from the line and the system can be restored. If the fault persists the line would have to be taken out of service until the fault path can be cleared.

Underground cable is almost completely immune to line-to-line faults, as insulation, conduit and the earth separate the cables. However, they can still occur. The insulation of the cable can fail due to improper installation, excessive voltage/current, and exposure to the environment (water, soil, etc) or cable aging. When this occurs, the broken insulation will allow a path for current to flow to ground. As the fault persists the integrity of the insulation is reduced causing the fault to worsen. A ground fault may also occur when a person inadvertently cuts through one of the lines. This generally happens during construction projects. In either case the fault will always be permanent and will require a complete shutdown of the line as well as a costly repair.

This causes an imbalance of the DC link voltage between the positive and negative poles. As the voltage of the faulted line begins to fall and high currents flow. These high currents may damage the converter [12]. A single line to ground fault on positive terminal of line is shown

in Fig.6.

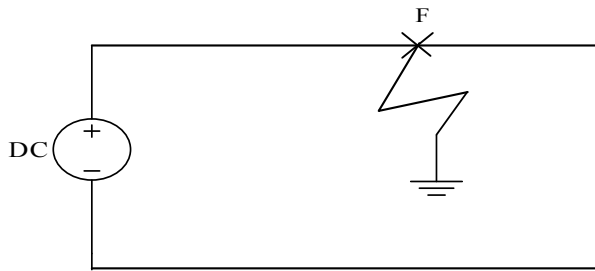


Fig.6 Single Line to ground fault.

b. Double line fault (Line to line fault)

A line to line fault on a cable-connected system is less likely to occur on the cable. In an overhead system, line-to-line faults can be caused by an object falling across the positive and negative line, they may also occur in the event of the failure of a switching device causing the lines to short. A switching fault, which is independent of how the converter stations are connected together, causes the positive bus short to the negative bus inside the converter [12]. Fig.7 depicts the line to line fault between positive and negative line.

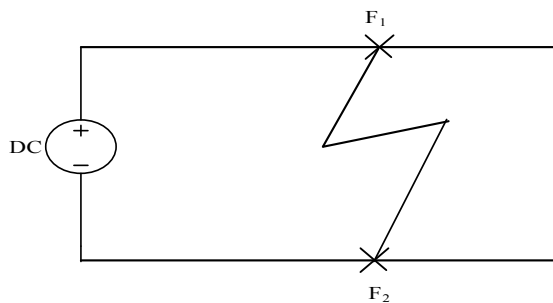


Fig.7 Line to line fault.

c. Overcurrent

While overcurrent protection is important during line-to-line and line-to ground faults, it must also operate when the system is being overloaded. Overload conditions may occur in two-terminal systems when the load increases past the rating of the converter or as a result of a fault on another part of the system. For example, if three VSC's are feeding a common load and one VSC is dropped due to a permanent fault, the remaining two must supply the load. This will result in elevated currents that may overload the converters. In this situation the overcurrent protection would need to operate. Another

option to avoid a wide spread blackout would be to shed non-critical loads [12]

V. CONVENTIONAL FAULT ISOLATION TECHNIQUES

The common practice in DC power systems is not to install any protection on the DC side, and protection only provide on AC side using AC circuit breakers. Upon fault detection the AC CBs that link the AC and DC systems are opened, and disconnect DC link from AC grid. However, this method completely de-energizes the DC system until the fault is removed and the systems can be re-energized. It works for HVDC and medium-voltage DC (MVDC) transmission systems where the DC system is a conduit between the AC systems and loads.

However, this method can create unnecessary outages in LVDC micro-grids where multiple sources and loads are connected to a common bus [13], [14]. Fuses also used for protection, but fuses have limitations and ac circuit breaker cannot use in DC systems [7]. There are several alternatives for solid-state devices for the CBs, such as gate turn-off thyristors (GTOs), insulated-gate commutated thyristors (IGCTs), and Insulated-gate bipolar transistor (IGBTs).

VI. NEW FAULT ISOLATION SCHEME

Instead of shutting down the whole system or limiting the bus current, the presented scheme detects the fault and separates the faulted section so that the rest of the system keeps operating. The loop-type DC bus is suggested for the presented scheme to make the system robust under faulted conditions. It has also been reported that the loop-type bus has a good system efficiency especially when the distribution line is not long [16].

In this scheme current sensors placed at the sending end and receiving end of DC micro grid. These current sensors continuously sense the line current and give information to the controller. In healthy operating condition the current at the two end of line is approximately same. But when single line to ground or the line to line fault occurs in the bus, there is a current difference between the two ends of the line is occurs. When this current difference exceeds the threshold value, controller will operate and gives

command to the power switches.

Fig.8 depicts only one bus protection. It is shown that, current sensors placed at two ends bus and near to power switches/circuit breaker. The controller operates when currents different between two ends exceeds a set value.

$$I_{operation} = I_1 - I_2$$

Where i_1 and i_2 is the line current at each end of the bus segment. When fault occurs in the system, current difference exceeds the threshold value. And the controller sends the appropriate commands to power switches/circuit breaker, so that the faulted segment can be separated from the system. Because this system uses the differential relaying principle monitoring only the relative difference of input and output current of a segment, it can detect the fault on the bus regardless of fault current amplitude or power supply's feeding capacity.

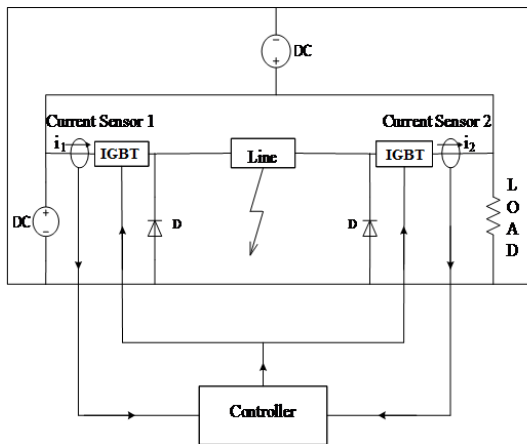


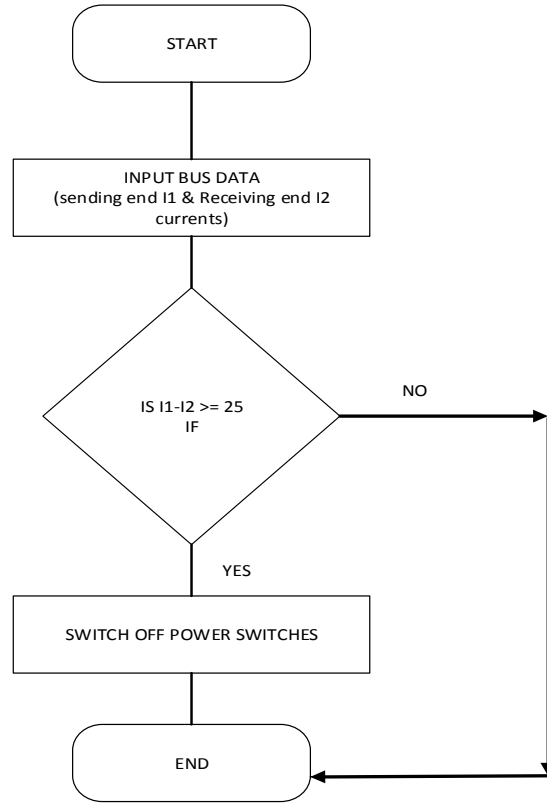
Fig. 8 Placement of current sensor and power switches.

Once the faulted segment has been isolated, the load voltage will be restored and remainder of the system can continue to operate on the loop-type bus. Even with multiple faulted segments, the system can operate partially if the segments from some power sources to loads are intact. The possibility of the fault around the device connection point can be minimized, if the sensors are installed as close to the connection point as possible.

When faulty section is isolated using switches (SW), the fault current in this section is

extinguished through the freewheeling resistors (R) and diode (D) is used for the freewheeling path. In healthy operating condition freewheeling diodes are in blocking mode, and there is no current passing through the freewheeling path. But when circuit breaker opens and isolates the faulted bus, diodes comes into conduction mode

Fig 9 shows a flow chart of proposed protection scheme



Fault current freewheel through diode, resistors and extinguished. How the fault current flows in the system and how this current extinguished through freewheeling path for single line to ground fault is shown in Fig. 9 (a) and 9 (b) respectively. Fault current path and freewheeling current path for line to line fault is shown in Fig.9 (c) and Fig.9 (d) respectively.

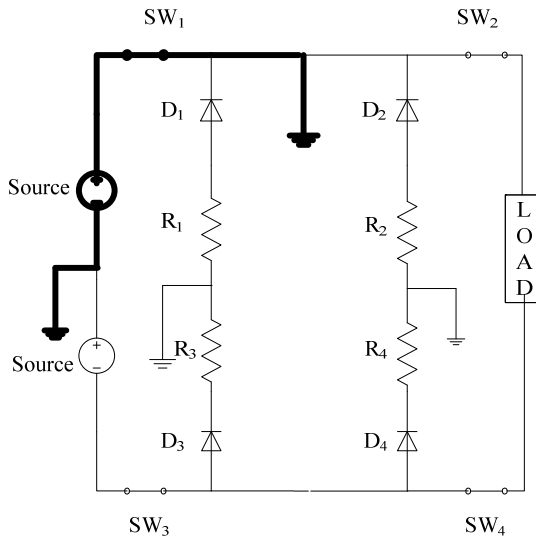


Fig a

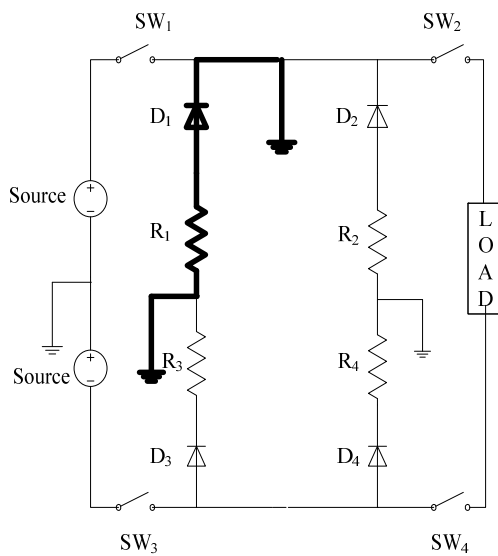


Fig b

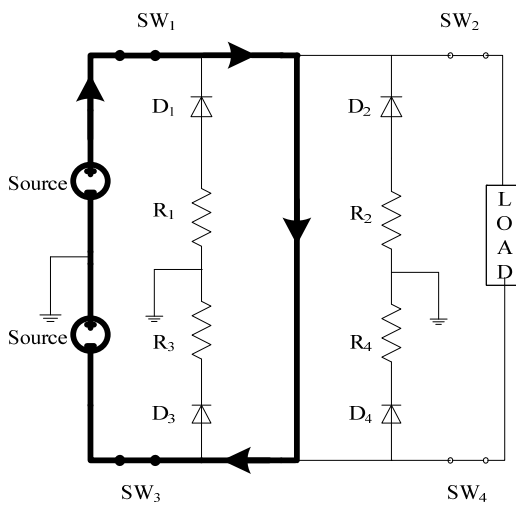


Fig c

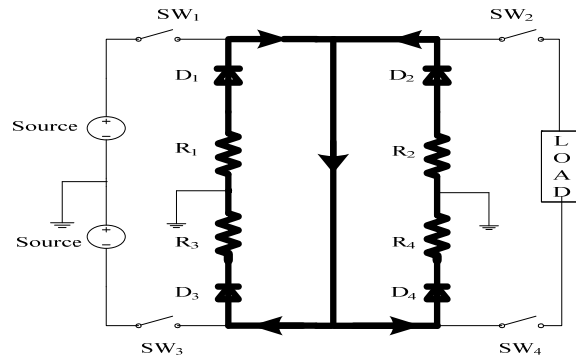


Fig d

Fig.9 Fault current path and extinction in presented scheme. (a) Fault current path in single line to ground fault. (b) Fault current extinction in single line to ground Fault. (c) Fault current path in line to line fault. (d) Fault current extinction in line to line fault.

Fault current extinction rate depends on resistance of freewheeling path. If the freewheeling resistance is large, current dissipates largely and fault current is extinguished quickly.

VII. RESULT

MATLAB-Simulink model created for a 400 meter bipolar dc bus with constant 120 volt dc supply between two terminals. A line-to-line fault in the middle of the line is simulated at 0.02 sec. The fault current magnitude depends on the impedance of the fault path. The currents at each end of the segment which has been identical before fault. When fault occurs in the system current at the both ends of segment shows clear difference. On this current difference controller will operate and opens the power switches, considering speed of controller and switching devices is fast. The simulation parameters of system are given in Table 1.

Table 1 Simulation Parameters.

Parameter	Specification
Bus voltage	120V
Bus length	400m
Line resistance	121mΩ/km
Line capacitance	12.1nF/km
Line inductance	0.97mH/km
Freewheeling resistance	50 Ω
Load	2 KW

The simulation results are shown in Fig.10 for line to line fault. Fig. 10(a) Shows that when there is no fault in the system i.e. in normal operating condition voltage across the load is constant, no disturbance in the system. When fault occurs at 0.02 second, voltage across the load is falls down rapidly. It is seen in the Fig 10 (b), when protection is applied to the system the controller will operate on current difference and opens the switches in 0.025 second. The voltage is immediately restore and the faulty section is isolated. The faulty bus is switched out from the operation and other buses will take care the load.

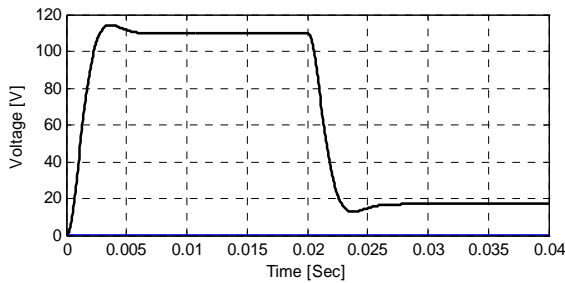


Fig 10 (a)

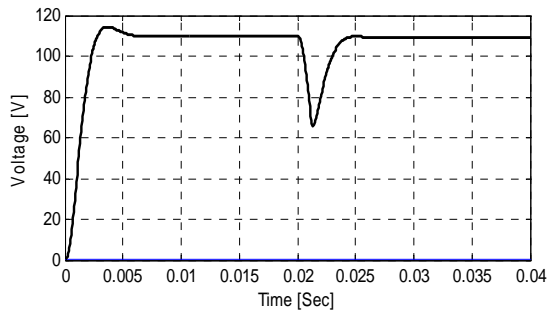


Fig 10 (b)

Fig. 10 (c) depicts that before occurrence of fault load current is constant. But during faulty condition load current is falls down quickly and it remains as it is if protection is not used. When said scheme is applied, section under trouble is isolated and load current is again maintained through loop system, as shown in Fig.10 (d).

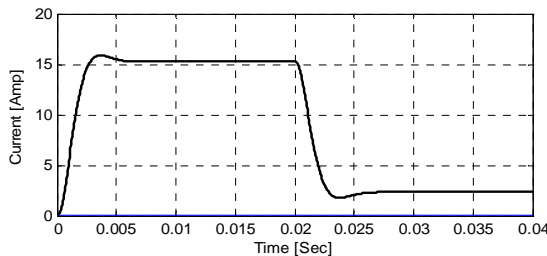


Fig 10 (c)

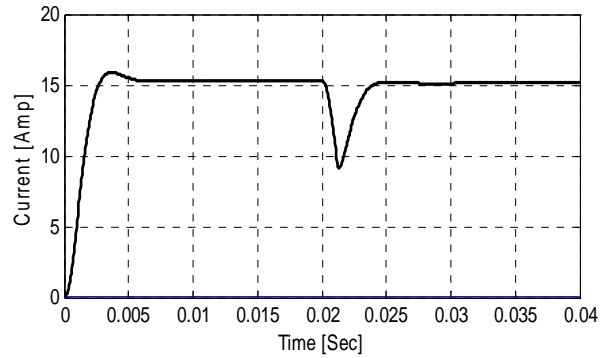


Fig 10 (d)

Fig. 4.4 Load voltage and current; without protection and with protection. (a) Load voltage without protection. (b) Load voltage with Protection. (c) Load current without protection. (d) Load current with Protection.

Bus current is normal during healthy condition, it is very high on the occurrence of fault, and it remains high without protection is shown in Fig.11.

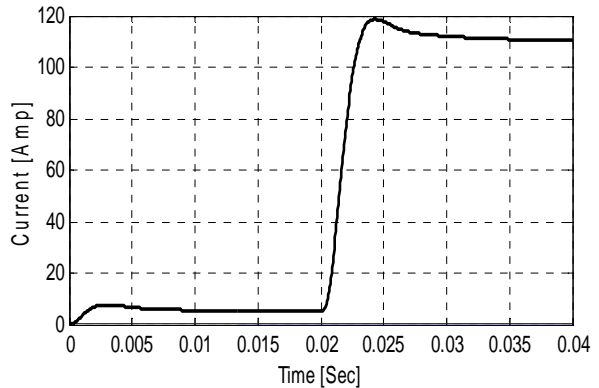


Fig.11 Fault bus current without protection.

Fig. 12 depicts the fault path current and also the current in the freewheeling path. When there is no fault in the system, no current difference occurs at the two ends of line and there is no controller action. Therefore zero current flows through the freewheeling path. But when fault happen in the system current difference at the two ends of line is occurred. The current sensors sense the difference if, this difference exceeds a defined value the controller will operate and switches are opened. When switches are opened diodes starts conduction, freewheeling current flows through it and extinguished through resistors. Depending upon the value of resistors the rate of fault current extinction is determined.

If high value resistors are used the fault current extinguish quickly.

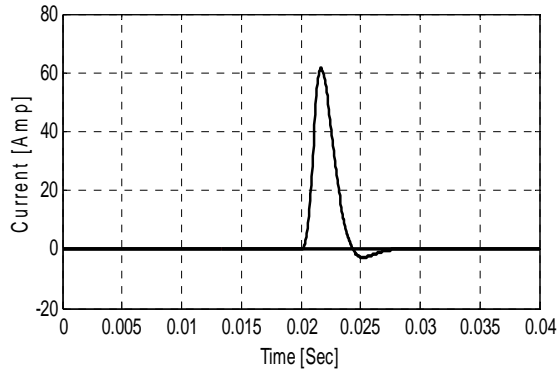


Fig. 12 Fault path current.

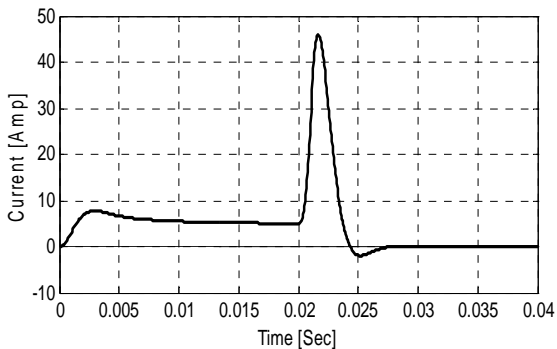


Fig. 13 Fault bus current with protection.

Fig.13 depicts the fault bus current which is high during faulty condition and goes to zero after the disconnecting or isolating this bus. Here only one bus protection is shown, while protection devices for other buses are not shown here.

VIII. CONCLUSION

With the new interest in green energy, the smart grid and distributed generation micro-grids may soon become an integral part of our electric grid. DC micro-grids have proven to be a viable competitor to AC micro-grids. Protection of the DC bus is an integral part to the DC micro-grid, and must be able to isolate faults with minimal impact to the overall system. It can be seen that the conventional techniques require a complete shutdown of the DC bus. This is not suitable for critical loads.

The new fault detection and isolation scheme for low-voltage DC-bus micro-grid system is shown here. The loop-type bus allows multiple paths for power to flow when a section has been isolated. Successful fault detection and isolation was shown using MATLAB simulations and

hardware results. Though the fault detection and isolation proves successful for suppressing fault current, locating the faulted zone and isolating the zone for line-to-line fault. Also, when a fault occurs and a source is removed from the micro-grid, the remainder of the sources must accommodate the load. This will improve stability in the grid and maximize efficiency from all of the sources.

REFERENCES

- [1] R. Dugan, T. McDermott, "Distributed generation," *IEEE Ind. Appl. Mag.*, vol. 8, no. 2, pp. 19-25, Mar./Apr. 2002.
- [2] "Comparison of Costs and Benefits for AC and DC Transmission" OAK RIDGE NATIONAL LABORATORY.
- [3] Roberto Rudervall, J.P. Charpentier, Raghuvveer Sharma "High Voltage Direct Current (HVDC) Transmission Systems Technology Review Paper" Presented at Energy Week 2000, Washington, D.C, USA, March 7-8, 2000.
- [4] R. Lasseter and P. Paigi, "Microgrid: A conceptual solution," in *Proc. 35th Annu. IEEE Power Electron. Specialists Conf.*, 2004, pp. 4285–4290.
- [5] H. Nikkhajoei and R. Lasseter, "Distributed generation interface to the CERTS microgrid," *IEEE Trans. Power Del.*, vol. 24, no. 3, pp. 1598–1608, Jul. 2009.
- [6] F. Katiraei, R. Iravani, N. Hatziargyriou, and A. Dimeas, "Microgrids management," *IEEE Power EnergyMag.*, vol. 6, no. 3, pp. 54–65, May/ Jun. 2008.
- [7] J. Park, J. Candelaria, "Fault detection and isolation in low voltage DC-Bus microgrid system" *IEEE Trans. Power Del.*, vol. 28, no. 2, pp. 779-787, Apr. 2013.
- [8] M. Saeedifard, M. Graovac, R. Dias, and R. Iravani, "DC power systems: Challenges and opportunities," in *Proc. IEEE Power Energy Soc. Gen. Meeting*, July 2010, pp. 1–7
- [9] P. Salonen, P. Nuutinen, P. Peltoniemi, and J. Partanen, "LVDC distribution system protection: Solutions, implementation and measurements," in *Proc. 13th Eur. Conf. Power Electron. Appl.*, 2009, pp. 1–10.
- [10] D. Salomonsson, L. Soder, and A. Sannino, "Protection of low-voltage DC microgrids,"

- IEEE Trans. Power Del., vol. 24, no. 3, pp. 1045–1053, Jul. 2009.
- [11]R. Cuzner and G. Venkataramanan, “The status of DC micro-grid protection,” in Proc. IEEE Ind. Appl. Soc. Annu. Meeting, Oct. 2008, pp. 1–8.
- [12]J. Candelaria and J.-D. Park, “VSC-HVDC system protection: A review of current methods,” in Proc. IEEE/Power Energy Soc. Power Syst. Conf. Expo., Mar. 2011, pp. 1–7.
- [13]P. Cairoli, R. Dougal, U. Ghisla, and I. Kondratiev, “Power sequencing approach to fault isolation in dc systems: Influence of system parameters,” in Proc. IEEE Energy Convers. Congr. Expo, 2010, pp. 72–78.
- [14]L. Tang and B. Ooi, “Locating and isolating DC faults in multi-terminal DC systems,” IEEE Trans. Power Del., vol. 22, no. 3, pp. 1877–1884, Jul. 2007.
- [15]R. Schmerda, S. Krstic, E. Wellner, and A. Bendre, “IGCTs vs. IGBTs for circuit breakers in advanced ship electrical systems,” in Proc. IEEE Electric Ship Technol. Symp., Apr. 2009, pp. 400–405.
- [16]M. Saisho, T. Ise, and K. Tsuji, “Configuration of DC loop type quality control center,” in Proc. Power Convers. Conf., 2002, vol. 2, pp. 434–439.



ANALYSIS OF SMART METER DATA USING HADOOP

¹Balaji K. Bodkhe, ²Dr. Sanjay P. Sood

MESCOE Pune, CDAC Mohali

Email: ¹balajibodkheptu@gmail.com, ²spsood@gmail.com

Abstract— The government agencies and the large multinational companies across the world focuses on energy conservation and efficient usage of energy. The need of using energy in a efficient way is the need of developing countries like India and China .The emergence of smart grid meters gave us access to huge amount of energy consumption data. This data provided by smart meters can be used efficiently to provide insights into energy conservation measures and initiatives. Various energy distribution companies harness this data and get unpredictable results about customer’s usage pattern; they then after performing analysis predict the demand and consumption of users. This analysis helps them to decide the tariff at different point of time. The companies are trying to overcome the bottleneck in capital investment cost of data .Further, processing Big Data for chart generation and analytics is a slow process and is not fast enough to support real-time decision making. Our paper showcases a Business Intelligence tool which uses Apache Hadoop to efficiently handle the existing problems. Taking the advantage of this tool, energy distribution companies can reduce the investment by using community hardware that runs Hadoop. The usage of distributed computing tools also reduces the processing time significantly to enable real-time monitoring and decision making .This tool will also reduce carbon footprint and other related problems in energy distribution including loses and theft .In future this same analysis

can be done on other utility resources such as gas and water.

Index Terms—About four key words or phrases in alphabetical order, separated by commas.

I. INTRODUCTION

Analytics of energy consumption data to gain insights into customer usage patterns is what energy distributors are trying to achieve for several target applications such as time-of use tariff, demand response management and billing accuracy. This smart meter collects data every minute which results in generating large amount of data while the old mechanical meter collects data by hourly or monthly. This huge data storage capabilities and the complexity of data processing intelligence varies significantly with different applications. Traditional RDBMS of utility companies is a bottleneck in executing this approach. As a result, for the industry to truly benefit from the smart grid investment, it is critical that the massive amount of data made available by smart meters be handled efficiently in an organized manner that helps grid operators make timely decisions to operate grid safely, economically and reliably. Apache Hadoop is the solution available to tackle above problems which runs on commodity machines only. It is distributed computing tool which have large storage as well as processing capability.

We are using Apache Hadoop framework that allows for the distributed processing of large data sets across clusters of computers. Hadoop MapReduce is a system for parallel processing of large data sets. Traditional RDBMS or other applications are much slower and inefficient in handling big data generated by smart meters as

compared to Hadoop framework. So for the industry and customers to gain benefits like billing accuracy, energy theft detection, analyzing customer usage patterns and demand response management etc. It is always profitable to use Hadoop which runs on cheap commodity hardware.

With the evolution of smart meters for smart distribution and efficient use of energy, electricity, the generated power should be utilized properly with fair economy gains to distributors and the consumers. Thus with this focus of energy distribution in the domain of energy consumption, which will result in reduction of carbon prints, the analytics for the data received from the smart meters should be done. This massive size of analytics will need large computation which can be done with the help of distributed processing framework, Hadoop. The framework's use will provide multipurpose beneficial outputs which include: billing accuracy, time-of-use tariff plans etc. Thus this concept, smart meter data analytics, is implemented with a view of future use.

II. HADOOP

Smart meters send energy consumption data to the server at regular intervals of time which results in generating big amount of data and existing tools were not capable of handling such large amounts of data. Apache Hadoop is an open source framework for developing distributed applications that can process very large amounts of data. It is a platform that provides both distributed storage and computational capabilities.

Hadoop has two main layers:

1. Computation layer: The computation tier uses a framework called MapReduce.
2. Distributed storage layer: A distributed file system called HDFS provides storage.

Hadoop Advantages:

- Hadoop is an open source, versatile tool that provides the power of distributed computing.
- By using distributed storage & transferring code instead of data, Hadoop reduces the costly transmission step when working with large data sets to a great extent.
- Redundancy, hadoop can recover from a situation when a single node fails.

- Ease to create programs with Hadoop As it uses the MapReduce framework. You did not have to do worry about partitioning the data, determining which nodes will perform which tasks, or handling communication between nodes as it is all done by Hadoop for you.
- Hadoop leaving you free to focus on what is most important to you and your data and what you want to do with it.

Hadoop Key Features:

Distributed computing is the very vast field but following key features has made Hadoop very distinctive and attractive.

A. Accessible:

Hadoop runs on large clusters of commodity machines or on cloud computing services such as Amazon's Elastic Compute Cloud (EC2).

B. Robust:

As Hadoop is intended to run on commodity hardware, it is architected with the assumption of frequent hardware malfunctions. It can gracefully handle most such failures.

C. Scalable:

Hadoop scales linearly to handle larger data by adding more nodes to the cluster.

III. SYSTEM ARCHITECTURE

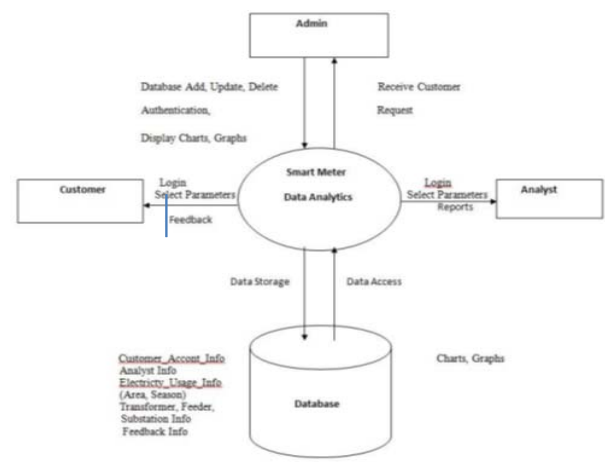


Fig. 1 System Architecture

IV. SMART METER DATA ANALYSIS

Electricity generation in India majorly depends upon the non-renewable sources [1]. Though India is rich in these resources but these resources are depleting at an alarming rate such that they will be exhausted very soon whereas

the renewable resources are not utilized to their capacity. Thus India needs to concentrate more on the renewable sources of energy such as wind energy harvesting in southern and western India where wind velocity is high.

Poor metering, power theft, lack of proper planning, overload on the resources are the few reasons to the present poor grid conditions in India. The transmission and distribution costs are so high that the government loses a lot of money on every unit of electricity sold.

Keeping all the above factors in mind the government of India has taken many steps towards the betterment and improvement of the electricity grid. Smart metering, Variable tariffs, the Electricity act 2003, etc. are some of the initiatives taken.

The Smart grid concept presented in this paper is a step by step process specially tailored to Indian conditions which when followed will lead to a very effective and well managed smart electricity grid by 2024. This will include well established production and transmission devices, smart metering, transparency in the working of the management, visual analytics for both the provider and the consumer.

Various hurdles will have to be jumped over to reach this stage the biggest one will be that of corruption, once that is overcome then rest of the problems can be collectively solved by heuristic methods. Secondly government should try and involve the IT companies into this so that experts from these companies can make necessary amendments. The top ranked colleges can be involved in this process where the students might provide some valuable insights.

To save energy, reduce cost, and increase reliability, billions of dollars are being invested by the U.S. government and private industries to build the smart grid infrastructure [2]. Higher resolution measurements are made available to more equipment at wider areas by the wide deployment of modern information technology into power grid control and communication networks.

Consider Fig.2 for example. According to this figure, data is collected by a smart meter by the minute while the data is collected hourly or monthly by an old mechanical meter; 30-60 data points are collected by a phasor measurement unit (PMU) per second which is much faster than the sampling rate of the traditional mechanical

system named supervisory control and data acquisition (SCADA) system, which is 1 data point per 1-2 second.

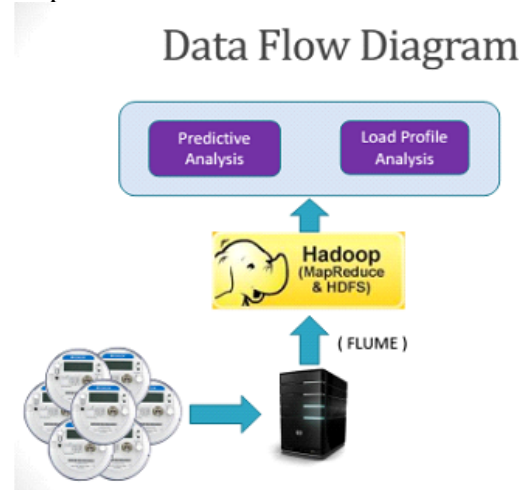


Fig.2: Data Flow Diagram

V. IMPLEMENTATION AND RESULTS

The system that we implemented is useful for both electricity providers and customers in terms of cost efficiency and analysis. Smart meters collect and send electricity consumption data at particular intervals which results in generating large amount of data. The best software that we can use for handling such big data is Hadoop. Hadoop is infrastructure developed by Apache and leading distributed computing platform. Hadoop was derived from Google's MapReduce and Google File System (GFS). Hadoop is open-source platform and works on master-slave configuration. Hadoop runs on commodity hardware.

In our implementation HDFS (Hadoop Distributed File System) acts as our database where we are going to store all the data which includes electricity consumption data, user account information.

GUI (Graphical User Interface):

Our main module is the GUI which tells entirely about the project that we have implemented. It describes different functionalities provided to user of the system. Here two types of user can gain access to the system, one is the analyst and another is consumer. Only authenticated users can be allowed to use the system. Both users can view electricity consumption data of their choice based on different given parameters (week, month etc.) available in the system. Then depending upon their selected choice, graph is

generated so that they can analyze the consumption of electricity and further achieve various objectives mentioned. Main aim of GUI is to provide flexible and efficient system to users.

ANALYSIS MODEL 1:

Module Name	Energy Consumption Prediction
Functionality	Following functionality is provided in this module 1. Can access different parameters (week, season etc.) 2. Can access graph of choice
General Workflow	Following steps are included in general workflow of module 1. Login 2. Select Parameters 3. Select Graph
Dependency	Following module on which this module is dependent Login for username and password

Table I Analysis Model 1

ANALYSIS MODEL 2:

Module Name	Drill Down
Functionality	Following functionality is provided in this module 1. Can access different parameters (week, season etc.) 2. Can access graph of choice
General Workflow	Following steps are included in general workflow of module 1. Login 2. Select Parameters 3. Select Graph
Dependency	Following module on which this module is dependent Login for username and password

Table II Analysis Model 2

CONSUMER MODEL:

Module Name	Customer
Functionality	Following functionality is

	provided in this module 1. Can access different parameters (week, season etc.) 2. Can access graph of choice
General Workflow	Following steps are included in general workflow of module 3. Login 4. Select Parameters 5. Select Graph
Dependency	Following module on which this module is dependent Login for username and password

Table III Customer Model

The fig 4 shows the comparison of energy consumption in the month of February and fig 5 shows the running hadoop job on slave 3

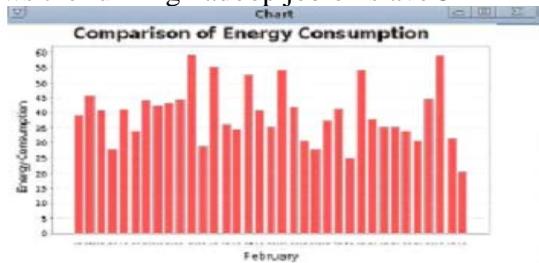


Fig. 4: Comparison of energy consumption

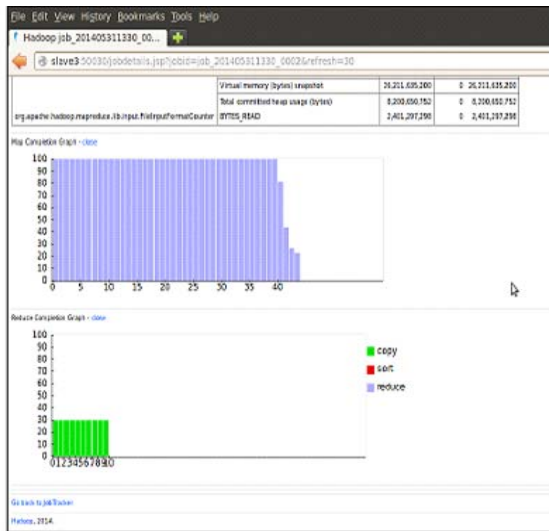


Fig. 5: Ongoing Hadoop Jobs of Slave 3

VI. CONCLUSION

To reach the 2020 energy efficiency as well as renewable energy targets and also for the future smart grids, effective use of smart metering technology is crucial. Rational energy use is a

must for a larger group of companies, municipalities and public organizations because of the gain in importance of the energy costs and environmental issues. Hence proper information about their consumption is needed by them along with and its distribution between different activities. A total picture of their energy use, potential for savings, along with costs can be given to them by smart meter data analytics, enabling effective energy management. Smart meter sends energy consumption data at small intervals resulting in generating big data. Time and storage are two important factors that affect a lot on building any application. The solution for handling such big data is Hadoop.

VII. FUTURE SCOPE

For a good understanding of how customer, environmental and structural features affect the usage, the techniques for the analysis of energy consumption data by using smart meters will be helpful. Analysis of customer behavior can be performed easily by analyzing this data which will be helpful to reduce energy consumption. A utility for better management of power outages and restoration events as well as reduction in outage duration and costs is allowed by Outage Management System (OMS). Reduced CO₂ emission is resulted by demand response because of avoided use of polluting power plant. Also, as a result, reduced peak prices are found because of avoided use of expensive peak load production. Because of customers' awareness, reduced consumption is found as a result of feedback as well as load management regarding energy consumption. Analysis of smart meter data in accordance with weather can also be performed. In India, main challenge is to install the smart meter all over the country as internet facility is still not present in most of the regions.

REFERENCES

- [1] Amir-Hamed Mohsenian-Rad, Member, IEEE, and Alberto Leon-Garcia, Fellow, IEEE, "Optimal Residential Load Control With Price Prediction in Real-Time Electricity Pricing Environments", IEEE TRANSACTIONS ON SMART GRID, VOL. 1, NO. 2, SEPTEMBER 2010
- [2] Ning Lu, Pengwei Du, Xinxin Guo, and Frank L. Greitzer , "Smart Meter Data Analysis.
- [3] Dr. Sanjay Gupta, Ashish Mohan Tiwari, Cognizant, "How to Generate Greater Value from Smart Meter Data."
- [4] Sanjay Ghemawat, Howard Gobioff, and Shun-Tak Leung Google, "The Google File System."
- [5] Amir-Hamed Mohsenian-Rad, Member, IEEE, and Alberto Leon-Garcia, Fellow, IEEE, "Optimal Residential Load Control With Price Prediction in Real-Time Electricity Pricing Environments", IEEE TRANSACTIONS ON SMART GRID, VOL. 1, NO. 2, SEPTEMBER 2010
- [6] Li Ping Qian, Member, IEEE, Ying Jun (Angela) Zhang, Senior Member, IEEE, Jianwei Huang, Senior Member, IEEE, and Yuan Wu, Member, IEEE, "Demand Response Management via Real-Time Electricity Price Control in Smart Grids", IEEE JOURNAL ON SELECTED AREAS IN COMMUNICATIONS, VOL. 31, NO. 7, JULY 2013
"SMART METER DATA ANALYTICS USING HADOOP (SMDA)"
MES COLLEGE OF ENGINEERING, PUNE 87
- [7] Giuseppe DeCandia, Deniz Hastorun, Madan Jampani, Gunavardhan Kakulapati, Avinash Lakshman, Alex Pilchin, Swaminathan Sivasubramanian, Peter Vosshall and Werner Vogels Amazon.com, "Dynamo: Amazon's Highly Available Key-value Store"
- [8] Fahad Javed, Naveed Arshad, Fredrik Wallin, Iana Vassileva , Erik Dahlquist, "Forecasting for demand response in smart grids: An analysis on use of anthropologic and structural data and short term multiple loads forecasting"
- [9] Shannon Warner, Samrat Sen, Cognizant, "How Predictive Analytics Elevate Airlines' Customer Centricity and Competitive Advantage"2, Aug. 1987, pp. 740–741 [Dig. 9th Annu. Conf. Magnetics Japan, 1982, p. 301].



AN EXPERIMENTAL WORK ON MULTI-ROLLER BURNISHING PROCESS ON ALUMINUM ALLOY

Kundan Kumar D¹, Dr. K. Eshwara Prasad²

¹Research Scholar, JNTUH R&D, JNTU Hyderabad, Telangana, India,

²Professor, Department of Mechanical Engineering, JNTU CEH, Hyderabad, Telangana, India

Email: ¹dkundankumar@gmail.com

Abstract

Burnishing is a cold working and chipless machining carried out to improve surface roughness, surface hardness, fatigue, compressive stress and corrosion resistance by using sliding speed, feed rate and depth of penetration. The process smooth out peaks valleys on the surface. This paper described the process carried out by multi-roller burnishing fitted in housing and rotated freely in a horizontal axis. The work material used was Aluminum alloy Al -4V The process produced good surface roughness and hardness at high rotation of spindle coupled with high feed rate and high depth of penetration.

Keywords: Burnishing, Plastic deformation, Surface hardness, Surface Roughness.

1. INTRODUCTION

During recent years, considerable attention are being paid to the post metal finishing operations, such as burnishing process, which improves the surface characteristics by plastic deformation.

Burnishing is a cold working process, in which the metal near a machined surface is displaced from protrusion to fill the depressions. Along with good surface roughness, the burnishing process has additional advantages over other machining processes, such as increased surface hardness, corrosion resistance, and fatigue life as result of producing compressive residual stress. Burnishing distinguishes itself from chip-forming finishing, processes such as grinding, honing, lapping and super finishing which induce residual tensile stresses at the machined

surface layer. The burnishing is a simple and cheap process, requiring little time and no skill required to operate to obtain a high quality surface finish [4]. A simple burnishing process by ball and roller are shown in the Fig. 1- (a) and (b) respectively. The burnishing process can be carried out by simple designed tool with conventional machines like lathe or vertical milling machine depending on the process.

Roller burnishing is similar to ball burnishing process where as multi hardened rollers are pressed against a surface. The pressure generated by the rollers exceeds a plastic deformation stage and create a new surface. The machined surface consists of a series of peaks and valleys of irregular heights and spacing, plastic deformation created by roller is a displacement of the material in the peaks which cold flows under pressure into the valleys. Grain size is condensed, refined and the compacted surface is smooth, hardened and layer wearing than ground or honed surfaces. It was suggested by many researchers that an improvement in wear resistance can be achieved by burnishing [5-6]. Rajasekariah and Vaidyanathan [7] studied the influence of several parameters of ball burnishing such as the diameter of the ball, feed rate, the burnishing force and the initial surface roughness on the finish, surface hardness and wear resistance of steel components.

2. EXPERIMENT DETAILS

A multi roller burnishing tool are hardened rollers fitted in a housing and are rotates freely in a horizontal axis. The rollers project by 1 mm from housing surface. The tool used have 8

rollers and as shown in the Fig.2 (a). The process of vertical roller burnishing is shown in the Fig. 2-(b). The work material used was Aluminum alloy Al-4V. Al-4V material was cut from stock of material and machined to 45 x 45 x 120 mm. The surface of the work material was skin ground to have smooth surface before burnishing. The surface roughness was measured by using Mitutoyo SJ 400 tester. The micro hardness was measured by digital micro hardness tester make – HWMMT –X3 manufactured by M/s TT unlimited INC, of Japan. The plastic deformation was measured by Scanning Electron Microscope (SEM) Joel 6380 LA. A Pinnacle vertical milling machine was used for burnishing process. Before the experiment was conducted the initial surface roughness and hardness were recorded. The initial surface roughness measured was 0.41 microns and hardness 270 HV. The operating parameters are the spindle speeds of 700, 1050, 1400 and 1750 RPM, 100, 200, 300 and 400 mm/ min as the feed rate and depth of penetration (DOP) of 0.20, 0.25, 0.30 and 0.35 mm.

3. RESULTS AND DISCUSSIONS

3.1. Surface roughness

The Fig.1 (a) and (b) show typical ball and roller burnishing process respectively. The Fig. 2 shows multi roller burnishing tool used for this experiments. The Figs. 3 to 6 show the feed rate against surface roughness for depth of penetration of 0.20, 0.25, 0.30 and 0.35 mm for various spindle rotation 700, 1050, 1400 and 1750. Hassan and Maqableh [8] have identified that reduction in the surface roughness and the increase in hardness with increase in the initial hardness of the burnished work material.

The plastic deformation of asperities depends on the normal force, and mechanical properties of the work piece materials, as well as geometric characteristics of the original asperities. The initial surface roughness before burnishing was 0.41 μm . At feed rate of 100 with DOP 0.20 mm having the spindle speed of 700, the surface roughness obtained was 0.25 μm with sudden reduction of approximately 40 % from the initial roughness value. As the depth of penetration was increased to 0.25, 0.30 and 0.35 mm for the same operating parameters, the surface roughness values are 0.17, 0.19, and 0.13 microns respectively. The reductions in percentages are 58 %, 53 % and 68 % for 0.25,

0.30 and 0.35 DOP respectively. As the DOP was increased, the deformation of material taken place and peaks and valleys were reduced. This is shown in the Fig. 3. At feed rate of 200 at spindle rotation of 1050 with DOP of 0.20, 0.25, 0.30 and 0.35 mm, the roughness values are 0.15, 0.18, 0.15 and 0.14 microns respectively. This is shown in the Fig.4. The percentage difference between 100 and 200 feed rate was 40 % 0.10 %, 21 % and 7. Figs. 5 and 6 show the roughness values at feed rate of 300 and 400 mm/min for spindle rotation of 1400 and 1750 rpm. The roughness values are 0.12, 0.13, 0.14 and 0.13 microns for feed rate 300 and for the feed rate of 400 mm/min, values are 0.12, 0.24, 0.18 and 0.18 microns. As the feed rate was increased to 400 mm/min, there was deterioration surface roughness and the deformation was ineffective. i.e. the peaks and valleys again formed. The higher the depth of penetration by the roller, the peaks and valleys reduced and better surface finish is obtained. It was not advisable to further deepen the penetration which may lead to micro-cracks on the surface which may not be seen by the naked eye. It was clear that depth of 0.20 mm is the better option to get good surface finish even though, 0.25, 0.30 and 0.35 mm DOP produced almost same effect. Consequently an indication that surface roughness started to increase. The ideal operating parameters are spindle rotation of 1400 rpm; feed rate of 300 mm/min and depth of penetration 0.20 mm.

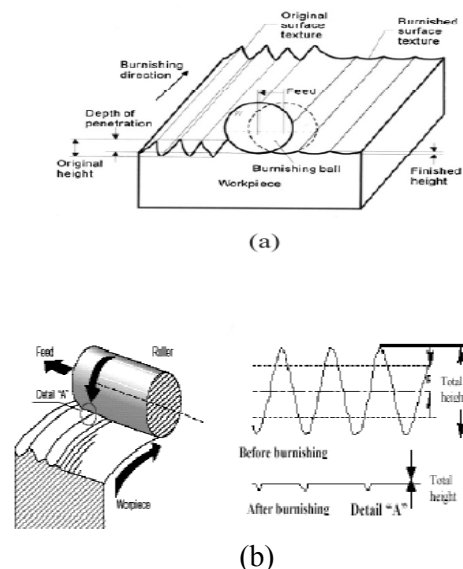


Fig.1. Schematic diagram of burnishing process – (a) ball and (b) – roller [11-12]

3.2. Surface hardness

Hassan [9] studied burnishing force or number of tool passes to certain limits increases the wear resistance of brass components under different rotating disc velocities or applied contact forces of the wear testing device. When a metal is continuously moving over a surface, plastic deformation takes place. This produces work hardening effect and produce harder surface than other surfaces. The surface hardness is directly proportional to applied force, i.e. an increase in compressive force increases surface hardness. This is due to the increase in depth of penetration, increases in metal flow that leads to an increase in the amount of deformation and voids present in the metal. When the burnishing process continued for a longer period of time, hardness of the disturbed layer of the surface increased significantly. The heat produced at the deformation zone and friction zones overheat the tool and work material [10]. The surface hardness is based on the initial surface hardness of the work materials to be burnished [11–12]. Figs. 7 to 10 show the surface hardness against depth of penetration. When a metal is continuously moving over a surface, a plastic deformation takes place. This produces work hardening effect and this surface is harder than other surface. The hardness of distributed layer increased significantly. At feed rate of 100 with DOP of 0.20, 0.25, 0.30 and 0.35 mm, the surface hardness increased 308, 375 302 and 323. Between the initial hardness and this test, the hardness values increased by 12%, 28%, 10% and 16% for DOP of 0.20, 0.25, 0.30 and 0.35 mm respectively. When the depth of penetration was 0.25 the hardness value was 375 for feed rate of 100 at 700 spindle rotation. This is shown in the Fig.8. This is similar to number of passes. It was clear that there was decrease in the surface hardness at spindle rotation of 1050 with feed rate of 200 mm/min with the same DOP as that of 100 mm/min. At feed rate of 300 with spindle rotation of 1400 rpm, the hardness values were increased to 388, 375, 360 and 350 HV.



(a)



(b)

Fig.2. Multi-roller burnishing tool and vertical roller burnishing process

This was due to initial surface hardness before burnishing. At 400 feed rate, the hardness values are 330, 355, 290 and 310 which is far below from the hardness as shown in figure 8. Any further increase in the DOP will only produce flaking effect on the surface with out any increase in hardness. This is shown in the Fig.9. From Fig. 10, it is understood that high surface hardness value was possible by 1400 spindle rotation with feed rate of 300 , m/min at DOP of 0.25 mm. Fig.11 shows the SEM view on deformation taken at spindle rotation of 1400 for feed rate of 300 with 0.2 DOP.

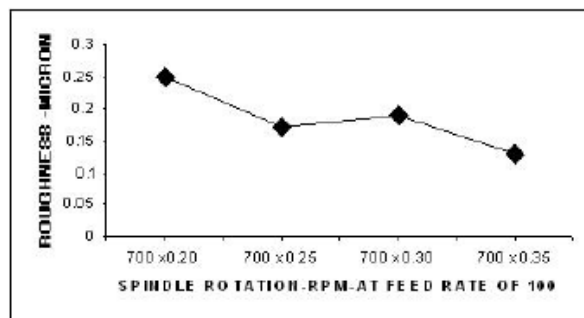


Fig.3. Feed rate Vs Roughness at 700 RPM

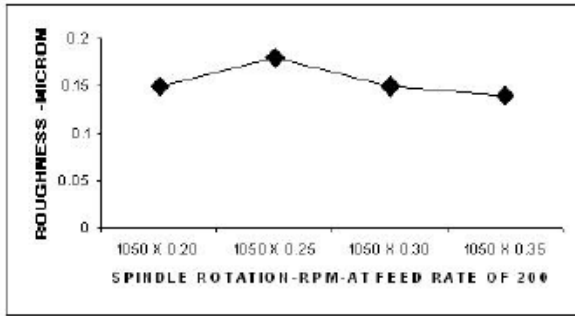


Fig.4. Feed rate Vs Roughness at 1050 RPM

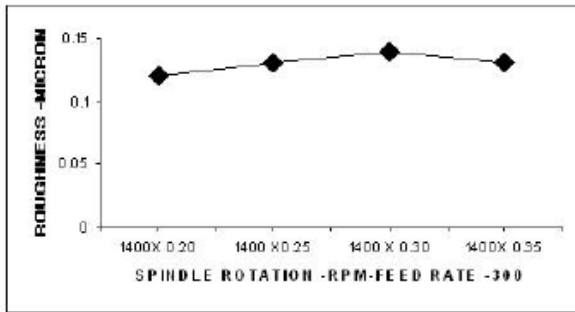


Fig.5. Feed rate Vs Roughness at 1400 RPM

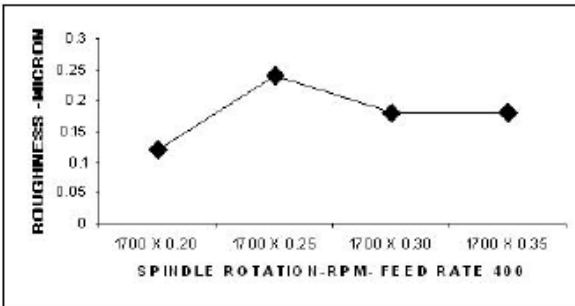


Fig.6. Feed rate Vs Roughness AT 1700 RPM

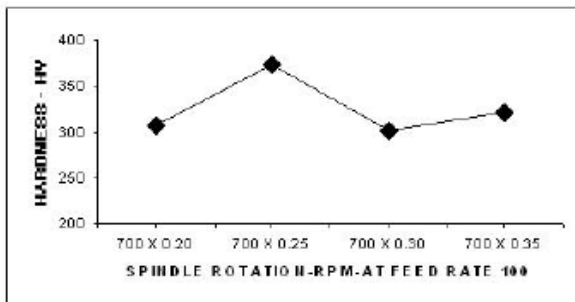


Fig.7. Feed rate Vs Hardness – 700 RPM

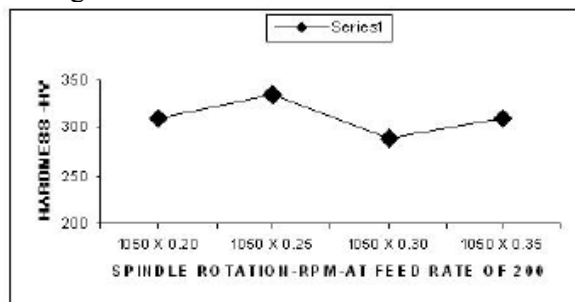


Fig.8.Feed rate Vs Hardness-1050 RPM

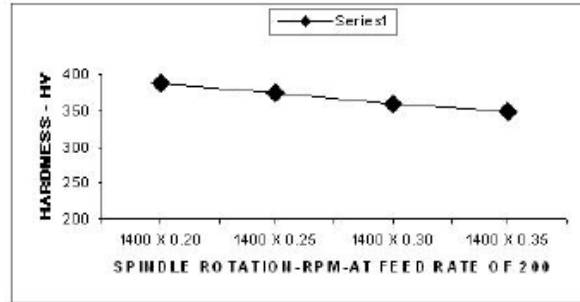


Fig.9.Feed rate Vs Hardness -1400 RPM

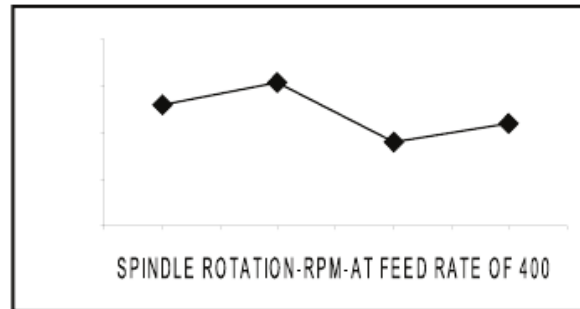


Fig.10.Feed rate Vs Hardness -1750 RPM



Fig.11.Deformation of material

4. CONCLUSION

The following conclusions were drawn from the multi-roller burnishing process on Aluminum alloy.

01. At 1400 spindle rotation with feed rate of 300 mm/min at 0.30 DOP produced low surface roughness value.
02. The depth of penetration increased the burnishing force on the surface and hardness was also increased. High surface hardness of 388 HV was obtained at 1400 spindle rotation with feed rate of 300 mm/min at depth of penetration of 0.20 mm.
03. High Depth of penetration smooth out peaks and valleys. This produced more plastic

deformation on the surface and in turn produced good surface roughness and more hardness.

REFERENCES

- [1] N.H.Loh, S.C.Tam and S.Miyazawa, A study of the effects of burnishing parameters on surface roughness using factorial design, *Journal Mech. Working Technology*, 18 (1989), 53-61.
- [2] M.H.El-Axir and Ibrahim, Some surface characteristics due to center rest ball burnishing, *Journal of Materials Processing Technology* 167(2005), 47-53.
- [3] T.Sivaprasad and Kottiveerachari, External burnishing of aluminum Components, *J.Inst.Eng. india*, 69 (1988), 55-58.
- [4] N.H.Loh, S.C.Tam and S. Miyazawa, Application of experimental design in ball burnishing, *Int. J. Mach. Tools Manuf.* 33 (1993), 841-852.
- [5] R.L. Murthy, and Kotiveerachari, Burnishing of metallic surfaces – a review, *Precision Engineering*, 3 (1981), 172-179.
- [6] M. Fattough, M.M.El-Khabeery and S.M.Serage, (1985), Residual stress distribution in burnishing solution treated and aged 7075 aluminum alloy, *International Journal of Machine Tools and Manufacture*, 29 (1) 1985 153-160.
- [7] R.Rajasekariah and S.Vaidyanathan, Increasing the wear resistance of tool components by ball burnishing, *Wear* 43 (1975) 183-188.
- [8] A.M.Hassan and A.M.Maqableh, The effect of initial burnishing parameters on non-ferrous components, *Journal of Materials Processing Technology*, 102 (200) 115-121.
- [9] A.M.Hassan, The effects of ball and roller burnishing on the surface roughness and hardness of some non-ferrous metals, *Journal of Materials Processing Technology*, 72 (1997), 385-391.
- [10] Binu C.Yeldose and Ramamoorthy, An investigation into the high performance of tin coated rollers in burnishing process, *Journal of Materials Processing Technology*, 107 (2008), 350-355.
- [11] Fang-Jung Shiou and Chih-Cheng Hsu, Surface finish of hardened and tempered stainless steel using sequential ball grinding, ball burnishing and ball polishing process on a machining centre, *Journal of Materials Processing Technology*, 205(2008),249-258
- [12] S.Thamizhmanii, B.Saparudin and S.Hasan, A study of multi - roller burnishing on non-ferrous metals, *Journal of Achievements in Mechanical and Manufacturing Engineering*, Volume 22, Issue 2, (2007), 95-98.



OPTIMIZATION OF PARAMETERS TO MINIMIZE THE SKIN FRICTION COEFFICIENT IN ABRASIVE WATER SUSPENSION JET MACHINING THROUGH TLBO

Rakesh Kumar Sahu¹, Saurabh Verma², Santosh Kumar Mishra³

^{1, 2, 3}Department of Mechanical Engineering
Bhilai Institute of Technology, Durg, India

Email: ¹rakeshkumarsahu10@rediffmail.com, ²san810@gmail.com,

Abstract

Abrasive water suspension jet (AWSJ) machining is material removal process where the material is removed by high velocity stream of water and abrasive mixture. Abrasive particles moving with the flow cause severe skin friction effect which reduces the life of nozzle for effective machining. In the present work, According to the structure of nozzle computational domain has been modeled using commercially available pre-processor routine called GAMBIT, and CFD Analysis has been performed in ANSYS (fluent) to obtain the values of SFC for different values of parameters. Based on the Analysis at the critical section of nozzle an empirical formula has been developed for SFC. TLBO algorithm has been used to optimize the parameters to minimize the SFC in AWSJ machining. To validate the result CFD Analysis has been performed to obtain the value of SFC for optimized value of parameters.

Key Words: Abrasive water suspension jet (AWSJ) machining, nozzle geometry, nozzle wear, fluid flow, MRR, Erosion rate, Teaching-Learning-Based Optimization (TLBO).

Broad Area - Mechanical Engineering.

Sub-Area - Fluid Mechanics.

1. Introduction

Abrasive water suspension jet (AWSJ) machining is a well-established non-traditional machining process which uses the principles of

both abrasive jet machining and water jet machining. AWSJ machining is a non-conventional machining process where material is removed by impact erosion of high pressure high velocity of water and entrained high velocity of grit abrasives on a work piece [8]. In abrasive water suspension jet machining process pure water (tap water) is used and for abrasive particles like sand (SiO_2), glass beads, Aluminum oxide, and silicon carbide is generally used. In AWSJ machining in which suspended abrasive particles in liquid medium called slurry is pressurized and expelled through the nozzle. Slurry is accelerated through a fine orifice to produce a high velocity stream, which is capable of machining a range of materials [2]. The rapid advances in AWSJ machining is due to high capability of the process to machine complex shapes that need to be produced from brittle and heat sensitive materials and also from the need to machine different variety of composites. One of the plaguing problems faced by AWSJ machining is nozzle wear mainly due to the suspension particles in the jet [27]. M. Hashish et al [2] experimentally investigated observations of wear of abrasive-waterjet nozzle materials and found that Tube made with tough section at the entry and a hard section at the exit has an improved wear performance. M. Nanduri et al [6] analyzed experimentally nozzle wear in abrasive waterjet machining process. The result founded in this paper is that the effect of nozzle length, inlet angle, diameter, orifice diameter, abrasive flow rate, and water pressure on nozzle

wear was studied and the nozzle wear model was developed for prediction the wear. J. John et al. [10] has done experimental work and gave strategy for the efficient and quality cutting of materials and suggest that to achieve higher efficiency and desired quality, it is required to monitor the condition of nozzles and considering the change in the dimension of orifice and focusing nozzle.

H. Liu et al. [9] carried out Computational Fluid Dynamic (CFD) analysis to study the jet dynamic characteristics of flow downstream. Kyriaki et al. [11] proposed a finite element-based model for pure waterjet process simulation and the main objective was to investigate and analyzed in detail the work piece material behavior under waterjet impingement; a non-linear FE model (using LS-DYNA 3D code) had been developed which simulates the erosion of the target material caused by the high pressure waterjet flow. The simulation model can provide a lot of results to the user and it can be useful in studying the overall waterjet process and for the optimization of the waterjet parameters. Deepak D et al. [20] analyzed the effect of inlet operating pressure on skin friction coefficient and jet exit kinetic energy in single step nozzle. It is found that an increase in inlet operating pressure causes a significant increase in skin friction coefficient and also results in proportional increase in the exit kinetic energy of the jet.

Rao et al. [23] proposed a new efficient optimization method, called ‘Teaching–Learning-Based Optimization (TLBO)’, for the optimization of mechanical design problems. This method works on the effect of influence of a teacher on learners. Pawar et al. [24] presented TLBO algorithm to find the optimal combination of process parameters for the considered machining processes. It was observed that TLBO algorithm is slightly better in terms of accuracy of solution. Rao & Patel (2012a) proposed an elitist teaching learning based optimization algorithm for solving complex constrained optimization problems. The results show that elitism consideration produces better results than without elitism consideration.

Nomenclature

d Focus tube diameter (mm)

dp Diameter of abrasive particles (μm)

D Inlet diameter of nozzle (mm)

FLift Lift force (N)

Fs External body force (N)

Fvm Virtual mass force (N)

K Momentum exchange co-efficient

l Length of flow domain (mm)

L Particle spacing (mm)

$m\dot{\square}$ Mass flow rate of mixture (m^3/s)

St Stokes number

ts system response time (s)

V Velocity of phase (m/s)

α Volume fraction of the phase

β Particulate loading

ρ Density of suspension mixture (kg/m^3)

γ Density ratio

τ_d Particle response time (s)

μ Viscosity ($\text{kg}/\text{m}\cdot\text{s}$)

Subscripts

p, q phases

l liquid phase

s solid phase

2. Theoretical formulation

2.1 Numerical Model and Assumptions

The numerical region for flow analysis is made up of flow geometry given in the Fig. 1 for the single step AWSJ nozzle. Computational domain consists of converging nozzle of diameter 4mm, nozzle length 4mm straight duct is introduced. There is a focus tube of diameter 1.3mm and length 17mm. The Abrasive water suspension mixture is let into the nozzle at the inlet and is carried down through the converging cone to the focus tube and exits as coherent jet at the nozzle exit, in which the focus tube is used for stabilizing the flow.

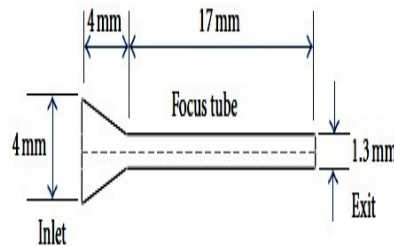


Fig.1: Computational domain of single step nozzle according to Deepak et al. [20].

The numerical model adopted closely follows the work of G.Hu et al [4] in which liquid solid two-phase flow is considered and the following assumptions are valid for the present work.

- I. The primary liquid phase is continuous and incompressible.
- II. Flow is taken to be two-phase flow in which the primary liquid phase mixes homogeneously with the particles of equal diameter, constituting the solid phase.
- III. Two-phase flow assumed is steady and characterized by turbulent flow.

The average distance between the individual particles (particle size $d_p=63\mu\text{m}$) of the particulate phase is

$$L=1.7925 \times d_p = 1.7925 \times 0.063 = 0.1129\text{mm}$$

Estimating the value of the stokes number helps to select the most appropriate multiphase model. The stokes number is defined as the ratio of the particle response time to the system response time is calculated below.

$$\tau_d = \frac{\rho_d d^2 p}{18\mu_t} = \frac{2300x(63x10^{-6})^2}{18x0.001004} = 5.05123x10^{-4}$$

(7)

$$t_s = \frac{l}{v} = \frac{0.0364}{25.6} = 1.4218x10^{-3} \quad (8)$$

$$S_t = \frac{\tau_d}{t_s} = \frac{5.05129x10^{-4}}{1.4218x10^{-3}} = 0.3552 \quad (9)$$

For silicon carbide abrasive:

$$\gamma = \frac{\rho_s}{\rho_l} = \frac{3170}{998} = 3.18 \quad (10)$$

$$k = \frac{\beta}{\gamma} = \frac{0.318}{3.18} = 0.1 \quad (11)$$

$$L = 1.7925 \times 0.063 = 0.1129\text{mm}$$

$$\tau_d = \frac{\rho_d d^2 p}{18\mu_t} = \frac{3170x(63x10^{-6})^2}{18x0.001004} = 6.96200x10^{-4}$$

(12)

$$t_s = \frac{l}{v} = \frac{0.0364}{25.6} = 1.4218x10^{-3} \quad (13)$$

$$S_t = \frac{\tau_d}{t_s} = \frac{5.05129x10^{-4}}{1.4218x10^{-3}} = 0.3551 \quad (14)$$

For Aluminum oxide abrasive:

$$\gamma = \frac{\rho_s}{\rho_l} = \frac{2719}{998} = 2.72 \quad (15)$$

$$k = \frac{\beta}{\gamma} = \frac{0.272}{2.72} = 0.1 \quad (16)$$

$$\frac{L}{d_p} = \left(\frac{\pi}{6} \frac{1+k}{k}\right)^{\frac{1}{3}} = \left(\frac{\pi}{6} \frac{1+0.1}{0.1}\right)^{\frac{1}{3}} = 1.7925 \quad (17)$$

$$L = 1.7925 \times 0.063 = 0.1129\text{mm}$$

$$\tau_d = \frac{\rho_d d^2 p}{18\mu_t} = \frac{2719x(63x10^{-6})^2}{18x0.001004} = 5.97151x10^{-4}$$

(18)

$$t_s = \frac{l}{v} = \frac{0.0364}{25.6} = 1.4218x10^{-3} \quad (19)$$

2.2 The computation of particulate loading and stokes number

Particulate loading and the stokes number are important parameters that help to identify the appropriate multiphase model. Particulate loading has a major impact on phase interactions and is defined as the mass density ratio of the dispersed phase to that of the carrier phase.

The particulate loading for garnet abrasive is

$$\beta = \frac{\alpha_s \rho_s}{\alpha_l \rho_l} = \frac{0.1x2300}{998} = 0.230 \quad (1)$$

For silicon carbide abrasive is

$$\beta = \frac{\alpha_s \rho_s}{\alpha_l \rho_l} = \frac{0.1x3170}{998} = 0.318 \quad (2)$$

For aluminum oxide abrasive is

$$\beta = \frac{\alpha_s \rho_s}{\alpha_l \rho_l} = \frac{0.1x2719}{998} = 0.27 \quad (3)$$

The degree of interaction between the phases is intermediate loading, the coupling is two-way i.e., the fluid carrier influences the particulate phase via drag and turbulence, but the particles in turn influence the carrier fluid via reduction in mean momentum and turbulence. All multiphase models can handle this type of problem but it is found that the Eulerian multiphase model seems to be the most accurate one. The average distance between the individual particles of the particulate phase can be estimated by equation developed by Crowe et al (2009).

For garnet abrasive:

$$\gamma = \frac{\rho_s}{\rho_l} = \frac{2300}{998} = 2.3 \quad (4)$$

$$k = \frac{\beta}{\gamma} = \frac{0.230}{2.30} = 0.100 \quad (5)$$

$$\frac{L}{d_p} = \left(\frac{\pi}{6} \frac{1+k}{k}\right)^{\frac{1}{3}} = \left(\frac{\pi}{6} \frac{1+0.10}{0.10}\right)^{\frac{1}{3}} = 1.7925 \quad (6)$$

$$S_t = \frac{\tau_d}{t_s} = \frac{5.05129 \times 10^{-4}}{1.4218 \times 10^{-3}} = 0.3552 \quad (20)$$

For Stokes number less than unity, particles will closely follow the fluid flow and any one of the three multiphase models namely Volume of fluid model, Mixture model or Eulerian multiphase model is applicable. Also from the calculation of the effect of particulate loading it is clear that coupling between two phases is intermediate. Hence present numerical simulation is carried using Eulerian multiphase model which through is most expensive in computation, but gives most accurate results. Eulerian Multiphase model is embedded in fluent software. Fluent solves a multi-fluid granular model to describe the flow behavior of fluid solid mixture. The stresses induced in the solid phase are deduced through an analogy between the random particle motion arising from particle to particle collisions and the thermal gradient of molecules in the fluid stream taking into effect the inelasticity of the granular phase. Intensity of the particle velocity fluctuations determines the stresses, viscosity and pressure of the solid phase.

The governing equations for mass and momentum conservation are solved for the steady incompressible flow. The coupling between velocity and pressure has been attempted through the phase couples SIMPLE algorithm developed by Patankar S.V. using the power law scheme for the solution. The turbulence is modeled using Realizable k-ε turbulence model. The governing partial differential equations, for mass and momentum conservations are detailed below.

Continuity Equation:

$$\frac{1}{\rho_{pq}} \left[\frac{\partial}{\partial t} (\alpha_q \rho_q) + \nabla \cdot (\alpha_q \rho_q v_q) \right] = \sum_{p=1}^N (m_{pq} - m_{qp}) \quad (21)$$

Where p,q phases, α_q = vol.fraction of the secondary phase, ρ_{pq} = density of suspended mixture(kg/m³), v= velocity, m= mass flow rate, N= lift force

Fluid-solid Momentum Equation:

The conservation of momentum equation for the solid phase is as follows:

$$\frac{\partial}{\partial t} (\alpha_s \rho_s v_s) + \nabla \cdot (\alpha_s \rho_s v_s^2) = -\alpha_s \nabla p - \nabla p_s + \nabla \cdot \tau_s + \alpha_s \rho_s g + \sum_{l=1}^N [k_{ls} (v_l - v_s) + (m_{ls} v_{ls} - m_{sl} v_{sl})] + (F_s + F_{lift,s} + F_{vm,s}) \quad (22)$$

Where α_s =vol. fraction of solid phase, ρ_s = density of the solid phase, v_s =velocity of the solid phase, τ_s = particle response time, l= length of flow domain (mm), F_s =external body force, $F_{vm,s}$ =virtual mass force of solid phase, F_{lift} = lift force of solid phase, m = mass flow rate, K= momentum exchange coefficient

The conservation of momentum equation for the fluid phase is as follows.

$$\frac{\partial}{\partial t} (\alpha_q \rho_q v_q) + \nabla \cdot (\alpha_q \rho_q v_q^2) = -\alpha_q \nabla p + \nabla \cdot \tau_q + \alpha_q \rho_q g + \sum_{l=1}^N [k_{pq} (v_p - v_q) + (m_{pq} v_{pq} - m_{qp} v_{qp})] + (F_q + F_{lift,q} + F_{vm,q}) \quad (23)$$

2.3 Numerical Scheme

Computational domain is modeled using commercially available pre-processor routine called GAMBIT, and meshing is carried out using grid cells of 30000 control volumes. According to the structure of nozzle computational domain is built axi-symmetric model shown in figure 2.

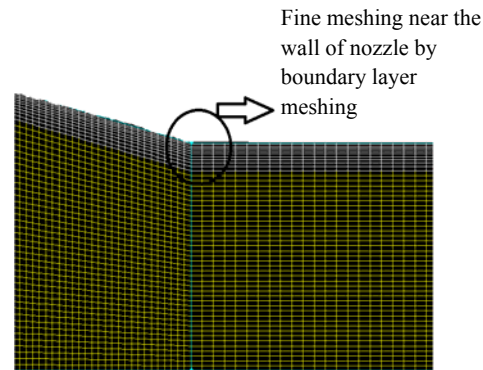


Fig. 2 A meshed domains near the wall of nozzle

2.4 Boundary Condition and Operating Parameters

Suitable boundary conditions are imposed on the computational domain, as per the physics of the problem. Inlet boundary condition is specified by the operating pressure entering the nozzle. It is assumed that velocity at inlet is uniform across

the cross section. At the exit, static pressure of refluxing flow is taken to be zero (gauge), so that the computation would proceed by the relative pressure difference across the grid volumes for the entire domain of the flow. Wall boundary conditions are impressed to bound fluid and solid regions. In viscous flow models, as in the present case velocity components at the wall are set to zero in according with the no-slip and impermeability conditions that exist on the wall boundary. The axis of the nozzle is used to solve the computational domain as axis-symmetric problem and suitable boundary conditions are imposed for the same i.e., the gradient of fluid properties are set to zero across the axis line. In the present numerical simulation suspended liquid is treated as primary phase and abrasive is treated as secondary phase.

2.5 Validation of the Numerical Model

The present model is benchmarked against the numerical work according to Deepak et al. (2012) cited in [20]. The graph of the velocity distribution of one of the phases (liquid phase) has been calibrated in the present work as shown in Fig.4 with that of the work cited in the literature according to Deepak et al. (2012) as shown in Fig.3. According to fig.3 and fig.4 in both figure Velocity magnitude first increases length along the nozzle then the velocity is constant. It is clear that there is good agreement between the two models as regards to the velocity distribution.

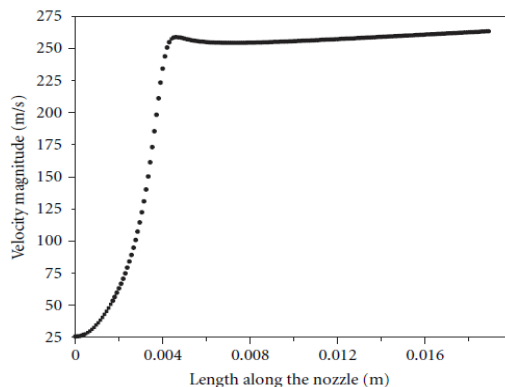


Fig. 3: The velocity distribution along the length of the single step nozzle as given in reference literature [20].

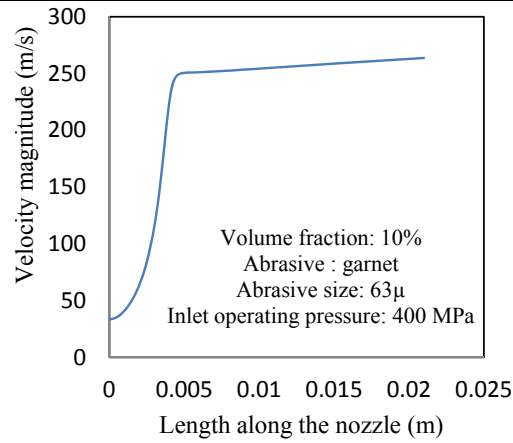


Fig. 4: The velocity distribution along the length of the single step nozzle as per the present model.

3. Method of solution

3.1 CFD Analysis of nozzle for different geometry models

CFD Analysis has performed in ANSYS (fluent) 14.0 to obtain values of SFC for various sets of parameters (Table 2). Range has been selected as given in Table 1.

Table 1

Parameters	Range	Units	Typical values
P (Inlet Operating Pressure)	100- 400	Bar	400
D (Nozzle diameter)	3.50 - 4.50	mm	4.2
d (orifice diameter)	1 -1.5	mm	1.0
ρ (density of Abrasive Particle)	2300- 3170	kg/m ³	2300
L (focus length)	17-18.2	Mm	17.0

Table 2

P (Bar)	D (mm)	d (mm)	ρ (kg/m ³)	L (mm)	SFC
100	4.2	1.00	2300	17.0	0.0012314
200	4.2	1.00	2300	17.0	0.0023365
300	4.2	1.00	2300	17.0	0.0033984
400	4.2	1.00	2300	17.0	0.0044333
400	3.5	1.00	2300	17.0	0.0041870
400	3.8	1.00	2300	17.0	0.0043370
400	4.2	1.00	2300	17.0	0.0045268
400	4.5	1.00	2300	17.0	0.0046625
400	4.2	1.00	2300	17.0	0.0044333
400	4.2	1.25	2300	17.0	0.0040493
400	4.2	1.35	2300	17.0	0.0039247
400	4.2	1.50	2300	17.0	0.0037604

Optimization Of Parameters To Minimize The Skin Friction Coefficient In Abrasive Water Suspension Jet Machining Through TLBO

400	4.2	1.00	2300	17.0	0.0044333
400	4.2	1.00	2600	17.0	0.0042512
400	4.2	1.00	2900	17.0	0.0040954
400	4.2	1.00	3170	17.0	0.0039726
400	4.2	1.00	2300	17.0	0.0044333
400	4.2	1.00	2300	17.5	0.0043477
400	4.2	1.00	2300	18.0	0.0042657
400	4.2	1.00	2300	18.2	0.0041870

3.2 Based on the Analysis development of Empirical Relation for nozzle geometry

Based on the Analysis at the critical section of nozzle an empirical formula developed for the Range as given in Table 1.

$$\text{Skin friction coefficient} = \frac{K (P)^{0.924} (D)^{0.428}}{(d)^{0.206} (\rho)^{0.342} (L)^{0.838}} \quad (24)$$

Where $K = 1.027 \times 10^{-5} = \frac{mm^2}{kgN}$

3.3 Teaching-learning-based optimization algorithm

Teaching-Learning based Optimization (TLBO) algorithm is a global optimization method originally developed by Rao et al. [23]. TLBO is an optimization algorithm based on teaching and learning process in a classroom. The searching process consists of two phase, i.e. Teacher phase and Learner Phase. In teacher phase, learners first get knowledge from a teacher and then from other classmates in learner phase. In the entire population, the best solution is considered as the teacher (Xteacher). On the other hand, learners seek knowledge from the teacher in the teacher phase. In this phase, the teacher tries to improvise the results of other individuals (Xi) by increasing the mean results of the classroom (Xmean) towards his/her position Xteacher. In order to maintain uncertain features of the search, two randomly-generated parameters r and Tf are applied in update formula for the solution Xi as:

$$X_{new} = X_i + r(X_{teacher} - T_f * X_{mean})$$

Where r is a randomly selected number in the range of 0 and 1 and Tf is a teaching factor which can be either 1 or 2:

$$T_f = \text{round} [1 + \text{rand}(0,1)\{2-1\}]$$

Moreover, Xnew and Xi are the new and existing solution of i.

In the learner phase, the learner attempt to increase their information by interacting with other learners. Therefore, an individual learns new knowledge if the other individuals have more knowledge compared to the other learner. Throughout this phase, the student Xi interacts randomly with another student Xj (where i ≠ j) in order to improve his/her knowledge. In the case that if Xj is better than Xi (then f(Xj) < f(Xi) for minimization problem), Xi is moved towards Xj. Otherwise it is moved away from Xj :

$$X_{new} = X_i + r.(X_j - X_i) \text{ if } f(X_i) > f(X_j)$$

$$X_{new} = X_i + r.(X_i - X_j) \text{ if } f(X_i) < f(X_j)$$

If the solution Xnew is better, it is accepted in the population. The algorithm will continue until the termination condition is met.

3.4 Optimization of parameters of SFC through TLBO

Optimization performance of TLBO is determined by the Analyzed data and mathematical modeling as considered here..A computer code is developed using MATLAB R2013a for the parametric optimization in AWSJ machining process considering the Population size 12 and Objective of using TLBO is to minimize the SFC given by the eq. 24.

Generation – 1

Table 3: Initial Population

P (Bar)	D (mm)	d (mm)	ρ (kg/m³)	L (mm)	SFC
200	3.8	1.20	2500	17.4	0.0021
240	4.2	1.30	2600	17.5	0.0025
280	3.8	1.40	2700	17.6	0.0027
320	4.2	1.25	2800	17.7	0.0032
360	3.8	1.35	2900	17.8	0.0033
230	4.2	1.45	3000	17.9	0.0022
370	3.8	1.20	2400	17.9	0.0037
350	4.2	1.30	2470	17.8	0.0036
300	3.8	1.40	2550	17.7	0.0029
180	4.2	1.25	2630	17.6	0.0019
250	3.8	1.35	2750	17.5	0.0024
300	4.2	1.40	2850	17.4	0.0030

Optimization Of Parameters To Minimize The Skin Friction Coefficient In Abrasive Water Suspension Jet Machining Through TLBO

Table 4: Teacher Phase

P _{new} (Bar)	D _{new} (mm)	d _{new} (mm)	ρ _{new} (kg/m ³)	L _{new} (mm)	SFC _{new}
135.95	3.906	1.1695	2474	17.3685	0.0015
175.95	4.306	1.2695	2574	17.4685	0.0019
215.95	3.906	1.3695	2674	17.5685	0.0022
255.95	4.306	1.2195	2774	17.6685	0.0026
295.95	3.906	1.3195	2874	17.7685	0.0028
165.95	4.306	1.4195	2974	17.8685	0.0017
305.95	3.906	1.1695	2374	17.8685	0.0031
285.95	4.306	1.2695	2444	17.7685	0.0030
235.95	3.906	1.3695	2524	17.6685	0.0024
115.95	4.306	1.2195	2604	17.5685	0.0013
185.95	3.906	1.3195	2724	17.4685	0.0019
235.95	4.306	1.3695	2824	17.3685	0.0024

Table 6: Modified value after learner phase

P _{mod} (Bar)	D _{mod} (mm)	d _{mod} (mm)	ρ _{mod} (kg/m ³)	L _{mod} (mm)	SFC _{mod}
123.350	4.1180	1.1910	2543	17.4945	0.0014
138.150	4.3060	1.2480	2590	17.5315	0.0015
152.950	4.1180	1.3050	2637	17.5685	0.0016
152.950	4.1180	1.3050	2637	17.5685	0.0018
182.550	4.1180	1.2765	2731	17.6425	0.0019
134.450	4.3060	1.3335	2778	17.6795	0.0014
186.250	4.1180	1.1910	2496	17.6795	0.0020
178.850	4.3060	1.2480	2529	17.6425	0.0019
160.350	4.1180	1.3050	2566	17.6055	0.0017
115.950	4.3060	1.2195	2604	17.5685	0.0013
141.850	4.1180	1.2765	2660	17.5315	0.0015
160.350	4.3060	1.3050	2707	17.4945	0.0017

Table 4: Modified value after teacher phase

P _{mod} (Bar)	D _{mod} (mm)	d _{mod} (mm)	ρ _{mod} (kg/m ³)	L _{mod} (mm)	SFC _{mod}
135.950	3.9060	1.1695	2474	17.3685	0.0015
175.950	4.3060	1.2695	2574	17.4685	0.0019
215.950	3.9060	1.3695	2674	17.5685	0.0022
255.950	4.3060	1.2195	2774	17.6685	0.0026
295.950	3.9060	1.3195	2874	17.7685	0.0028
165.950	4.3060	1.4195	2974	17.8685	0.0017
305.950	3.9060	1.1695	2374	17.8685	0.0031
285.950	4.3060	1.2695	2444	17.7685	0.0030
235.950	3.9060	1.3695	2524	17.6685	0.0024
115.950	4.3060	1.2195	2604	17.5685	0.0013
185.950	3.9060	1.3195	2724	17.4685	0.0019
235.950	4.3060	1.3695	2824	17.3685	0.0024

Generation – 2

Modified values after learner phase of First generation are taken as Initial population for the Second generation and then same operations are performed and the best set of solution of optimum values of parameters for minimum value of SFC after second generation is given in the Table no. 8.

Table 8: Modified value after learner phase

P _{mod} (Bar)	D _{mod} (mm)	d _{mod} (mm)	ρ _{mod} (kg/m ³)	L _{mod} (mm)	SFC _{mod}
105.90 5	4.264 5	1.203 1	2555	17.498 5	0.00119 7

Table 5: Learner phase

P _{nbest} (Bar)	D _{nbest} (mm)	d _{nbest} (mm)	ρ _{nbest} (kg/m ³)	L _{nbest} (mm)	SFC _{nbest}
123.35	4.1180	1.1910	2543	17.4945	0.0014
138.15	4.3060	1.2480	2590	17.5315	0.0015
152.95	4.1180	1.3050	2637	17.5685	0.0016
152.95	4.1180	1.3050	2637	17.5685	0.0018
182.55	4.1180	1.2765	2731	17.6425	0.0019
134.45	4.3060	1.3335	2778	17.6795	0.0014
186.25	4.1180	1.1910	2496	17.6795	0.0020
178.85	4.3060	1.2480	2529	17.6425	0.0019
160.35	4.1180	1.3050	2566	17.6055	0.0017
27.750	4.3060	1.2195	2514	17.5055	0.0004
141.85	4.1180	1.2765	2660	17.5315	0.0015
160.35	4.3060	1.3050	2707	17.4945	0.0017

4. RESULT AND DISCUSSION

Optimized values of parameters for minimum SFC are:

Inlet Operating Pressure	105.95
Bar	
Nozzle diameter	4.2645
mm	
Orifice diameter	1.2031
mm	
Density of Abrasive article	2555 kg/m ³
Focus length	17.4985 mm

The minimum value of SFC for optimized value of parameters is 0.001197.

4.1 Confirmation Analysis for optimum value

The confirmation analysis has performed at optimum value of parameters using commercially available pre-processor routine called GAMBIT. CFD Analysis has performed to obtain the value of SFC for optimized set of parameters and the Analyzed value of SFC is 0.001127 and it is closer to the predicted value.

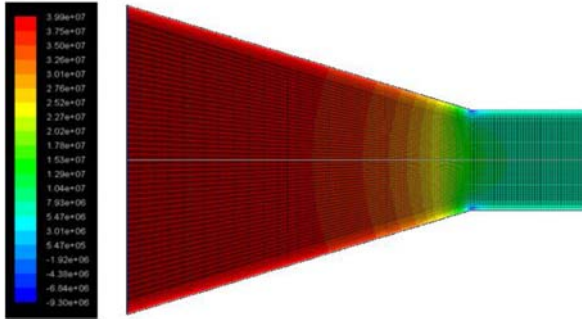


Fig. 5: Contours of static pressure (mixture) (Pascal) as per the present model.

5. CONCLUSION

The optimized value of SFC through TLBO is 0.001197 and it is closer to Analyzed value of SFC. In the present work, According to the structure of nozzle computational domain has been modeled using commercially available pre-processor routine called GAMBIT, and CFD Analysis has been performed in ANSYS (fluent) to obtain the values of SFC for different values of parameters. Based on the Analysis at the critical section of nozzle an empirical formula has been developed for nozzle geometry. TLBO algorithm has been used to optimize the parameters to minimize the SFC in AWSJ machining. To confirm the result CFD Analysis has been performed to obtain the value of SFC for optimized value of parameters.

References

- [1] N. C. Markatos, "Modelling of two-phase transient flow and combustion of granular propellants." *International Journal of Multiphase flow*, vol. 12, no. 6, pp. 913-933, 1986.
- [2] M. Hashish, Observation of wear of abrasive-waterjet nozzle materials, *Journal of Tribology* 116 (1994) 439-444.
- [3] Fluent User's Guide, vol. 3, Fluent Incorporated Publishers, Lebanon, 1998.
- [4] G. Hu, W. Zhu, T. Yu, and J. Yuan, "Numerical simulation and experimental study of liquid-solid two-phase flow in nozzle of DIA jet", *Proceedings of the IEEE International conference industrial informatics (INDIN 2008)*, Daejeon, Korea, July 13-16th 2008
- [5] G. J. Brown, "Erosion prediction in slurry pipeline teejunctions," *Applied Mathematical Modelling*, vol. 26, no. 2, pp. 155-170, 2002.
- [6] Nanduri M, Taggart DG, Kim TJ (2002), The effects of system and geometric parameters on abrasive waterjet nozzle wear. *Int J Mach Tools Manuf* 42: 615-623.
- [7] J. Chahed, V. Roig, and L. Masbersnat, "Eulerian-eulerian two-fluid model for turbulent gas-liquid bubbly flows," *International Journal of Multiphase Flow*, vol. 29, no. 1, pp. 23-49, 2003.
- [8] P.K. Mishra; Non-conventional machining, Narosa publishing house, Third reprint- 2005.
- [9] H. Liu, J. Wang, N. Kelson, R. Brown, A study of abrasive waterjet characteristics by CFD simulation, *Journal of Materials Processing Technology* 153-154 (2004) 488-493.
- [10] J. John RozarioJegaraj, N. Ramesh Babu, A strategy for efficient and quality cutting of material with abrasive waterjets considering the variation in orifice and focusing nozzle diameter, *Int. J. Mach. Tools Manuf.* 45 (12-13) (2005) 1443-1450.
- [11] K. Maniadaki, T. Kestis, N. Bilalis, A. Antoniadis, A finite element-based model for pure water-jet process simulation, *Int. J. Adv Manuf. Technol.* (2007) 31: 933-940.
- [12] B. S. Nie, J. Q. Meng, and Z. F. Ji, "Numerical simulation on flow field of pre-mixed abrasive water jet nozzle," in *Proceedings of the Asia Simulation-7th International Conference on System*

- Simulation and Scientific Computing (ICSC '08)*, pp.247–251, October 2008.
- [13] D. S. Srinivasu, N. Ramesh Babu, A neuro-genetic approach for selection of process parameters in abrasive waterjet cutting considering variation in diameter of focusing nozzle, in *applied soft computing* 8 (2008) 809-819.
- [14] T. Nguyen, D.K. Shanmugam, and J. Wang, “Effect of liquid properties on the stability of an abrasive waterjet” *International Journal of Machine Tools and Manufacture*, vol, 48, no. 10, pp.1138-1147, 2008.
- [15] H.Z. Li, J. Wang, J.M. Fan, Analysis and modeling of particle velocities in micro-abrasive air jet, *International Journals of Machine Tools & Manufacture* 49 (2009) 850-858.
- [16] N. Pi and N. Q. Tuan, “A study on nozzle wear modeling in abrasive waterjet cutting,” *advanced Materials Research*, vol.76, pp. 345–350, 2009.
- [17] M.G. Mostofa, K. Yong Kil, A. J. Hwan, computational fluid analysis of abrasive waterjet cutting head, *Journal of Mechanical Science and Technology* 24 (2010) 249-252.
- [18] M. Zohoor, S.HadiNourian, Development of an algorithm for optimum control process to compensate the nozzle wear effect in cutting the hard and tough material abrasive water jet cutting process, *Int. J AdvManufTechnol* (2012) 61:1019-1028.
- [19] Help documentation of ‘GAMBIT 2.3.16’ Software.
- [20] D. Deepak, D. Anjaiah D, K. VasuudevaKaranth, and N. Yagnesh Sharma, CFD Simulation of flow in an Abrasive Water Suspension Jet: The Effect of Inlet Operating Pressure and Volume Fraction on Skin Friction and Exit Kinetic Energy, *Hindawi Publishing Corporation, Advance in Mechanical Engineering, Volume 2012, Article ID 186430*.
- [21] Help documentation of ‘Fluent 6.3.26’ Software
- [22] S. Anwar, D. Axinte and A.A Becker, Finite element modelling of abrasive waterjet milled footprints Faculty of Engineering, Department of Mechanical, Materials and Manufacturing Engineering, University of Nottingham, NG7 2RD, UK, Volume 213, Issue 2, February 2013, Pages 180–193.
- [23] Rao, R.V., Savsani, V.J. & Vakharia, D.P. (2011). Teaching-learning-based optimization: A novel method for constrained mechanical design optimization problems. *Computer-Aided Design*, 43 (3), 303-315.
- [24] Rao, R.V., Pawar, P.J. and Shankar, R., 2008. Multi-objective optimization of electrochemical machining process parameters using a particle swarm optimization algorithm. *Proceedings of the Institution of Mechanical Engineers, Journal of Engineering Manufacture*, 222, 949–958.
- [25] MATLAB, user manual of MATLAB (2013).
- [26] U. Anand and J. Katz, “Prevention of nozzle wears abrasive water suspension jet (AWSJ) using porous lubricated nozzle, “*Journal of Tribology*, vol.125, no.1, pp.168-180,2003.
- [27] Deepak. D, Anjaiah D and Yagnesh Sharma, “Numerical analysis of flow through abrasive water suspension jet: the effect of abrasive grain size and jet diameter ratio on wall shear”, *International Journal of Earth Sciences and Engineering*, Vol. 04, no 04 spl, pp. 78-83, ISSN 0974-5904.
- [28] Rao, R.V., & Patel, V. (2012). An elitist teaching-learning-based optimization algorithm for solving complex constrained optimization problems. *International Journal of Industrial Engineering Computations*, 3(4), 535-560.
- [29] M. J. Steinkamp, T. T. Clark, and F. H. Harlow, “Two-point description of two-fluid turbulent mixing-II. Numerical solutions and comparisons with experiments,” *International Journal of Multiphase Flow*, vol. 25, no. 4, pp. 639–682, 1999.



A REBROADCAST ROUTE DISCOVERY IN MANET FOR REDUCING ROUTING OVERHEAD

¹Mr. Prasad R. Patil, ²Prof. R.S.Nipanikar

¹PG Scholar, ²Assistant Professor, E&TC Engineering, PVPIT Pune,
Savitribai Phule Pune University, Pune, India

Email:¹prasad.patil201@gmail.com, ²rohiniipanikar@gmail.com

Abstract- Due to no infrastructure in MANET, there are frequent link breakages which lead to frequent path failures and route discoveries. Because it does not have a route to the destination a mobile node blindly rebroadcasts the first received route request packets, and thus it causes the broadcast storm problem. So, the rebroadcast is very costly and requires too much network resource. In the existing AD-hoc On-demand Distance Vector Routing System, a broadcasting technique is used in which the receiver node blindly rebroadcast the first received route request (RREQ) packet unless it has route to the destination. This mechanism incur retransmission which causes overhead and decrease the packet delivery ratio and increase the end-to-end delay, which cannot be avoided.

In this paper we proposed a protocol for reducing routing overhead in mobile ad hoc network using Neighbor knowledge. In this we have proposed a additional coverage ratio and connectivity factor. This approach can significantly decrease the routing overhead by decreasing the number of retransmission and improvement in routing performance.

Keywords- AODV, MANET, RREP, RREQ

I. INTRODUCTION

During route discovery traditional on-demand routing protocols produce a large amount of routing traffic by blindly flooding the entire network with RREQ packet which causes routing overhead. In this protocol we have proposed a technique which reduces end to end

delay and improves packet delivery ratio.

For this, we are finding the rebroadcast delay and uncovered neighbours set. Which include following methodology:

After receiving RREQ packet from its previous node, it can use the list of neighbours in the RREQ packet to estimate how many its neighbours have not been covered by the RREQ packet from previous node. If node has more neighbours uncovered by the RREQ packet from previous node, which means that if node rebroadcasts the RREQ packet, the RREQ packet can reach more additional neighbour nodes. For this, we define the UnCovered Neighbours (UCN) set of node. The rebroadcast delay is to determine the forwarding order. The node which has more common neighbours with the previous node has the lower delay. If this node rebroadcasts a packet, then more common neighbours will know this fact. Therefore, this rebroadcast delay enables the information that the nodes have transmitted the packet spread to more neighbours, which is the key to success for the proposed scheme.

II. RELATED WORK

Broadcasting is very effective mechanism in route discovery, but there is a routing overhead associated with the broadcasting can be very large, in high dynamic networks [7]. Ni et al. [5] showed that after the study of broadcasting protocol the rebroadcasting consumes large network resource and is costly too. Because of large routing overhead in broadcasting which causes problems like redundant retransmissions,

contentions, and collisions [5]. Therefore, optimizing the broadcasting in route discovery is an effective solution to improve the packet delivery and to reduce end-to-end delay and hence to improve the routing performance.

Each node forwards a packet with a probability in gossip based approach proposed by Haas et al.[9]. They showed that gossip-based approach can save overhead compared to the flooding. But, as the network density is high or the traffic load is heavy, the improvement in the gossip-based approach is limited [8]. A probabilistic broadcasting scheme based on coverage area and neighbour confirmation is proposed by Kim et al. [7] which uses the coverage area to set the rebroadcast probability, and also uses the neighbour confirmation to guarantee reach ability. SBA is proposed by Peng and Lu [10] which is nothing but Scalable Broadcast Algorithm (SBA) which determines the rebroadcast of a packet according to the fact whether this rebroadcast would reach additional nodes.

Based on neighbour coverage Dynamic Probabilistic Route Discovery (DPR) proposed by Abdulai et al. [11]. In which a forwarding probability is determined by each node according to the number of its neighbours and the set of neighbours which are covered by the previous broadcast. This DPR scheme only considers the coverage ratio by the previous node and does not consider the neighbours receiving the duplicate RREQ packet. Hence, there is a room of further optimization and extension for the DPR protocol. In recent years there are many robust protocols have been proposed besides the above optimization issues for broadcasting. Chen et al. [12] proposed an AODV protocol with Directional Forward Routing (AODV-DFR) which considers the directional forwarding used in geographic routing into AODV protocol. While a route breaks, for packet forwarding this protocol can automatically find the next-hop node.

Keshavarz-Haddad et al. [13] proposed two deterministic timer-based broadcast schemes namely Dynamic Reflector Broadcast (DRB) and Dynamic Connector-Connector Broadcast (DCCB). They showed that these schemes can achieve full reach ability over an idealistic lossless MAC layer, and their schemes are robustness for the situation of node failure and

mobility. Stann et al. [14] proposed a Robust Broadcast Propagation (RBP) protocol to provide near-perfect reliability for flooding in wireless networks, and this protocol also has a good efficiency. They presented a new perspective for broadcasting: not to make a single broadcast more efficient but to make a single broadcast more reliable, which means by reducing the frequency of upper layer with the help of flooding to improve the overall performance of flooding. Every node in the network retransmits a message to its neighbours upon receiving it for the first time this is nothing but the flooding mechanism. Although flooding is extremely simple and easy to implement, it can lead to serious problem, named as broadcast storm problem, which is characterized by redundant packet retransmissions, network bandwidth contention and collision and is also very costly. Flooding protocol is studied analytically and experimentally by Ni et al. [5] and showed that a rebroadcast can provide only 59% additional coverage at most and only 40% additional coverage in average over that already covered by the previous transmission. Therefore the rebroadcasts are very costly and should be used with caution.

III. PROPOSED WORK

During route discovery traditional on-demand routing protocols produce a large amount of routing traffic by blindly flooding the entire network with RREQ packet. In MANET the network topology frequently changes causing routing overhead due to dissemination of routing control packet such as RREQ. Therefore to reduce the routing overhead associated with route discovery in on demand routing protocols is very important.

A neighbour knowledge based rebroadcasting protocol is proposed in this article which combines both neighbour coverage and probabilistic methods.

A. UCN Set and Rebroadcast Delay :

The node can use the list of neighbours in the RREQ packet to find how many its neighbours have not been covered by the RREQ packet from previous node after receiving RREQ packet from its previous node. If it has more uncovered neighbours by the RREQ packet from previous node, which is nothing but if node rebroadcasts the RREQ packet, the RREQ packet can reach

more additional neighbour nodes. For this, we define the UnCovered Neighbours (UCN) set of node. The rebroadcast delay is to determine the forwarding order. The node which has more common neighbours with the previous node has the lower delay. If this node rebroadcasts a packet, then more common neighbours will know this fact. Therefore, this rebroadcast delay enables the information that the nodes have transmitted the packet spread to more neighbours.

B. Neighbour Knowledge and Rebroadcast Probability:

The RREQ is nothing but the Route REQuest which can be sent by the sensor nodes to all their neighbors. The rebroadcast probability which can be used to reduce the number of rebroadcasts of the RREQ packet, to improve the routing performance. The rebroadcast probability is given by combining the additional coverage ratio and the connectivity factor.

The node which has a larger rebroadcast delay may listen to RREQ packets from the nodes which have lowered one. For example, if node 'ni' receives a duplicate RREQ packet from its neighbour 'nj', it knows that how many its neighbours have been covered by the RREQ packet from 'nj'. Thus, node 'ni' could further adjust its UCN set according to the neighbour list in the RREQ packet from 'nj'. When the timer of the rebroadcast delay of node ni expires, the node obtains the final UCN set. The nodes belonging to the final UCN set are the nodes that need to receive and process the RREQ packet. Note that, if a node does not sense any duplicate RREQ packets from its neighbourhood, its UCN set is not changed, which is the initial UCN set.

C. Additional coverage ratio

The additional coverage ratio ($R_a(n_i)$) of node n_i defined as

$$R_a(n_i) = \frac{|U(n_i)|}{|N(n_i)|}$$

This formula shows that the ratio of the number of nodes that are additionally covered by the rebroadcast to the total number of neighbors of node n_i . The nodes that are additionally covered need to receive and process the RREQ packet. As the value of R_a becomes larger, more nodes will be covered by this rebroadcast, and more nodes need to receive and process the

RREQ packet, and therefore the rebroadcast probability should be set to be higher.

D. Connectivity Factor

If each node connects to its nearest neighbour more than $5:1774 \log n$, then the probability of the network being connected is approaching 1 as n increases, where n is the number of nodes in the network[15]. Now, we can use $5.1774 \log n$ as the *connectivity factor* of the said network. Let us assume $F_c(n_i)$ be the ratio of the number of nodes that need to receive the RREQ packet to the total number of neighbours of node n_i .

So let's define the minimum $F_c(n_i)$ as a *connectivity factor*, which is

$$F_c(n_i) = \frac{N_c}{|N(n_i)|}$$

where $N_c = 5:1774 \log n$, and n is the number of nodes in network.

IV. PLATFORM USED

- (1)**VMware Workstation** : Virtual Machine For visualization of virtual operating system
- (2)**CentOS** : operating system to work on VMware for installation and simulation of NS-2
- (3)**NS-2 (v2.35)**: Network Simulator version 2.35 for implementation of source code of protocols

Simulation Parameter	Value
Simulator	NS-2 (v2.35)
Topology Size	450m × 550m
Number of Nodes	5,10, 15,.....,30
Transmission Range	150m
Bandwidth	2Mbps
Interface Queue Length	50
Traffic Type	CBR
Packet Size	512 bytes
Packet Rate	4 Packets/sec
Min speed	1 m/s
Max Speed	5 m/s

V. RESULTS

Following graphs of comparison between the two protocols that is AODV and NKR for the two parameters Packet Delivery Ratio (PDR)

and Packet delay with respect to the number of nodes clearly shows that the proposed NKRP protocol has better performance than that of AODV.

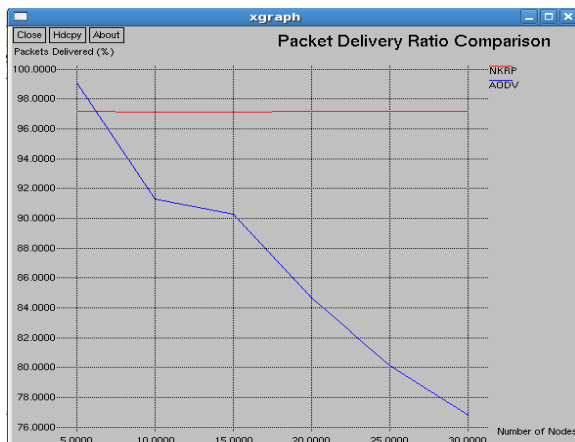


Fig 1. Comparison graph for Packet delivery ratio

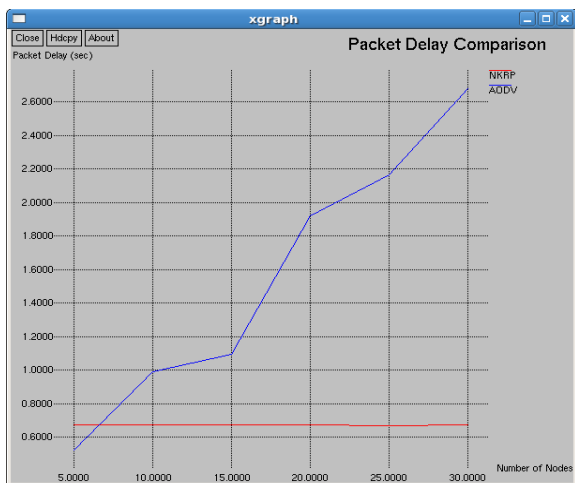


Fig 2. Comparison graph for Packet delay

```

Applications Places System
root@localhost:~/Desktop/Project/Project
File Edit View Terminal Tabs Help
[root@localhost Project]# ns aodv.tcl 20 2 9
num_nodes is set 20
warning: Please use -channel as shown in tcl/ex/wireless-mitf.tcl
INITIALIZE THE LIST xListHead
channel.cc:sendUp - Calc highestAntennaZ_ and distCST_
highestAntennaZ_ = 1.5, distCST_ = 550.0
SORTING LISTS ...DONE!
[root@localhost Project]# awk -f aodv.awk aodv.tr
Packet Delivery Ratio = 86.17
[root@localhost Project]# awk -f aodv_delay.awk aodv.tr
Packet Delay = 1.786
[root@localhost Project]# awk -f nkpr.awk nkpr.tr
Packet Delivery Ratio = 97.14
[root@localhost Project]# awk -f nkpr_delay.awk nkpr.tr
Packet Delay = 0.673
[root@localhost Project]# ns nkpr.tcl 20 2 9
    
```

Fig. 3 Calculated PDR and Delay for 20 nodes

VII. CONCLUSION

In this article we proposed a protocol for reducing routing overhead in mobile ad hoc network using Neighbor knowledge. In this we have proposed a additional coverage ratio and connectivity factor. With the help of neighbor coverage knowledge we can find out the Packet Delivery Ratio and Packet Delay. From the comparison between the AODV and our proposed NKRP protocol for above two parameters and found results we can conclude that our proposed Neighbor Knowledge based Rebroadcast Protocol (NKRP) is much better than existing protocol. The result of proposed protocol shows the Packet Delivery Ratio about 97.14% and Packet Delay is about 0.673sec for variations of number of nodes. This is much better than the existing AODV protocol. This proposed protocol can significantly decrease the number of retransmissions so as to reduce the routing overhead, and can also improve the routing performance.

REFERENCES

- [1]C. Perkins, E. Belding-Royer, and S. Das, *Ad Hoc On-Demand Distance Vector (AODV) Routing*, IETF RFC 3561, 2003.
- [2] D. Johnson, Y. Hu, and D. Maltz, *The Dynamic Source Routing Protocol for Mobile Ad Hoc Networks (DSR) for IPv4*, IETF RFC 4728, vol. 15, pp. 153-181, 2007.
- [3] H. AlAamri, M. Abolhasan, and T. Wysocki, "On Optimising Route Discovery in Absence of Previous Route Information in MANETs," Proc. IEEE Vehicular Technology Conf. (VTC), pp. 1-5, 2009.
- [4] X. Wu, H.R. Sadjadpour, and J.J. Garcia-Luna-Aceves, "Routing Overhead as a Function of Node Mobility: Modeling Framework and Implications on Proactive Routing," Proc. IEEE Int'l Conf. Mobile Ad Hoc and Sensor Systems (MASS '07), pp. 1-9, 2007.
- [5] S.Y. Ni, Y.C. Tseng, Y.S. Chen, and J.P. Sheu, "The Broadcast Storm Problem in a Mobile Ad Hoc Network," Proc. ACM/IEEE MobiCom, pp. 151-162, 1999.
- [6] B. Williams and T. Camp, "Comparison of Broadcasting Techniques for Mobile Ad Hoc Networks," Proc. ACM MobiHoc, pp. 194-205, 2002.
- [7] J. Kim, Q. Zhang, and D.P. Agrawal,

- “Probabilistic Broadcasting Based on Coverage Area and Neighbor Confirmation in Mobile Ad Hoc Networks,”* Proc. IEEE GlobeCom, 2004.
- [8] J.D. Abdulai, M. Ould-Khaoua, and L.M. Mackenzie, *“Improving Probabilistic Route Discovery in Mobile Ad Hoc Networks,”* Proc. IEEE Conf. Local Computer Networks, pp. 739-746, 2007.
- [9] Z. Haas, J.Y. Halpern, and L. Li, *“Gossip-Based Ad Hoc Routing,”* Proc. IEEE INFOCOM, vol. 21, pp. 1707-1716, 2002.
- [10] W. Peng and X. Lu, *“On the Reduction of Broadcast Redundancy in Mobile Ad Hoc Networks,”* Proc. ACM MobiHoc, pp. 129-130, 2000.
- [11] J.D. Abdulai, M. Ould-Khaoua, L.M. Mackenzie, and A. Mohammed, *“Neighbour Coverage: A Dynamic Probabilistic Route Discovery for Mobile Ad Hoc Networks,”* Proc. Int’l Symp. Performance Evaluation of Computer and Telecomm. Systems (SPECTS ’08), pp. 165-172, 2008.
- [12] J. Chen, Y.Z. Lee, H. Zhou, M. Gerla, and Y. Shu, *“Robust Ad Hoc Routing for Lossy Wireless Environment,”* Proc. IEEE Conf. Military Comm. (MILCOM ’06), pp. 1-7, 2006.
- [13] A. Keshavarz-Haddady, V. Ribeiro, and R. Riedi, *“DRB and DCCB: Efficient and Robust Dynamic Broadcast for Ad Hoc and Sensor Networks,”* Proc. IEEE Comm. Soc. Conf. Sensor, Mesh, and Ad Hoc Comm. and Networks (SECON ’07), pp. 253-262, 2007.
- [14] F. Stann, J. Heidemann, R. Shroff, and M.Z. Murtaza, *“RBP: Robust Broadcast Propagation in Wireless Networks,”* Proc. Int’l Conf. Embedded Networked Sensor Systems (SenSys ’06), pp. 85-98, 2006.
- [15] F. Xue and P.R. Kumar, *“The Number of Neighbors Needed for Connectivity of Wireless Networks,”* Wireless Networks, vol. 10, no. 2, pp. 169-181, 2004.
- [16] V.V.V. Pradeep Sastry, Dr S.Arvind, *“A Survey of Coverage-Based Broadcast for Reducing Routing Overhead in Mobile Ad Hoc Networks,”* IJCTT – volume 11 number 2 – May 2014
- [17] Richa Sharma, Maninder Singh Nehra , *“Improving the Performance of Routing Protocol Using Neighbor Coverage Based Probabilistic Rebroadcast in Mobile Ad Hoc Network”* IJRITCC | Volume: 1 Issue: 12 December 2013.



BACKGROUND AND RESIDUAL NOISE REDUCTION FOR SPEECH ENHANCEMENT: SPECTRAL SUBTRACTION AND MEDIAN FILTER APPROACH

¹Disha Desai

¹Post Graduate Student, Department of Electronics & Communication,
Sarvajanik College of Engineering & Technology, Surat, Gujarat, India
Email:¹disha.ec20@gmail.com

Abstract - Analysis of speech signal is used to illustrate parts of speech that comprise momentary the speech component and develop an algorithm to extract those components. In noisy environment in which channel is bit noisy, speaker and listener may experience several annoying noises which causes significant degradation in efficiency of communication system which makes communication bit difficult. It may happen that speaker has to speak much louder and listener has to give more concentration in listening process to maintain fruitful communication. Spectral subtraction method is normally used for background noise removal but there will be still some residual noise is present in this enhanced speech that needs to be suppressed for efficient communication system. Median filter can be used for second stage enhancement which removes residual noise from already enhanced speech in first stage.

Keywords- Segmental SNR(SNR), Perceptual evaluation of speech quality(PESQ), Signal to Noise Ratio (SNR)

I. INTRODUCTION

Speech enhancement is one of the major parts of any communication block. Analysis of speech signal is used to illustrate parts of speech that comprise momentary the speech component and develop an algorithm to extract those components. Many speech enhancement techniques remove background noise very

efficiently from noisy speech. But the musical effect of residual noise appears in the enhanced speech.

In simple speech enhancement, only background noise can be removed from noisy speech. Output of this speech enhancement is called as a pre-processed speech which contains some amount of noise after enhancement. So quality of speech is degraded and cannot get proper desired speech signal. This noise can be called as 'Musical Residual Noise'. This effect of musical noise is appearing due to some spectral patches of residual noise randomly appearing or disappearing in successive frames and over the neighboring sub bands. The majority of the speech enhancement system suffers from this musical residual noise which significantly degrades the perception quality of pre-processed speech. This type of residual noise is infuriating to human ear. If this residual noise is too prominent in nature, then it is more disturbing than the interference before speech enhancement. So for all these reasons it is required to remove residual noise for better speech quality.

II. SPEECH ENHANCEMENT

There are mainly two stages to reduce residual noise. First stage contains background noise reduction using speech enhancement algorithm. Output of this stage is called as pre-processed speech which contains some amount of residual noise after enhancement. And second stage is used to reduce the residual noise from pre-processed speech. Residual noise is reduced using post-processed algorithm for improved

speech quality. Output of second stage contains enhanced speech quality with reduction of residual noise.

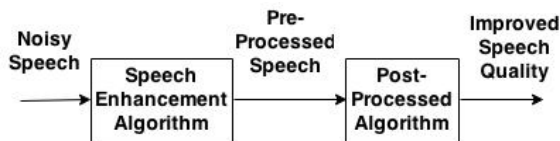


Figure 1 Process for Reduction of Residual Noise from Speech

A) First stage speech enhancement

First stage speech enhancement contains background noise reduction. Different approaches are used to remove background noise (e.g. Spectral subtraction, Wiener filtering, Wavelet denoising)^[1]. Spectral subtraction is used to remove background noise from noisy speech.

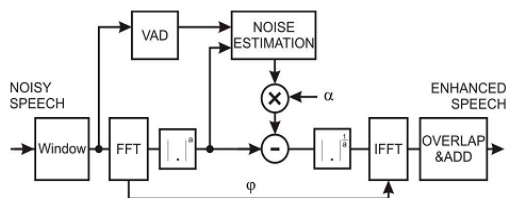


Figure 2 Spectral Subtraction Method ^[5]

Spectral subtraction is one of the noise reduction techniques that try to approximate the short-time spectrum of an additive noise which is used to corrupt a speech signal. In spectral subtraction, an approximation of the short-time spectrum of original speech is obtained by difference between estimated noise spectrum and spectrum of noisy speech. Estimation of original speech is obtained by combining estimated spectrum with the phase of noisy speech.

These processes can be used to improve the signal-to-noise ratio by attenuating the short-time spectrum when the signal-to-noise ratio is relatively low and there will be no attenuation in short time spectrum when SNR is high. Various spectral subtraction methods are decided by estimation method of short time spectrum of AWGN.

B) Second Stage Speech Enhancement

Enhanced speech after first stage may contain residual noise. Zero crossing detector is used to

identify noisy portion and speech portion available in first stage enhanced speech. Number of zero crossing in a given signal tells about ZCR. More number of zero crossing shows that there are too quick changes in signal and it may contain high frequency information. On another hand, less number of zero crossing shows changes are gradual and it can be understood that signal may contain low frequency information. Frequency contents of a signal can be fetched out indirectly from parameter ZCR. Low ZCR value indicates voiced signal and high ZCR value indicates unvoiced signal.

For speech signal ZCR is given by,

$$z(n) = \frac{1}{2N} \sum_{m=0}^{N-1} s(m) \cdot w(n - m) \quad (2.1)$$

Musical residual noise can be removed by a two-stage speech enhancement approach. Two-step noise reduction algorithm contains Two-Step-Decision-Directed approach. Basic goal of this method is to detect musical tone and attenuate the tone for the enhanced speech signal. When the spectral distance changes largely among the neighbors, the reference spectrum is notified as isolated spectrum which can be further adapted by the median filter. Conversely, the reference is declared as harmonic spectrum if the spectral distance changes easily among the neighbors. Now no more processing is done on this spectrum to preserve speech quality and kept it as it is. The central spectrum is terms as reference spectrum. Initially the optimum motion direction of the reference spectrum is detected. Neighboring directions are selected. The decision rule is used to find the minimum spectral distance between those directions. The spectral-distance measure is given by

$$d^{(i)}(m, \omega) = \sum_{\Delta m} \sum_{\Delta \omega} \frac{[|X(m + \Delta m, \omega + \Delta \omega)| - |X(m, \omega)|]^2}{|X(m, \omega)|^2} \quad (2.2)$$

The minimum spectral-distance measure is given in equation 2.2 and it is confirmed as the motion direction for the reference spectrum. Based on the value of spectral distance for the optimum direction, the decision is taken if the reference spectrum is speech spectrum or not. The optimum spectral distance measure is given as

$$d^{(i*)}(m, \omega) = \min\{d^{(i)}(m, \omega), 1 \leq i \leq 4\} \quad (2.3)$$

If the reference spectrum is an isolated musical tone, the spectrum varies seriously over the neighbors of the reference spectrum. The value of the spectral-distance is large on the optimum direction. Hence, optimum spectral-distance is used to classify the reference spectrum is either speech or musical tone. The decision rule can be given by

$$d^{(i^*)}(m, \omega) > \theta(m, \omega) : \text{residual noise}$$

$$d^{(i^*)}(m, \omega) < \theta(m, \omega) : \text{speech}$$

(2.4)

If musical tone is detected in reference spectrum then it is replaced by the weighted median value of the window what is analyzed. The modified spectrum is given as

$$\hat{S}(m, \omega) = \gamma(m, \omega) \cdot \tilde{S}(m, \omega) + [1 - \gamma(m, \omega)] \cdot M(m, \omega) \quad (2.5)$$

Where, Replacing flag and modified spectrum are denoted as $\gamma(m, \omega)$ and $M(m, \omega)$ respectively. Reference spectrum is modified if replacing flag shows zero value. Unity value of replacing flag is set when reference spectrum is classified as speech. Fluctuation of random spectral peaks can be diminished by weighted median filter is used that modifies the isolated reference spectrum. Best direction of those different directions decides the weight of reference spectrum. The weighted median filter is given as

$$M(m, \omega) = \text{median}\{\tilde{S}(m + \Delta m, \omega + \Delta \omega)\} \quad (2.6)$$

Block and directional median (BDM) filter^[3] that is post processing which reduces musical effect of residual noise presented in first stage enhanced speech. Directional median filtering is employed to slightly decrease musical effect of residual noise in speech like spectrum and on other hand vowel spectrum which have strong harmonic spectrum is well maintained. Then the quality of post-processed speech is assured. Spectral changes in noise dominant area are reduced by median filtering which smoothens spectral peaks of musical noise. Based on the speech presence probability, both preprocessed and post-processed spectra are integrated.

III. IMPLEMENTED WORK

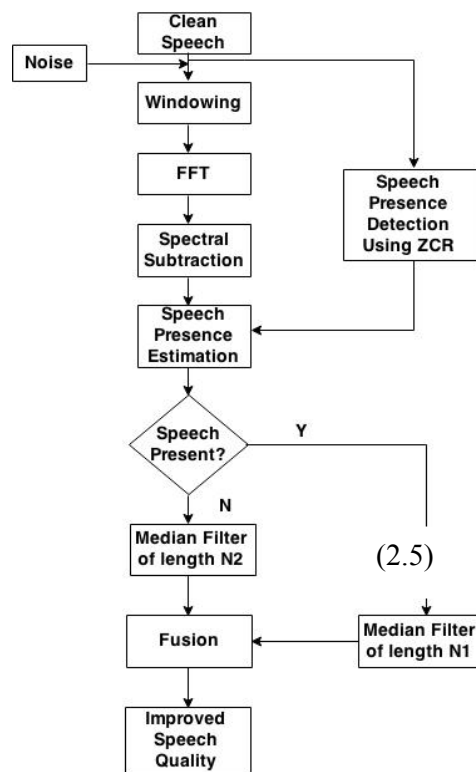


Figure.3 Flow chart of Proposed Work

IV. SIMULATION RESULTS

Simulation is carried out on NOIZEUS speech database with airport, car and babble noise for different input SNR values. SNR, SSSNR and PESQ are used for performance measurement.

Software used:	MATLAB R2009
Speech Database:	NOIZEUS speech Corpus for Evaluation of Speech Enhancement Algorithm)

(2.6)

Table 1 SNR Results in dB for Female and Male Voice for AWGN Noise

Male/ Female	Noisy Speech	Spectral Subtraction	Proposed Method
Female	-5.0173	2.1476	9.7314
	-0.0724	7.0833	8.3779
	0.9971	8.0141	8.2852
Male	-5.0187	0.7415	10.2264
	0.0048	5.5907	8.2924
	2.0292	7.6293	8.1469

Table 2 SNR Results in dB for Male Voice with Different Noise

Type of Noise	Noisy Speech (dB)	Spectral Subtraction	Proposed Method
Airport	-0.6669	3.5642	8.3453
	4.3331	8.1861	8.6017
Babble	-0.6668	3.6147	8.6259
	4.3331	7.9708	8.6115
Car	-0.6668	3.4560	10.0459
	4.3332	8.2772	8.2313

Table 1 PESQ Results for Male Voice for Different Noise

Type of Noise	SNR of Noisy Speech	PESQ	
		Spectral Subtraction	Proposed Method
Airport	-0.6669	2.5553	4.3154
	4.3331	2.9150	4.1222
Babble	-0.6668	2.5645	4.1817
	4.3331	2.9718	4.0309
Car	-0.6668	2.4582	3.9549
	4.3332	2.8447	4.2076

Table 2 SSNR Results for Male Voice for Different Noise

Type of Noise	Noisy Speech	Spectral Subtraction	Proposed Method
Airport	-4.4125	-1.8151	0.1610
	-1.8234	1.7360	2.1605
Babble	-4.3520	-1.4235	0.4358
	-1.4040	2.4222	2.7495
Car	-4.4421	-2.3841	-1.7550
	-1.5324	1.7572	2.2691

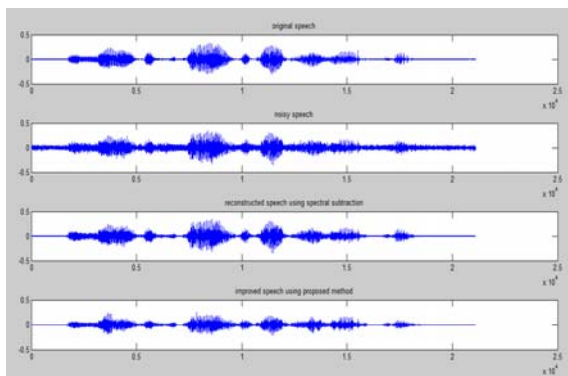


Figure. 4 For Male Voice (a) Clean Speech (b) Noisy Speech with Airport Noise at 5 dB (c) Reconstructed Speech using Spectral Subtraction Method (d) Improved Speech Quality using Proposed Method

V. CONCLUSION

Plenty of noises are always present during ongoing communication in practical world and those noises are main culprit for degradation of efficiency of communication system. Elimination or suppression of these noises is essential for fruitful communication. Major work is carried out over here is removal of background noise and residual noise which is still present after first stage of noise removal process. Spectral subtraction method is used for removal of background noise. Although output of this method contains some part of residual noise which is degrading the quality of speech. Removal of this residual noise is necessary. For that, first detection of speech part and noise part is done. Here ZCR approach is used to differentiate between speech part and noisy part. Median filter is used in last stage enhancement.

Experiments are carried out on free available NOIZEUS speech database with different noises (e.g. car, babble, airport, AWGN, F16, factory and machine). Performance of algorithm is measured using parameters like SNR, SSNR and PESQ. It has been noted that application of spectral subtraction method removes noise from noisy speech but not in significant way. Second stage speech enhancement (using median filter) improves speech quality which can be seen from comparison of SNR, SSNR and PESQ of first stage and second stage of enhancement.

It is observed that after second stage enhancement, output SNR increases around 4 to 5 dB from first stage enhanced SNR values for 0 dB (lower SNR) input SNR with airport, babble and car noises. This SNR increment is around 1dB when input SNR is around 5 dB.

REFERENCES

- [1] Marwa A. Abd El-Fattah, Moawad I. Dessouky, Alaa M. Abbas, Salaheldin M. Diab, El Sayed M. El-Rabaie, Waleed Al-Nuaimy, Saleh A. Alshebeili, Fathi E. Abd El-samie, "Speech Enhancement with an Adaptive Wiener Filter," Springer Journal on Int J Speech Technol, 17, PP 53-64, August 2013.
- [2] Ching-Ta Lu, Kun-Fu Tseng, Chih-Tsung Chen, "Reduction of Residual Noise Using Directional Median Filter," IEEE Conference on Computer Science

- and Automation Engineering, Vol. 3, PP 475-479, June 2011.
- [3] Ching-Ta Lu, "Reduction of Musical Residual Noise using Block-and-Directional Median Filter Adapted by Harmonic Properties," Elsevier Journal on Speech Communication Vol. 58, PP 35-48, March 2014.
- [4] Thomas Esch, Peter Vary, "Efficient Musical Noise Suppression for Speech Enhancement Systems", IEEE International Conference on Acoustics, Speech and Signal Processing, PP 4409-4412, April 2009.
- [5] Ekaterina Verteletskaya and Boris Simak, "Noise Reduction Based on Modified Spectral Subtraction Method", in IJCS, February 2011.
- [6] Yi Hu and Philipos C. Loizou, "Evaluation of Objective Quality Measures for Speech Enhancement", IEEE Transactions on Audio, Speech, and Language Processing, Vol. 16, No. 1, PP 229-238, January 2008.
- [7] Thomas F. Quatieri, "Discrete-Time Speech Signal Processing: Principles and Practice", New Jersey: Prentice Hall, 2001.



WATERMARKING FOR VIDEO AUTHENTICATION

¹Pathak Utsav A

Department of Electronics and Communication
Sarvajanik College of Engineering and Technology
Surat, India

Email:¹utsavpathak.3787@gmail.com

Abstract— In law examples like surveillance and forensics video is presented as proof. Because of that it is extreme importance to establish the validity and dependability of the video data. Since the H.264 / AVC-based video products are becoming increasingly popular, are issues of copyright protection and authentication that are appropriate for this very important standard. Here in this dissertation different techniques for video authentication are studied. Here different types of spatial and temporal tampering attacks are considered for video and to check authenticity of video intelligent technique like SVM based machine learning is used to identify temporal attacks like frame adding, frame removing etc. For authentication different parameters are studied for video like PSNR, NC, BER.

Keywords—watermarking, authentication, embedding, extracting, DWT, DCT, DFT, H.264/AVC, SVM, SVD

I. INTRODUCTION

Today in multimedia creation and delivery from authoring content provider to the receivers everything seems to be digital. The benefits of digital processing and distribution, example transmission without noise, software in place of hardware processing and superior re-configurability of systems, are well recognized and obvious. But distribution of digital media is main disadvantage. For example, in terms of media generators and content providers, the opportunity of infinite replication of computerized data without loss of loyalty is not desirable for the reason that it tends to substantial

economic losses. Digital copy or copy protection, since access to plain text versions of protected data must be a minimum estimate of the receiver, which then produce and distribute illegal copies are issued, it may be of limited value. In actuality tries of preventing copy are always get bypass.

Another method of protecting intellectual property rights (IPR) is the embedding of digital watermarks in the multimedia data. The watermark is a computerized code unsolvable, robust, and imperceptibly implanted in the host information and for the most part contains data about the starting point, status and target of the information. Although unutilized specifically for copy safety, it can help identify the starting place and ending point of multimedia information and as a "last line of defense", allow proper proceedings in case of doubt of copyright violation.

Although copyright protection is the mainly popular application of watermarking techniques, there are other, plus data validation means fragile watermarks that impaired or damaged by manipulations implanted transfer of worth added services in the multimedia data, and embedded data identification for purposes other than protection of copyright, some example tracking and monitoring of data. An illustration of a data monitoring system is the automatic registration and monitoring of radio broadcasting, to automatically pay the royalties the IPR owner of the broadcast data.

The progress of watermarking methods has some of the design compromises. Watermark should be robust. It is compared with standard data manoeuvring, including digital-to-analog conversion and digital format conversion. Security is a particular concern, and watermark

should withstand attack attempts by competent persons. On the second note watermark should not be perceptible and as many information as it can. Generally watermark embedding and recovery should have little complication, since for a variety of applications, a synchronized watermark is popular.

A. Requirement of Digital Watermarking

- 1) A watermark will transmit to great extent information possible, which means that the watermark data should have high data rate.
- 2) A watermark should be generally kept undisclosed and accessible only by sanctioned person. This necessity is known as watermark security and it is typically achieved by using cryptographic keys.
- 3) Including all signal processing that can happen and how unauthorized person try to change a watermark is in the host data is stayed with it. This scheme is known to watermark robustness. It is an important prerequisite for protection of data or access control applications, but also applications for which the watermarks are not essential to cryptographically sure, for illustration, applications where watermark transmit the information to the public less important.
- 4) A watermark should however as non-removable, are imperceptible.

This fundamental set of needs may be supplemented with extra needs depending on media in which watermark is to be embedded and the application.

- 1) Watermark recovery may or may not get approved to employ unwatermarked original host data.
- 2) Based on purpose watermark embedding like video fingerprinting may require concurrent example. Embedding in real may need compressed domain embedding techniques for complication reasons.
- 3) Depending on use watermark is needed to be capable to transmit random information. While in different applications just some predefined watermarks must be installed and for disentangling it might be adequate to verify vicinity of one of the predefined watermarks.

According to ^[6] some of these desires and the consequential design issues will be painted in greater detail.

1) Watermark Security and Keys: If the security, that is, confidentiality of the embedded

information is essential, for embedding and extraction one or more than one secure keys are used. For example, in lots of systems, pseudo-random signals are embedded as a watermark. In this situation, the description and the seeds of the pseudo-random number generator are used as keys. Here two security levels are used. Users which are not authorized can't decode embedded watermark in the first stage, but can know whether it have watermark. Now in second level users which are not authorized can't sense that data have watermark or not however the embedded data can't be read without secret key. Here systems embed two watermarks one with public key and other with secret key. On the other hand, a scheme was introduced that use combined public key with a private key, and embeds it instead of multiple watermarks. There are some issues such as generation of secret key, distribution and management needs to consider as well as other aspects of system integration.

2) Robustness: When making any watermarking algorithm robustness is the main issue because robustness introduced again by standard data processing and data attacks distortion is an important prerequisite. Standard Data Processing includes all data manipulation and modifications that the data could in the normal distribution chain to undergo, such as data processing, printing, enlargement and format conversion. "Attack" is the data manipulation with the purpose of affecting, disrupting or removing the embedded watermark. Although it is possible to design robust watermark method, it should be noted that a watermark is only robust, as long as it is private, the as long as they will not be of anyone reading device.

3) Imperceptibility: Perceptual clearness in important requirement of watermarking. The embedding procedure must not launch artifacts in host data which are noticeable by viewer. On the other part, it is important that watermark amplitude is as high as promising for good robustness. Thus, there is always trade-off between imperceptibility and robustness in construction of watermarking method. Normally, watermark should be embedded just below some threshold so that no one can notice its presence. However, for genuine image, video and audio signals it is hard to find such threshold value.

4) Watermark Recovery With or Without the Original Data: In watermark recovery if the original unwatermarked data is available then recovery generally becomes more robust. Also easy use of new data set in recovery process the finding of distortion that alter geometry of the data. For example, if watermarked image has been rotated by an assailant this thing will help. However in some application such as data monitoring and data tracking right to use to the unique data is impossible in every cases. In video watermarking because of the large volume of data it is not practically good to use the original data even though it is available.

However for watermark extraction we can make techniques which do not require the original data. Some kind of modulations is performed in most watermarking techniques in which the distorted novel data set is considered. If we know this distortion or in recovery process if it can be modelled, clearly planned techniques permit its control without facts of the original. In fact, in most current methods there is no need of the original data for recovery.

B. Basic principle of watermarking

The basic idea of watermarking is to embed a watermark signal into the host data that is to be watermarked such that the watermark signal is unremarkable and secure in the mixture of signal but later on it can partly or fully be recovered from the signal mixture if the proper cryptographically secure key for recovery is used.

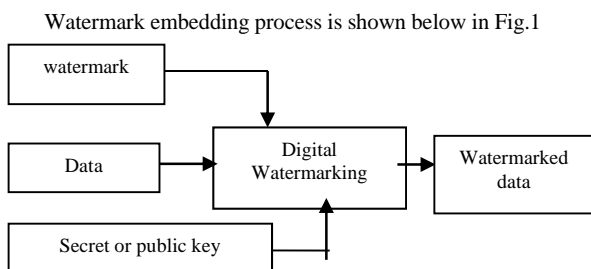
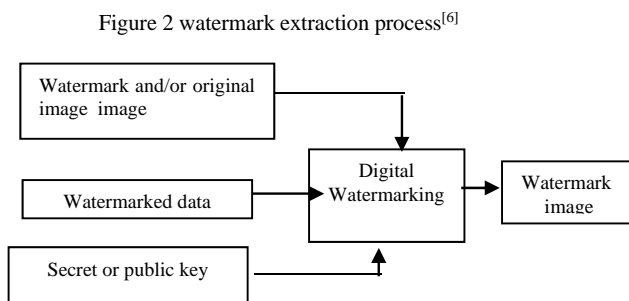


Figure 1 watermark embedding process^[6]



II. VIDEO WATERMARKING

A. Video watermarking principle:

There are three fundamentals part of total digital watermarking system ^[4]: generation of watermark, embedding of watermark and extraction/detection of watermark. In Figure 3 Block diagram for embedding and extraction of watermark is shown:

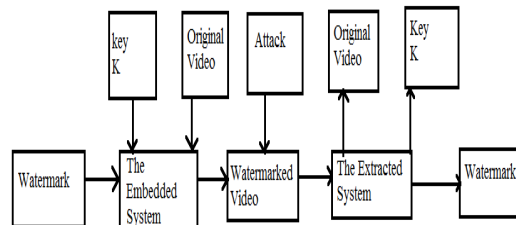


Figure 3 principle of video watermarking ^[4]

B. Video watermarking Characteristics

Video watermarking not only contain the features of image watermarking but also posses its own features ^[4].

- **High real-time.** Video that is three dimensional has more quantity of data than the image. So there is large computation quality and it requires large time for embedding/extracting. Using video compression standard such as VLC code word, motion vector coding are efficient algorithm for the procession of embedding.
- **Random detection.** This means that we can detect the watermark in video in any position not the place according to the video playback.
- **The combination of video codec standard.** In storage or transmission video is in compressed formats, so without specific video codec standard research of information hiding technology can't do anything. Video information hiding technology can accomplish the real time requirement combining with encoding and decoding standard.
- **Enhanced robustness.** This means that the scheme of video watermarking must guarantee that it can oppose almost all kind of attacks or processing.
- **Blind detection scheme.** If the detection scheme is Non-blind that it will require the

original data in extraction. But it is not very convenient to use the original data which is so large. While detection scheme of Blind type does not require any original data in extraction.

C. Video watermarking model

There are three types of solution for video watermarking algorithm based on the strategy of embedding^[4]:

- 1) The uncompressed video i.e. original video
- 2) video codec
- 3) The compressed video.

The type of the solution is shown in the figure 4.

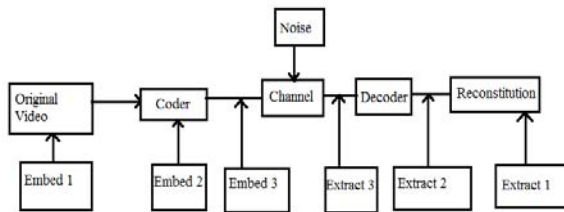


Figure 4 video watermarking model^[4]

The uncompressed video^[4]: In this type of video watermarking embedding of watermark is done directly into the original video sequence and then the encoding of watermark containing video is done. Here the advantage of watermarking technology of still image and combination with the structural characteristics of video frames makes the solution of video watermarking. The benefit of this watermarking algorithm is it is comparatively mature. We can apply methods like spread spectrum, the human vision model, image adaptive watermarking irreversible, synchronous detection mechanism to this video watermarking system. But the demerit of solution is video bit rate will be increased and it will effect video rate of constancy; and watermark may get lost after the compression and encoding of the video data. If the video is in compressed form than first we have to decode it and then after embedding watermark re-encoding of video has to be done. But with this process complexity will get increase and the quality of video will get decreased.

Solution based on video codec^[4]: In encoder embedding and detection module for watermarking are introduced. There are video compression standards like ISO / IEC of MPEG-

1, MPEG-2, MPEG-4 and ITU-T of H. 261, H. 263, etc in today's life. Block based transform coding and motion compensation prediction coding are the fundamental idea. Here the embedding is done in encoding phase of video. Characteristics of encoded data and principle of video data compression like transformation to the spatial redundancy, quantization and entropy coding, the motion compensation, motion estimation, etc are used here. The real time processing of watermark embedding and extracting is simple to achieve. The relative simple process of watermark embedding in the transform domain coefficient does not increase the bit rate of video; also we can make watermarking algorithm for multiple attacks, because embedding of watermark is done in transform domain and it is combined with the encoding process. GOP error accumulation is occurred because we need to modify the encoder and decoder and also the video codec in unable to perform common embedding and detection of watermark.

The compressed domain video^[4]: In this solution watermark is embedded straight into the compressed encoded bit stream of video. Here there is no requirement of decoding and re-encoding of video which is the advantages of this solution and because of that it will not degrade the video quality and there is low computation complexity. Here disadvantage is the bit-rate of compressed video constrain the size of watermark to be embedded. Error in video decoder will limit the strength of the watermark and the coding standard and the video compression algorithm will constrain the strategy of embedding. The computational complexity is low and rate of watermark embedded is high. But the capability to deal with channel interference is poor which is the disadvantage; by adding random bits in the VLC code using same algorithm can destroy the watermark; extraction of watermark will also get effected of traditional filtering, re-sampling and time-domain scaling processing.

D. Algorithm of video watermarking

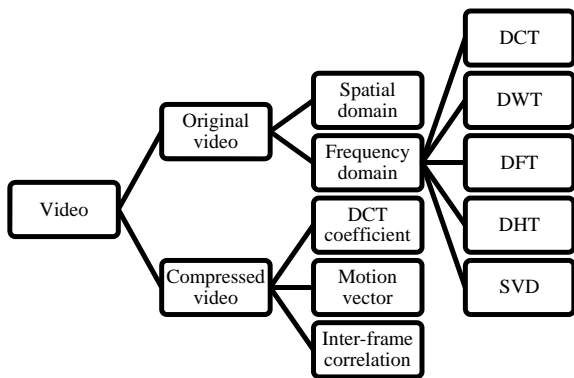


Figure 5 video watermarking algorithms [4]

Other than all this technique one technique is intelligent technique which is machine learning based technique in which the different classifiers (like SVM, NN etc.) are used to train the network first and after the network is trained it will provide whether the video is tampered or not. This technique is more suitable for temporal tampering like frame removal, frame dropping and frame shifting which is discussed in section III.

III. VIDEO TAMPERING ATTACKS

To change the content of video data there are several attacks are performed. Video data is the collection of consecutive frames with temporal or time dependency which is viewed in a three dimensional plane. This is known as the regional property of the video sequences. If malicious changes on video sequence is applied it can either attacks on the content of data like frames of video presenting visual information, or executed attacks on the temporal or time dependency within the frames. Therefore video tampering attacks are classified in three types based on the regional property of the video sequences: attacks of spatial tampering, attacks of temporal tampering and the combination of these two, attacks of spatio-temporal tampering

A. Attacks of Spatial Tampering^[5]

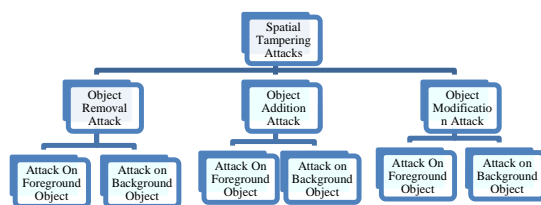


Figure 6 different spatial tampering attacks [5]

B. Object removal attack

In this type of attack in [5], the objects of the frames are removed from the frame by some technique. This type of attack is often carried out where a specific person wants hide his/her presence in particular sequence of frames. This attack can be carried out with two types of objects, object in the foreground and object in background.



Figure 7 object removal attack [5]

C. Object addition attack

In this type attack in [5], an object is added in a frame or in a series of frames, than this kind of manipulation is known as content or object addition attack. It can also be carried with both kinds of objects, objects in foreground and objects in background.



Figure 8 object addition attack [5]

D. Object modification attack

In this type of attack in [5], an existing object of the frame(s) modified in such a way that the existing identity of that object are lost, and a new appearance of object is obtained that is totally changed from the original object. Like example, the size and shape of the existing object to be changed, which may be to alter or discolour the color of object, and using additional effect of the nature of the subject and its relation with other object also be changed.

E. Temporal tampering

In this type the manipulation with the sequence of frame is performed. The concentration is on the time dependency. Temporal manipulation attacks are mainly based the temporal sequence of visual information captured from video recording device. Frame addition, frame removal and frame shuffling or rearranging are the common attacks in this type of tampering.

F. Frame addition attack

In this type of attack as shown in figure 9 another frame is added in between the original video frames at some random position.



Figure 9 frame addition attack [5]

G. Frame removal attack

In this type of attack as shown in figure 10 frames from the video sequence are removed intentionally from particular place to the fixed place or can be removed from various locations. Often this type of manipulation attack on video surveillance in which an attacker wants to remove his/her presence at all.



Figure 10 frame removal attack [5]

H. Frame shuffling attack

In this type of attack as shown in figure 13 position of frames are changed from its original place in a way that correct frame are mixed with this and compared to original video it will produce false information.



Figure 11 frame shuffling attack [5]

IV. RESULT AND ANALYSIS

A. Result for DWT and SVD based watermarking technique

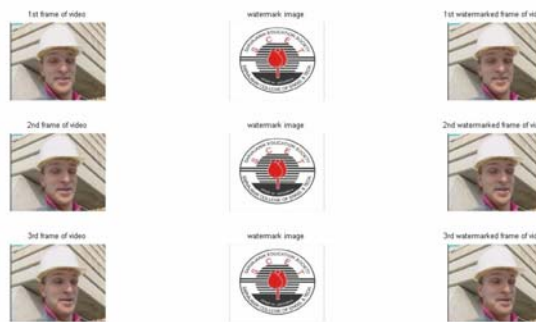


Figure 12 plot of original frame, watermark image and watermarked frame for foremen video sequences

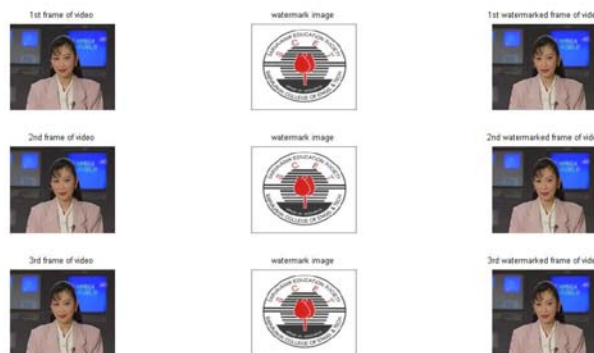


Figure 13 plot of original frame, watermark image and watermarked frame for akiyo video sequences

Table 1 effect of alpha on PSNR

Frame	PSNR for alpha=0.0 1	PSNR for alpha=0.2	PSNR for alpha=0.5
1	64.6296	38.01 36	30.734 4
2	64.7064	38.01 72	30.736 0
3	64.8109	38.01 31	30.737 5
4	64.7181	38.02 00	30.738 1
5	64.6689	38.01 15	30.744 5
6	64.6031	38.02 22	30.741 9
7	64.5421	38.01 78	30.744 5

8	64.5408	38.01 96	30.747 5
9	64.6031	38.02 77	30.745 1
10	64.5433	38.01 08	30.729 2
11	64.5421	38.00 81	30.732 1
12	64.6082	38.01 28	30.730 6
13	64.6812	38.00 34	30.730 9
14	64.6299	38.00 83	30.745 3
15	64.5603	38.01 83	30.745 0
16	64.5184	38.00 88	30.733 4
17	64.7123	38.00 13	30.721 8
18	64.6838	38.01 13	30.725 2
19	64.6484	38.00 01	30.729 2
20	64.8175	38.00 19	30.732 0
21	64.7751	38.00 88	30.724 0
22	64.8806	38.00 85	30.718 3
23	64.7646	38.00 64	30.718 1
24	64.6792	38.01 10	30.734 4
25	64.7285	38.00 60	30.717 8
26	64.9755	37.99 60	30.737 2
27	64.8462	37.99 88	30.734 6
28	64.8556	37.99 14	30.720 0
29	64.8449	38.00 37	30.736 6
30	64.8887	38.00 15	30.734 1

Table 2 different value of PSNR

Frame	Foren sequence	Akiyo sequence	Coastguard sequences	Mobile sequences
-------	----------------	----------------	----------------------	------------------

1	64.629 6	64.332 9	65.3159	65.731 7
2	64.706 4	64.409 8	65.5910	65.291 3
3	64.810 9	64.335 3	65.3889	65.445 5
4	64.718 1	64.295 0	65.6423	66.417 7
5	64.668 9	64.332 9	65.3144	66.127 3
6	64.603 1	64.371 2	65.6568	66.229 3
7	64.542 1	64.409 8	65.4617	66.225 6
8	64.540 8	64.335 3	65.1568	66.116 5
9	64.603 1	64.371 2	65.6487	65.889 1
10	64.543 3	64.409 8	65.3039	65.142 4
11	64.542 1	64.570 4	65.3204	65.378 3
12	64.608 2	64.451 2	65.5028	65.784 7
13	64.681 2	64.392 9	65.3323	66.123 7
14	64.629 9	64.354 4	65.4347	66.299 9
15	64.560 3	64.278 5	65.5696	66.371 7
16	64.518 4	64.203 8	65.2876	66.330 0
17	64.712 3	64.241 0	65.3904	66.833 5
18	64.683 8	64.128 2	65.2876	66.024 1
19	64.648 4	64.330 5	65.3836	66.371 7
20	64.817 5	64.325 8	65.3458	66.394 6
21	64.775 1	64.439 0	65.3700	66.210 9
22	64.880 6	64.321 0	65.1017	66.444 7
23	64.764 6	64.436 6	65.2891	66.116 5
24	64.679 2	64.510 4	65.0165	66.027 6
25	64.728 5	64.431 7	65.1066	66.052 3
26	64.975 5	64.431 7	65.1230	66.188 9

27	64.846 2	64.505 4	65.1632	65.689 2
28	64.855 6	64.636 3	65.0953	66.134 5
29	64.844 9	64.515 4	65.2250	66.487 5
30	64.888 7	64.608 3	65.2506	66.479 7



Figure 17 Plot of watermarked frame, original watermark and extracted watermark for foremen video sequence

B. Result of extraction for DWT-SVD based technique

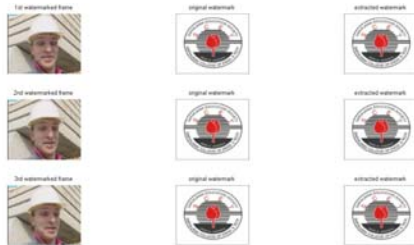


Figure 14 Plot of watermarked frame, original watermark and extracted watermark

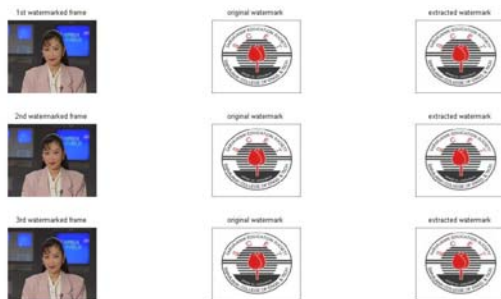


Figure 15 Plot of watermarked frame, original watermark and extracted watermark

C. Results for embedding algorithm for SVD based blind watermarking



Figure 16 Plot of watermarked frame, original watermark and extracted watermark for akiyo video sequence

Table 3 effect of alpha on PSNR

Frame	Akiyo video sequence	Coastguard video sequence	Foremen video sequence	Mobile video sequence	Stefan video sequence
1	34.9909	40.0441	46.0997	41.5930	48.3405
2	34.9654	39.7700	44.8927	41.0430	47.5796
3	34.9720	39.4477	43.6452	41.0286	46.7698
4	34.9997	39.0292	43.1152	40.7109	46.1011
5	35.0428	39.0046	42.5823	40.3819	45.1913
6	35.1261	39.1059	41.4183	40.1005	44.9520
7	35.1136	39.1436	39.9214	39.4494	47.0060
8	35.0739	38.8404	38.8685	39.0021	49.0354
9	35.0045	38.6690	38.5416	38.5619	48.3838
10	34.9673	38.4641	38.7939	38.1057	49.3549
11	34.9773	38.2944	38.9434	37.5686	50.7529
12	34.9108	38.2595	38.8975	37.0766	50.6056
13	34.8743	38.2148	39.7543	36.3896	49.3658
14	34.8567	38.2764	41.8741	36.1033	47.1649
15	34.8898	38.2906	45.2542	35.8666	46.4206
16	34.9145	38.3787	49.9624	35.7272	45.7651
17	34.8838	38.6268	46.1365	35.7811	47.8917

18	34.85 45	39.123 4	43.48 67	35.88 34	46.89 34
19	34.82 98	39.823 4	42.95 56	35.69 88	46.38 49
20	34.80 14	40.628 5	43.71 65	35.71 00	44.88 15
21	34.79 13	41.284 8	43.85 26	36.02 10	43.78 76
22	34.75 10	41.657 9	43.53 34	36.37 06	43.81 36
23	34.75 18	41.977 1	43.00 33	36.76 56	43.02 65
24	34.73 97	42.259 2	43.26 58	36.86 71	43.99 26
25	34.73 84	42.924 8	43.82 37	36.86 90	44.23 27
26	34.75 57	43.229 4	44.51 20	36.85 15	43.61 51
27	34.85 24	43.638 6	45.33 58	36.86 28	43.80 70
28	34.91 41	43.786 8	46.28 37	36.80 00	44.00 03
29	34.87 10	43.737 9	47.04 49	36.83 67	43.75 40
30	34.82 85	43.703 3	47.49 46	36.84 32	43.33 40

V. CONCLUSION

By doing this dissertation, for video authentication different methods have been studied. For video two types of attacks are possible one spatial tampering attack and the other one temporal tampering attack

For spatial tampering attacks different techniques has been studied and for implementation purpose two techniques SVD based blind video watermarking and DWT-SVD based watermarking algorithm has been employed. Both techniques have their merits and demerits. Former one is blind technique in which original watermark is not required to extract the watermark while latter is non-blind technique in which original watermark is required during the extraction. While value of PSNR is good in DWT-SVD based technique.

For temporal tampering attacks SVM based machine learning technique is studied. This technique is best suited for this type of attacks and gives good results with good accuracy.

REFERENCES

- [1] Dawen Xu, Rangding Wang, Jicheng Wang, "A novel watermarking scheme for H.264/AVC video authentication", *Signal Processing: Image Communication(Elsevier)* 26 (2011)267–279
- [2] Osama S. Faragallah, "Efficient video watermarking based on singular value decomposition in the discrete wavelet transform domain", *Int. J. Electron. Commun. (Elsevier)* 67 (2013) 189–196
- [3] Po-Chyi Su, Chin-Song Wu, Ing-Fan Chen, Ching-Yu Wu, Ying-Chang Wu, "A practical design of digital video watermarking in H.264/AVC for content authentication", *Signal Processing: Image Communication(Elsevier)* 26 (2011)413–426
- [4] Xing Chang, Weilin Wang, Jianyu Zhao, Li Zhang, "A Survey of Digital Video Watermarking", *Seventh International Conference on Natural Computation 2011 IEEE*
- [5] Richa Singh, Mayank Vatsa, Sanjay K. Singh, Saurabh Upadhyay, "Integrating SVM classification with SVD watermarking for intelligent video authentication", *Telecommun Syst(Springer)* (2009) 40: 5–15
- [6] Hartung, F.; Kutter, M., "Multimedia watermarking techniques," *Proceedings of the IEEE*, vol.87, no.7, pp.1079-1107, Jul 1999
- [7] Wenhai Kong; Bian Yang; Di Wu; Xiamu Niu, "SVD Based Blind Video Watermarking Algorithm," *Innovative Computing, Information and Control, 2006. ICICIC '06. First International Conference on*, vol.1, no., pp.265,268, Aug. 30 2006-Sept. 1 2006
- [8] Upadhyay, S.; Singh, S.K., "Learning based video authentication using statistical local information," *Image Information Processing (ICIIP), 2011 International Conference on*, vol., no., pp.1,6, 3-5 Nov. 2011
- [9] Mohd Shahidan Abdullah, Azizah Abd Manaf, "An Overview of Video watermarking Techniques",

- Postgraduate Annual Research Seminar
2007
- [10] Ankita Hood, N.J Janwe, "A Review on Video Watermarking and Its Robust Techniques", International Journal of Engineering Research & Technology (IJERT), vol.2 Issue 1, January-2013
- [11] Potdar, V.M.; Song Han; Chang, E., "A survey of digital image watermarking techniques," *Industrial Informatics, 2005. INDIN '05. 2005 3rd IEEE International Conference on* , vol., no., pp.709,716, 10-12 Aug. 2005
- [12] Bhattacharya, S.; Chattopadhyay, T.; Pal, A., "A Survey on Different Video Watermarking Techniques and Comparative Analysis with Reference to H.264/AVC," *Consumer Electronics, 2006. ISCE '06. 2006 IEEE Tenth International Symposium on* , vol., no., pp.1,6
- [13] Rashel Sarkar, Smitha Ravi, "A Survey of Digital VideoWatermarking", the international journal of computer science & application, vol.1, no.2, April-2012
- [14] Hamid shojanazeri, Wan Azizum Wan Adnan, Sharifah Mumtadzah Syed Ahmad, "Video Watermarking Techniques for Copyright protection and Content Authentication", International Journal of Computer Information Systems and Industrial Management Applications, volume 5(2013), pp.652-660
- [15] Saurabh Upadhyay, Sanjay Kumar Singh, "Video Authentication: Issues and Challanges", IJCSI International Journal of Computer Science Issues, Vol. 9, Issue 1, No 3, January 2012



WIRELESS SENSOR NETWORK LOCALIZATION USING SOCP RELAXATION

¹Pragnesh S Patel, ²Niteen B.Patel

¹M.E, ²Asst. Prof E&C Department

Sarvajanik college of engg. & tech. surat

E-mail ID: ¹pragnesh64146@gmail.com, ²niteen.patel@scet.ac.in

Abstract— In recent year node localization is one of the most important issue since it plays a critical role in many situation. The aim of the sensor network localization problem is to determine positions of all sensor nodes in a network given certain pair wise noisy distance measurements and some anchor node positions using distributed localization algorithm based on second-order cone programming relaxation. The distributed sensor network localization algorithm using SOCP Relaxation is implemented and Simulation for uniform network topologies shows, the anchor position and distance estimation errors, and the performance gains achievable in terms of localization accuracy and computational efficiency.

Index Terms— Distributed algorithms, convex optimization, relaxation methods , Localization

I. INTRODUCTION

The development of MEMS, chip systems and wireless communications technology has fostered, low-powered and multi-function sensor nodes, which can integrate information collection, data processing, wireless communications and other functions together within the small storage, to gain rapid progress [1]. WSN is a multi-hop self-organizing network, where a large number of sensor nodes are deployed. The aim of WSN is to perceive, collect and process the information

of sensor nodes within the coverage of the network [1].

In wireless sensor networks (WSN's), localization is often performed by using the information of time-of-arrival (TOA), time-difference of-arrival (TDOA), received-signal-strength (RSS) measurements, or a combination of them [2]. However, localization by using TOA or TDOA information (including the Global Positioning System (GPS)) requires the complicated timing and synchronization, which makes sensor node localization cost-expensive and is not suitable for sensor networks with small, simple and cheap nodes [9]. In indoor environments, the signal from the GPS satellites is too weak to penetrate most buildings, making GPS useless for indoor localization [4]. We here consider the problem by using the RSS information without the need of timing and synchronization.

Currently, most node localization schemes for WSNs are relying on a small fraction of beacons scattered throughout the sensor network.. Beacons are sensor nodes which know their own positions (through GPS or other manual configurations) and serve as a reference for other nodes whose positions are unknown as they are deployed. The position discovery for the unknown nodes in these cases intends to exploit the multi hop character of WSNs, and rely more on the node-to-beacon distance measurements. Moreover, due to some special limitations on the sensor nodes, such as low memory and bandwidth, short battery life, and limited

communication and computation capability, a node localization scheme is commonly required distributed, robust and energy efficient, and so on [5].

In this paper, we present a distributed algorithm based

on second-order cone programming (SOCP) for solving the sensor network localization problem. In the presence of distance estimation errors each sensor node determines its position by executing the localization algorithm independently using distance information to the anchor and sensor nodes with which it is directly linked (i.e., which are within its communication range). If in addition to the distance estimation errors, the anchor positions also have errors then the algorithm consists of three steps: using the local distance information and inaccurate anchor positions each sensor node estimates its position. Then, the anchors execute the localization algorithm using position information from their neighbouring nodes and the associated distance information to refine their positions. Finally, the sensor nodes execute the localization algorithm to refine their position estimates [9].

One of the significant advantages of our approach is that it is fully distributed and converges to an optimal (or near-optimal) solution. As a result of the distributed nature of the solution, the problem dimension at each node is a linear function of only the number of neighbours of the node. There is no significant increase in the computational effort per node even in large networks (for a given node connectivity level), whereas most existing methods result in an exponential increase in the computation time with network size gets reduced. Thus, the distributed SOCP approach is suitable for large-scale networks with thousands of nodes.

The rest of the paper is organized as follows. Section II provides an overview of existing approaches. Section III presents the mathematical formulation and the SOCP relaxation of the localization problem. In section IV we present the distributed localization algorithm based on the SOCP relaxation. The simulation study appears as sections V.

II. RELATED WORK

A more generalized form of the localization problem is the distance geometry problem. It has been studied extensively, mostly in the frame-

work of Euclidean distance matrix (EDM) completion. Schoenberg and Young and Householder [5] established some basic properties of distance matrices. Ideas presented therein form the basis of a class of algorithms known as Multidimensional Scaling. Algorithms based on MDS sometimes use objective functions (such as the STRESS criterion) that ensure low-dimensional solutions for the given incomplete distance matrix.[22] The problem with these techniques is that there is possibility of getting stuck in local minima due to non-convex nature of the problem, and there is no guarantee of finding a desired realization in polynomial time. apply distributed weighted MDS (dwMDS) to the localization problem and formulate the problem using a general form of the cost function we use in this paper. They solve the minimization problem using majorizing functions. Biswas and Ye [22] solve the problem using the semidefinite programming (SDP) relaxation. This approach can solve small problems effectively. The authors report a few seconds of PC execution time for a 50 node network. They have also proposed two techniques to improve the accuracy of the SDP solution. The first technique adds a regularization term to the objective function to force the SDP solution to lie close to a low dimensional subspace of Rd and the second technique improves the SDP estimated solution using a gradient-descent method. [23]

A few variations of the original problem include localization in NLOS sensor networks, with mobile sensors, etc. Sensor Localization forms a sub-problem of the larger set of Graph Realization Problems. Other problems including, but not limited to molecule structure prediction, data visualization, internet tomography and map reconstruction. The concept can also be extended to problems of dimensionality reduction. Examples include face recognition and image segmentation.

A. Computational Complexity of Sensor Localization

The problem with MDS based algorithms is that there is a possibility of getting stuck in local minima due to the nonconvex nature of the problem, and there is no guarantee of finding a desired realization in polynomial time. With this in mind, researchers have also attempted to pin down the exact computational complexity of this problem. Saxe proved that the EDM problem is

NP-hard in general. See also [2]. Aspnes et al. [3] proved a similar result in the context of sensor localization. More and Wu, who used global optimization techniques for distance geometry problems in the molecule conformation space, established that finding an optimal solution, when is small, is also NP-hard. Other general global optimization approaches which employ techniques like pattern search face similar problems.

Localization as such is a non-convex optimization problem with multiple local minima. It was formulated as a feasibility problem with convex radial constraints by Doherty et. al. [3]. However, it required centralized computation which made it unsuitable for large-scale networks. A distributed localization method MDS MAP(P,R) was proposed by Shang based on multi-dimensional scaling (MDS) [2]. However, it involved lots of redundant calculation while merging local data for sensors to get global data for the entire network.

The SDP relaxation problem proposed by Biswas and Ye [24] adds a regularization term in the objective function to reduce the rank of the SDP solution, thereby reducing the estimation error. Refining of the initial estimates is also done, using a gradient-descent method.

Computational efficiency becomes increasingly important in case of mobile sensor networks, requiring dynamic estimation of sensor positions.

III. SENSOR NETWORK LOCALIZATION: PROBLEM FORMULATION

Sensor nodes measure physical quantities at a given position. In most applications, the data reported by the sensors is relevant only if tagged with accurate position of the nodes. But equipping each node with a GPS is a costly affair. Also, it has geographical constraints (for instance, it doesn't work indoors). Hence, the sensor network localization problem is of extreme importance.

It can be formulated as follows:

“Assuming knowledge of the positions of some nodes and some pairwise distance measurements, determine the position of all nodes in the network. Nodes whose positions are known beforehand are called reference nodes (RN) or anchors, and nodes whose positions are unknown as the un-localized nodes (UN) or

sensors. The localization problem can be broken down into two sub problems:

(i) Ranging: To determine the distance (or range) between two neighboring nodes, for select nodes, depending on the model used. Usually, the constraints are noise in measurement and non-practicality of large distances between nodes, hence distances only less than a specified “RadioRange” are considered.

(ii) Positioning: To determine the position or location of the nodes given some pairwise distances.

Mathematically speaking, there are distinct points in \mathbb{R}^d ($d \geq 1$). We know the Cartesian coordinates of the last $n-m$ points (“anchors”) x_{m+1}, \dots, x_n and the Euclidean distance $d_{ij} > 0$ between “neighboring” points i and j for $(i, j) \in A$, where $A \subseteq (\{1, \dots, n\} \times \{1, \dots, m\}) \cup (\{1, \dots, m\} \times \{1, \dots, n\})$. We wish to estimate the Cartesian coordinates of the first m points (“sensors”).”

Here, we present a systematic approach towards sensor localization taking into account the statistical modeling of the ultra-wideband physical layer channel. This is accomplished through a distributed approach to refine sensor position estimates. Because most sensor localization approaches in the literature do not take into account the errors in node positions. But here, we have assumed erroneous node positions (both for sensors and anchors) and the localization is done in a three step process.

- (1) Sensor positions are estimated using information from their neighbors.
- (2) Anchor positions are refined using relative distance information exchanged with their neighbors.
- (3) Sensor positions are re-estimated using refined anchor positions of their neighbors.

Such a distributed approach goes a long way in discarding the effects of inaccurate node positions.

Simulations have performed on uniform and irregular network topologies, and dependency of localization accuracy and computational efficiency with various factors has been studied.

A. Convex Optimization using Matlab

MATLAB takes the help of certain “solvers” for solving convex optimization problems; common ones include CVX, SEDUMI, CPLEX, GUROBI etc. Different solvers are recommended for different optimization

problems. E.g. SEDUMI, SDPT3, CSDP, SDPA work best for Semidefinite Programming (SDP), while GUROBI and MOSEK are good for integer linear programming (LP). Now, which solver to choose depends on both the problem size and the type of the problem.[26] The variations in the type of problem can include constraints, which can be one the 5 types:

- None(unconstrained)
- Bound
- Linear (including bound)
- General (smooth)
- Discrete (integer)

As well as the type of optimization problem to be solved, which can be of one of the following types:

- Linear
- Quadratic
- Sum-of-squares (Least Squares)
- Smooth Nonlinear
- Non-smooth

IV. DISTRIBUTED SOCP LOCALIZATION ALGORITHM

1) SOCP Relaxation

SOCP has been chosen due to its simpler structure and computational efficiency. The SOCP relaxation was first studied by Tseng. Although it is weaker than SDP, its computational superiority enables the use of localization in mobile sensor networks.

In general, a second-order cone program (SOCP) is defined as:

$$\text{minimize } f^T x$$

$$\text{subject to } |A_i x + b_i|_2 \leq c_i^T x + d_i, \quad i=1, \dots, m$$

$$Fx = g,$$

where $x \in R^n$ is the optimization variable,

$$A_i \in R^{n \times n}, \text{ and } F \in R^{p \times n},$$

Now, the problem can be formulated as

$$\min_{x_1, \dots, x_m} \sum \left\| \|x_i - x_j\|^2 - d_{ij}^2 \right\| \quad (1)$$

where $\|\cdot\|$ denotes the Euclidean norm.

This can be rewritten in a convex form (by relaxing equality constraint to “greater than or equal to” inequality) as:

$$\min_{x_1, \dots, x_m} \sum_{(i,j) \in A} |y_{ij} - d_{ij}^2| \text{ s.t. } y_{ij} \geq \|x_i - x_j\|^2, \text{ for all } (i,j) \in A \quad (2)$$

The SOCP has $(d+3)|A| + m \cdot d$ variables and $(d+2)|A|$ equality constraints. In sensor network localization, $|A| = \Omega(m)$ and $d = 2$, so that (7) has $\Omega(m)$ variables and $\Omega(m)$ equality constraints.

Distributed Algorithm:

In a distributed algorithm, the optimal result is obtained in stages. Timing of computations at any one processor/node during a stage can be independent of the timing of computations at nodes in the same stage. All interactions and exchange of information / refining of positions takes place at the end of a particular stage. Here, in the SOCP it has been found in paper that each sensor can independently solve the minimization problem using position information only from its neighbor nodes.

Let $NB_A(i)$ denote the set of neighbor nodes for node x_i of the network. Above SOCP can be solved independently over the m sensor nodes, where each node uses information (x_j, d_{ij}) from its neighboring nodes $x_j, j \in NB_A(i)$. Thus, the SOCP decomposes to the following distributed formulation:

$$\begin{aligned} \min_{x_i, y_{ij}} \sum_{j \in NB_A(i)} t_{ij} \quad (3) \\ \text{s.t. } y_{ij} \geq \|x_i - x_j\|^2, \quad \text{for all } (i, j) \in A \\ t_{ij} \geq |y_{ij} - d_{ij}^2| \end{aligned}$$

The distributed SOCP algorithm consists of a phase where each sensor node estimates its position using local information and solving the SOCP (3). In an iterative distributed scheme, this would be followed by a communication phase wherein each node exchanges its position estimate with its neighbors. These iterations are repeated after fixed intervals of time or when any new information becomes available at a node. It should be noted that the algorithm uses information from neighboring anchors as well as sensors to position a given node. Thus to obtain a non-trivial position estimate each node needs at least 3 neighbors (for 2-D localization) with position estimates, as opposed to the more stringent requirement of having 3 anchors in the neighborhood that many triangulation/trilateration schemes impose. If the anchor positions are inaccurate, the distributed SOCP approach will consist of three steps: after the sensor nodes estimate their positions based on the inaccurate anchor positions and distance

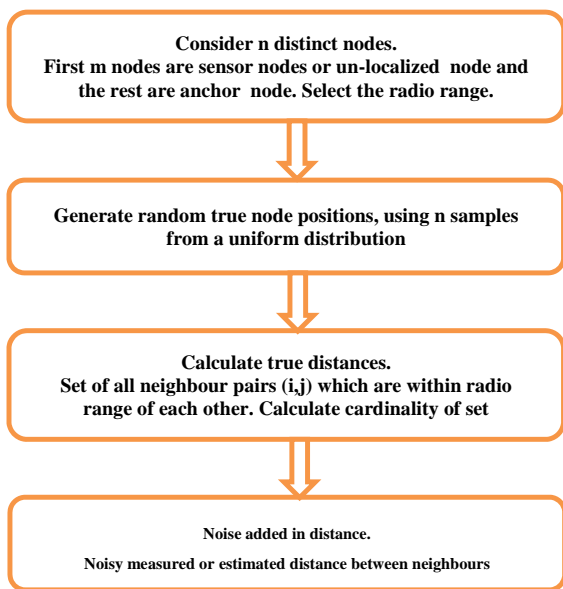
information, the anchors solve the local SOCP using position information from their neighboring nodes and the associated distance information to refine their positions. As we will show, this second step results in a significant improvement in the positioning accuracy of the inner anchors. Finally, another iteration of the local SOCP over the sensor nodes further refines their position estimates.

Let $n_i (=|N_A(i)|)$ represent the number of neighbors of the node x_i . SOCP has $2n_i+3$ variables, $2n_i$ conic constraints and 1 equality constraint. In sensor networks, due to the short radio range of the sensors, the number of neighbors of a given node is a small fraction of the total number of nodes in the network (i.e., $n_i \ll n$). Thus, the distributed SOCP approach results in significantly smaller problem sizes than approaches proposed in the literature. The SOCP problem can be efficiently solved by interior point methods. Here we use SeDuMi to solve this problem.

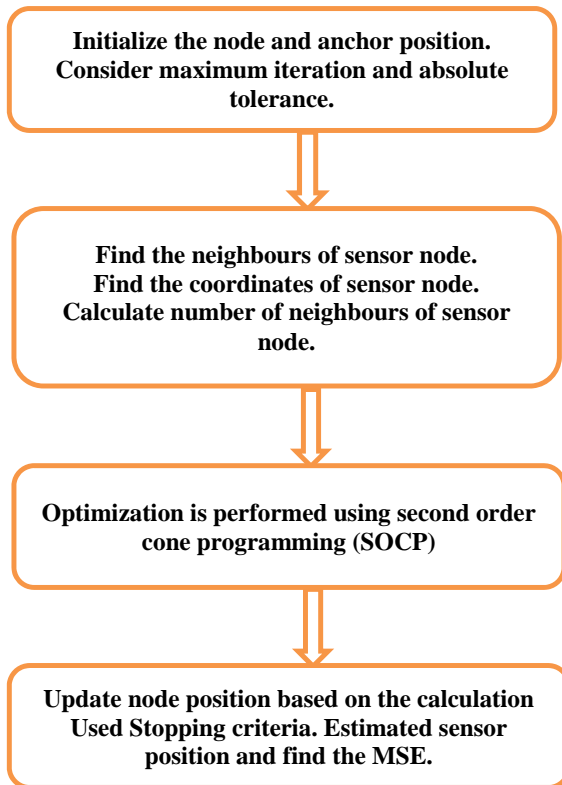
V. Algorithm and Simulation results

1. Distance Measurement Algorithm:

In this algorithm using anchor node and pair wise distance is measured. Position computation algorithm using this distance find the node position. finally find the error between true node position and estimated node position.



2. Position Computation and Localization Algorithm:



B. Simulation Results :

Simulation is performed in matlab. In this experiment using uniform distribution is used for node deployment. As shown in figure.1. number of nodes is 300, number of node is 0.15 percentage, RadioRange 0.06 and noise factor n_{fa} is 0.05. In figure 1 sensor node shown by anchor node shown by and estimated position of node is denoted by +. Line shows the true node position and estimated position difference.

fig.1. Distributed SOCP results for Uniform topology: $n = 300$, Radio Range = 0.6, $p = 0.15$ and $n_{fd} = 0.05$

Test case	n	Radio Range	p	CPU time per node (in sec)	Error
1	500	0.10	0.15	0.2188	0.0791
2	500	0.12	0.15	0.2500	0.1292
3	500	0.14	0.15	0.2836	0.0256

4	500	0.16	0.15	0.3438	0.0345
5	500	0.18	0.15	0.2344	0.0404
6	500	0.20	0.15	0.3906	0.0392
7	500	0.22	0.15	0.4688	0.0391
8	500	0.24	0.15	0.4844	0.0333
9	500	0.26	0.15	0.4688	0.0427

Table 1 . Different RadioRange for n=500,p=0.15

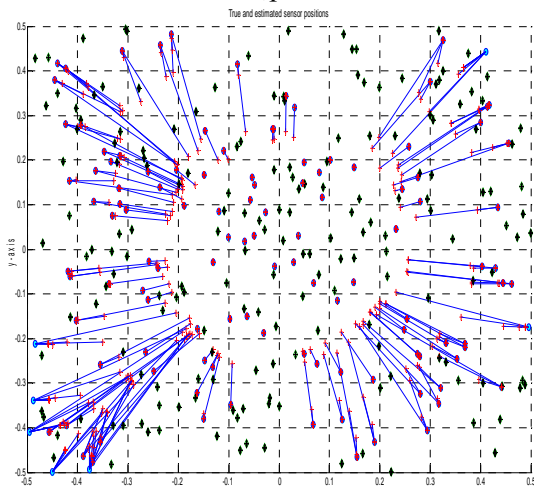


fig.1. Distributed SOCP results for Uniform topology: n = 300, Radio Range = 0.6, p = 0.15 and nfd = 0.05

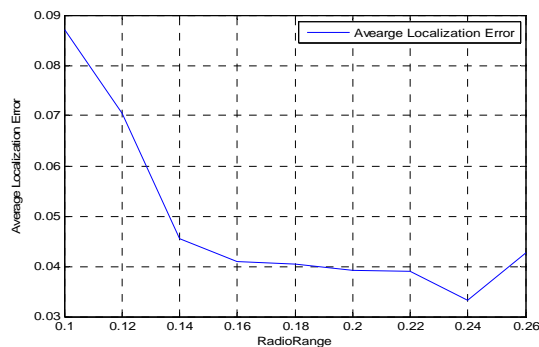


Fig.2.Average positioning error as a function of different RadioRange. (n = 500,p= 0.15 and nfd= 0.05)

Test case	n	p	nfa	Radio Range	CPU Time per node	Error
1	1000	0.15	0.05	0.08	0.2969	0.0497
2	1000	0.15	0.05	0.10	0.2656	0.0298
3	1000	0.15	0.05	0.15	0.3438	0.0281
4	1000	0.15	0.05	0.20	0.6719	0.0268
5	1000	0.15	0.05	0.25	0.8125	0.0294

Table.2 Different RadioRange for n=500,p=0.15

Fig.3.Average positioning error as a function of different RadioRange. (n = 1000,p= 0.15 and nfd= 0.05)

COMPARISON

Plot the graph noise factor and average node localization as shown in fig.4. Noise factor is increased average node localization accuracy is decrease. This graph shows that changes in distributed SOCP algorithm in k and pars. structure gives less error as compare to SOCP algorithm. Table shows parameter of the distributed SOCP algorithm. The performance increases is shown in graph and table.

As shwn in table implemented SOCP can give compare to paer (9). Taken 500 node , RadioRange 0.15, anchor percentage 0.15, noise factor for sensor node is difeerent different and noise factor for anchor node is taken 0.10 and simulate.

Test case	n	RadioRange	p	nfa	nfa	Implemented SOCP error	SOC P error
1	500	0.15	0.15	0.10	0.02	0.0406	0.0480
2	500	0.15	0.15	0.10	0.04	0.0411	0.0490

3	50 0	0.15	0.1 5	0.1 0	0.1 0	0.04 34	0.04 70
4	50 0	0.15	0.1 5	0.1 0	0.1 5	0.04 83	0.05 35
5	50 0	0.15	0.1 5	0.1 0	0.2 0	0.05 22	0.05 90

Table 5.3 Different noise factor for sensor node nfa and its parameter for n=500, RadioRange=0.15,p=0.15 and anchor node position nfa=0.10

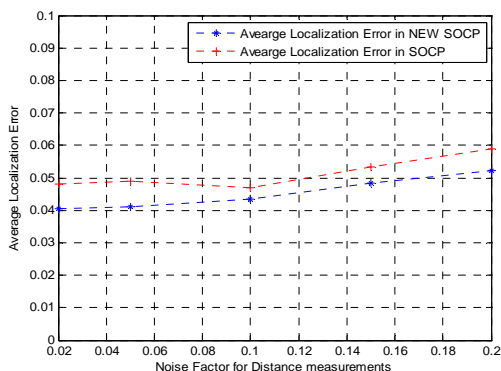


Fig. 4. Average positioning error as a function of the Noise Factor nfd. (n = 500, Radio Range = 0.15, p = 0.15)

CONCLUSIONS

Distributed approach goes a long way in discarding the effects of inaccurate node positions. Simulations have performed on uniform topology, and dependency of localization accuracy and computational efficiency with various factors has been done. Average node localization accuracy is improved as compared to the Distributed SOCP localization accuracy. In SeDuMi solver a Different parameter of second order cone constraints are used and get accurate result.

REFERENCES

1. Guangjie Han HuihuiXuTrung Q, Duong. Jinfang Jiang Takahiro Hara”Localization algorithms of wireless sensor network:a survey,” Telecommunication syst, springer, p.p.2419-2436,2013
2. Gang Wang; Kehu Yang, "A New Approach to Sensor Node Localization Using RSS Measurements in Wireless Sensor Networks," Wireless Communications, IEEE Transactions on , vol.10, no.5, pp.1389-1395, May 2011
3. Ouyang, R.W.; Wong, AK.-S.; Chin-Tau Lea, "Received Signal Strength-Based Wireless Localization via Semidefinite

Programming: Noncooperative and Cooperative Schemes," Vehicular Technology, IEEE Transactions on , vol.59, no.3, pp.1307-1318, March 2010

4. Ahmad, A; Serpedin, E.; Nounou, H.; Nounou, M., "Joint Node Localization and Time-Varying Clock Synchronization in Wireless Sensor Networks," Wireless Communications, IEEE Transactions on , vol.12, no.10, pp.5322-5333, October 2013
5. Stoleru, R.; Tian He; Mathiharan, S.S.; George, S.M.; Stankovic, J.A, "Asymmetric Event-Driven Node Localization in Wireless Sensor Networks," Parallel and Distributed Systems, IEEE Transactions on , vol.23, no.4, pp.634-642, April 2012
6. Patwari, N.; Ash, J.N.; Kyperountas, S.; Hero, AO.; Moses, R.L.; Correal, N.S., "Locating the nodes: cooperative localization in wireless sensor networks," Signal Processing Magazine, IEEE , vol.22, no.4, pp.54-69, July 2005
7. QinQin Shi. Hong Huo. Tao Fang. DerenLi,"A Distributed Node Localization Scheme for wireless Sensor Network,"WirelessPresComun, springer, p.p.15- 33,2010
8. F. Akyildiz, W. Su, Y. Sankarasubramaniam, and E. Cayirci, "A survey on sensor networks," IEEE Commun. Mag., vol. 40, no. 8, pp. 102–114, Aug. 2002.
9. SeshanSrirangarajan, Ahmed H. Tewfik, and Zhi-QuanLuo," Distributed Sensor Network Localization Using SOCP Relaxation ", IEEE Transactions on Wireless Communications, Vol. 7, NO. 12, DECEMBER 2008
10. Naddafzadeh-Shirazi, G.; Shenouda, M.B.; Lampe, L., "Second Order Cone Programming for Sensor Network Localization with Anchor Position Uncertainty," Wireless Communications, IEEE Transactions on , vol.13, no.2, pp.749,763, February 2014
11. G. Mao and B. Fidan, Localization algorithms and strategies for wireless sensor networks. Information Science reference, Hershey. New York, 2009.
12. Z. Sahinoglu, S. Gezici, and I. Guvenc, Ultra-wideband positioning systems: theoretical Limits, ranging algorithms, and protocols. New York: Cambridge University Press, 2008.

13. S. De, C. Qiao, D. A. Pados, M. Chatterjee, and S. J. Philip, "An integrated crosslayer study of wireless CDMA sensor networks," *IEEE Journal on Selected Areas in Communications*, vol. 22, no. 7, pp. 1271-1285, Sep. 2004.
14. A. H. Sayed, A. Tarighat, and N. Khajehnouri, "Network-based wireless location: challenges faced in developing techniques for accurate wireless location information," *IEEE Signal Processing Magazine*, vol. 22, no. 4, pp. 24-40, Jul. 2005.
15. S. Gezici, "A survey on wireless position estimation," *Wireless Personal Communications (Special Issue on Towards Global and Seamless Personal Navigation)*, vol. 44, no. 3, pp. 263-282, Feb. 2008.
16. S. Gezici, Z. Tian, G. B. Giannakis, H. Kobayashi, A. F. Molisch, H. V. Poor, and Z. Sahinoglu, "Localization via ultra-wideband radios: a look at positioning aspects for future sensor networks," *IEEE Signal Processing Magazine*, vol. 22, no. 4, pp. 70-84, Jul. 2005.
17. Y. C. Eldar, "Uniformly improving the Cram_er-Rao bound and maximum likelihood estimation," *IEEE Transactions on Signal Processing*, vol. 54, no. 8, pp. 2943-2956, Aug. 2006.
18. S. Slijepcevic, S. Megerian, and M. Potkonjak, "Location errors in wireless embedded sensor networks: sources, models, and effects on applications," *Sigmobile Mobile Computing and Communications Review*, vol. 6, pp. 67-78, Jul. 2002.
19. S. Slijepcevic, S. Megerian, and M. Potkonjak, "Location errors in wireless embedded sensor networks: sources, models, and effects on applications," *Sigmobile Mobile Computing and Communications Review*, vol. 6, pp. 67-78, Jul. 2002.
20. P. Biswas and Y. Ye, "Semidefinite programming for ad hoc sensor network localization," in *Proc. Int. Symp. on Information Processing in Sensor Networks (IPSN)*. Springer Verlag, , pp. 46-54 Apr. 2004.
21. P. Biswas, T.-C. Liang, K.-C. Toh, T.-C. Wang, and Y. Ye, "Semidefinite programming approaches for sensor network localization with noisy distance measurements," *IEEE Trans. Autom. Sci. Eng.*, vol. 3, no. 4, pp. 360-371, Oct. 2006.
22. Y. Shang, W. Ruml, Y. Zhang, and M. Fromherz, "Localization from connectivity in sensor networks," *IEEE Trans. Parallel Distrib. Syst.*, vol. 15, no. 11, pp. 961-974, Nov. 2004.
23. J. A. Costa, N. Patwari, and A. O. Hero, "Distributed weighted multidimensional scaling for node localization in sensor networks," *ACM Trans. Sensor Networks*, vol. 2, pp. 3964, Feb. 2006.
24. P. Biswas, T.-C. Liang, K.-C. Toh, T.-C. Wang, and Y. Ye, "Semidefinite programming approaches for sensor network localization with noisy distance measurements," *IEEE Trans. Autom. Sci. Eng.*, vol. 3, no. 4, pp. 360-371, Oct. 2006.
25. J. Strum, "Using SeDuMi 1.02, A Matlab Toolbox for Optimization Over Symmetric Cones (Updated for Version 1.05)," Oct. 2001.
26. S. Boyd and L. Vandenberghe, *Convex Optimization*. Cambridge University Press, 2004.



COMPARATIVE ANALYSIS OF DIFFERENT APPROACHES FOR HYPERSPECTRAL UNMIXING

¹Chirag Hirpara, ²Vankar Jyoti P.

M.E, Electronics and Communication Engineering,
Sarvajanik college of Engineering and Technology, Surat,
Email: ¹chiraghirpara0@gmail.com, ²jyoti.ec@gmail.com

Abstract - The hyperspectral cameras used for imaging are having low spatial resolution, and thus the pixels in the captured image will be mixtures of spectra of various materials present in the scene. Thus spectral unmixing comes as an unavoidable step in hyperspectral image processing. Spectral unmixing is an important problem in hyperspectral data exploitation. It amounts at characterizing the mixed spectral signatures collected by an imaging instrument in the form of a combination of pure spectral constituents (endmembers), weighted by their correspondent abundance fractions. This paper presents a comparative study and performance analysis of different approaches for unmixing. Three geometrical algorithms for spectral unmixing, namely PPI, N-FINDER VCA and MVSA are introduced in this paper. Also the paper represents the algorithms based on statistical approaches, those are NMF, NMF with piecewise smoothness constraint and NMF with sparseness constraint.

Index Terms-Hyperspectral imaging, Spectral signature, Spectral unmixing, PPI, N-FINDER, VCA, MVSA, NMF, nsNMF, NMFSC.

I. INTRODUCTION

HYPERSPECTRAL sensor collects 3-dimensional data with two spatial dimensions and one spectral dimension as shown in Fig. 1. Spectral dimension contain the data in hundreds of very narrow contiguous bands, and this

provides a good way for the identification of various materials over the observed scene captured by the sensor.

The various materials are discriminated on their unique spectral signatures as shown in Fig. 2. Hyperspectral imaging is having a wide range of applications in various fields as in agriculture, planetary remote sensing, military, environmental monitoring etc[1]. The hyperspectral imaging sensors can capture many contiguous bands which is having very high spectral resolution and this will be covering not only visible regions but also the infra red regions of electromagnetic spectrum(0.3-2.5 μm)[2],[3].

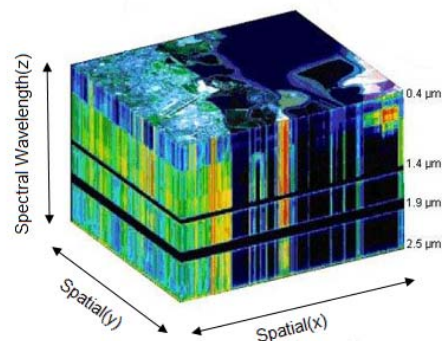


Fig. 1. An Example of a Hyperspectral Image

Advanced hyperspectral sensors like AVIRIS of NASA is now able to cover the above mentioned wave-length region using about 200 spectral channels. In the case of hyperspectral images, depending upon the spatial resolution of sensor, the individual pixels in the captured scene may comprise of more than one material.

Each pixel will be the mixture of various materials of the surface patch and thus the spectra observed will contain multiple endmembers (or spectral signatures) and thus the further analysis becomes difficult. This happens mainly because of the poor spatial resolution of the sensor used. There arises the need of hyperspectral unmixing. Hyperspectral unmixing aims at the decomposition of the observed spectra into a set of pure reference materials(endmembers)and their abundance fractions. Thus unmixing process gives both spectral signatures and corresponding abundance maps of materials present in the scene. This unmixing problem has been a subject to many investigative studies for the past many years.

Hyper Spectral unmixing is basically a blind source separation problem. Hyperspectral sense contain sources which are statistically dependent and they may combine either in a linear or nonlinear fashion. This makes spectral unmixing problem to be placed in higher level compared to other source separation problems.

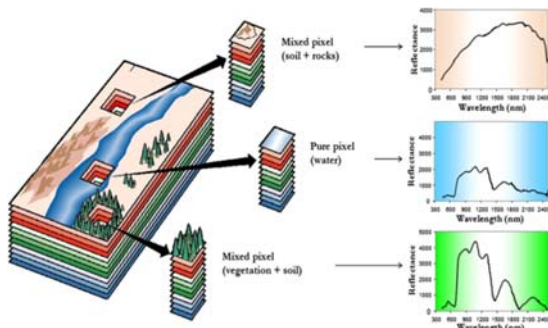


Fig. 2. Reflectance Spectrum of the pixels.

A. Mixing Models

Unmixing can be classified to linear[3] and Non linear[3].Linear models assume that the mixing scale is macroscopic, and the light which falls on the surface interacts with only one material. This type of mixing takes place due to the low spatial resolution of the sensor. Here multiple scatterings do not take place. In the case of Nonlinear mixing models the interaction between the light which is scattered by multiple materials occurs, and the mixed model becomes complicated. The interactions can be at Intimate or microscopic level. Thus non-linear unmixing becomes a difficult task. So here this paper concentrates in

linear unmixing due to its simplicity, and also it's the basis of many algorithms for more than 30 years.

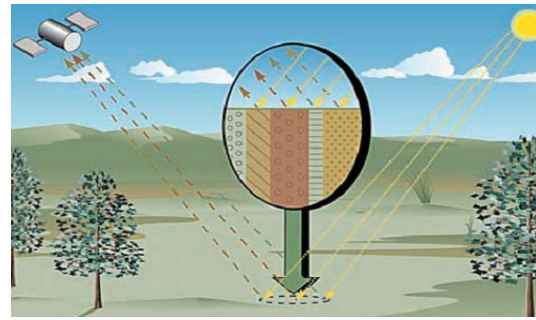


Fig. 3. Linear mixing model without any multiple scattering effects.

The linear mixing model assumes that the spectrum of a pixel in the acquired scene is a linear combination of all pure materials (endmembers) present in the scene. it is assumed that the hyperspectral sensor used for capturing the scene has L spectral bands, linear mixing model can be mathematically represented as in Fig. 4. The relation between them is given as per the follow.

$$R = X + n \quad (1)$$

Where, $X = MS$

$$R = MS + n(2)$$

Where, $S = \gamma\alpha$

$$R = M\gamma\alpha + n(3)$$

Here term \mathbf{R} is the original image cube. We can represent $\mathbf{R}_{ij} \in \mathbb{R}_L$ as an observation array at a single pixel. Matrix $\mathbf{M} \in \mathbb{R}_L \times \mathbb{P}$ is our observed spectral endmember signature matrix having each column $\mathbf{M}_p \in \mathbb{R}_L$ and here \mathbb{P} represents the total number of endmembers present in our image data. Matrix \mathbf{S} represents the relative abundance cube. Its every column $\mathbf{S}_{ij} \in \mathbb{R}_P$ is defined as an abundance vector related with \mathbf{R}_{ij} . In abundance matrix \mathbf{S} each element of it denoting the relative abundance fraction of endmember present in \mathbf{R}_{ij} .

For simplicity, “matrix-to-vector” alignment process is used. In this method all the rows in the matrix are concatenates together to form a single vector. This process is mainly applied for the conversion of band in \mathbf{R} and abundances in \mathbf{S} . So

our matrices will now change in dimensions. Original \mathbf{R} is of $i \times j \times L$, where $K=i \times j$, \mathbf{M} is of $L \times P$ and \mathbf{S} is of $i \times j \times P$. This dimensions will then transformed to \mathbf{R} is of $L \times K$, \mathbf{M} is of $L \times P$ and \mathbf{S} is of $P \times K$, respectively, where K is the number of pixels, P in the number of endmembers, L is the total spectral bands. In this modeling both \mathbf{M} and α have to be found by unmixing. Here basic two constraints are used.

ANC (abundance nonnegative constraint): It says that the each and every component present in our

Fig. 4. Simplified linear mixture model

II. GEOMETRICAL APPROACHES

As per the geometrical point of view the linearly mixed vectored generated by the mixing process are always stays in a simplex set of data (positive cone). It uses basically geometric properties of an image. These approaches take advantage of the analogy between mixing models and the geometric orientation of hyperspectral data in multidimensional spaces.

A. Endmember extraction algorithms overview

Geometrical approaches come as the third category of spectral unmixing algorithms. Basically it follows the fact that, under the linear mixing model spectral vectors belong to the simplex set whose vertices correspond to the endmembers. Thus by finding out the vertices it is possible to find out the endmember in the hyperspectral image.

There are two categories in this approach. Algorithms which assume the presence of pure pixels comes under the one category and algorithms which do not assume the presence of pure pixels comes under another category. MVSA (minimum volume simplex analysis) [11], MVES (minimum volume enclosing simplex), SISAL (simplex identification via split and augmented lagrangian), etc comes under the first category. In the second category to which this paper concentrates, come the following algorithms like SVMAX (successive volume maximization), AVMAX (Alternating volume maximization), ADVMM (alternating decoupled volume max-min), SDVMM (successive decoupled volume

signature matrix \mathbf{M} should always be nonnegative so it is given as eq. (4).

$$M_{lp} \geq 0, 1 \leq l \leq L \quad (4)$$

ASC (abundance sum to one constraint): It says that the sum of all the relative fraction of each pixel should be equal to unity as given as eq. (5).

$$\underline{S}_{ijp} \in [0,1], \sum_{p=1}^P \underline{S}_{ijp} = 1 \quad (5)$$

max-min), N-FINDR, VCA (vertex component analysis), IEA (iterative error analysis), PPI (pixel purity index), etc are some of the algorithms come under this section.

B. Pure pixels based geometrical algorithms

As discussed in the previous sections geometrical algorithms with pure pixel assumption assumes the presence of at least one pure pixel per endmember. These pure pixel algorithms still belong to minimum volume class. This assumption of pure pixel make these algorithms very efficient but still creates difficulty in some datasets. In this section a brief theoretical side of each of the 5 algorithms namely PPI, N-FINDER, VCA, MVSA is given.

C. N-FINDER

This is another popular algorithm used for spectral unmixing. This also works according to winter's belief [24]. This is a pure pixel based algorithm and this search for the set of pixels with largest possible volume by inflating a simplex inside the given dataset. The original N-FINDER algorithm [3] is having 4 steps as follows.

1) Feature reduction - In this the dimension of data is reduced from n to $P-1$ by some PCA [32] or MNF [33], where P is the number of endmembers to be identified.

2) Take some randomly selected endmembers from the dataset as $\{E_1^{(0)}, E_2^{(0)}, E_3^{(0)}, \dots, E_p^{(0)}\}$

3) At each iteration $k \geq 0$, calculate the volume by this set of endmembers as follows.

$$v(E_1^{(k)}, E_2^{(k)}, \dots, E_p^{(k)}) = \frac{\left| \det \begin{bmatrix} 1 & 1 \dots & 1 \\ E_1^{(k)} & E_2^{(k)} \dots & E_p^{(k)} \end{bmatrix} \right|}{(p-1)!} \quad (6)$$

4) Replacement- For each and every pixel the volume corresponding to it is checked by this way, if this pixel replaces one of the given endmember positions in matrix shown above. If the replacement of pixel results in an increase in volume, the pixel replaces the endmember. This process continues until there are no endmember replacements in the given data.

D. Vertex component analysis

The pseudo-code for the VCA method is shown in following steps. Symbols $[\hat{M}]_{:,j}$ and $[\hat{M}]_{:,i:k}$ stand for the j th column of \hat{M} and for the i th to k th columns of \hat{M} , respectively. Symbol \hat{M} stands for the estimated mixing matrix.

Step 1 Hyperspectral data cube (R) and number of endmembers (p) are known and can be an input of VCA.

Step 2 Find out value of SNR_{th} for given p .

Step 3 Test if the SNR is higher than SNR_{th} in order to decide whether the data is to be projected onto a subspace of dimension p or $p-1$. In the first case the projection matrix U_d is obtained by SVD from RR^T/N . In the second case the projection is obtained by PCA from $(R - \bar{r})(R - \bar{r})^T/N$ (recall that \bar{r} is the sample mean of $[R]_{:,i}$, for $i = 1, \dots, N$).

Steps 5 and 10 ensure that the inner product between any vector $[X]_{:,j}$ and vector u is non-negative, a crucial condition for the VCA algorithm to work correctly. The chosen value of $k = \text{argmax}_{j=1 \dots N} \|[X]_{:,j}\|$ ensures that the colatitude angle between u and any vector $[X]_{:,j}$ is between 0° and 45° , then avoiding numerical errors that otherwise would occur for angles near 90° .

Step 15 initializes the auxiliary matrix A , which stores the projection of the estimated endmembers signatures. Assume that there exists at least one pure pixel of each endmember in the

input sample R . Each time the loop for is executed, a vector f orthonormal to the space spanned by the columns of the auxiliary matrix A is randomly generated and y is projected onto f . Knowing that pure endmembers occupy the vertices of a simplex, then $a \leq f^T [Y]_{:,i} \leq b$, for $i = 1, \dots, N$, where values a and b correspond only to pure pixels. The endmember signature corresponding to $\max(|a| |b|)$ is stored. The next time loop for is executed, f is orthogonal to the space spanned by the signatures already determined. Since f is the projection of a zero-mean Gaussian independent random vector onto the orthogonal space spanned by the columns of $[A]_{:,1:i}$, then the probability of f being null is zero. Note that the underlying reason for generating a random vector is only to get a non null projection onto the orthogonal space generated by the columns of A . Figure 4.2 shows the input samples and the chosen pixels, after the projection $v = f^T Y$. Then a second vector f orthonormal to the endmember a is generated and the second endmember is stored. Finally, steps 25 and 27 compute the columns of matrix \hat{M} , which contain the estimated endmembers signatures in the L -dimensional space.

E. Minimum volume simplex analysis algorithm

Let $Y \equiv [y_1, y_2, \dots, y_N] \in R^{p \times n}$ is a matrix holding in its columns the spectral vectors $Y_i \in R^p$, for $i = 1, 2, \dots, n$, of a given hyperspectral data set. Although not strictly necessary, we assume in this version of the algorithm that a dimensionality reduction step has been applied to the data set and the vectors $Y_i \in R^p$ are represented in the signal subspace spanned by the endmember spectral signatures. Under the linear mixing model, we have spectral signatures. Under the linear mixing model, we have

$$Y = MS \quad (7)$$

$$\text{S.t.: } S \geq 0, 1_p^T S = 1_n^T$$

Where, $M \equiv [m_1, m_2, \dots, m_p] \in R^{p \times p}$ is the mixing matrix (m_i denotes the i th endmember signature and p is the number of endmembers), and $S \in R^{p \times n}$ is the abundance matrix containing

the fractions ($[S]_{i,j}$ denotes the fraction of material m_i at pixel j). For each pixel, the fractions should be no less than zero, and sum to 1, that is, the fraction vectors belong to the probability simplex. Therefore, the spectral vectors Y_i belong, as well, to a simplex set with vertices m_i , for $i = 1, 2, \dots, p$.

Given Y , and inspired by the seminal work, we infer matrices M and S by fitting a minimum volume simplex to the data subject to the constraints in eq. (7). This can be achieved by finding the matrix M with minimum volume defined by its columns under the constraints in eq. (7). It can be formulated as the following optimization problem:

$$M^* = \arg \min |\det(M)| \quad (8)$$

$$\text{s.t.: } QY \geq 0, 1_p^T QY = 1_N^T$$

Where, $Q \equiv M^{-1}$. Since $\det(Q) = 1 / \det(M)$, we can replace the problem in eq. (8) with the following:

$$Q^* = \arg \max \log |\det(Q)| \quad (9)$$

$$\text{s.t.: } QY \geq 0, 1_p^T QY = 1_N^T$$

Optimizations eq. (8) and (9) are nonlinear, although the constraints are linear. Problem eq. (8) is nonconvex and has many local minima. So, problem eq. (9) is nonconcave and has many local maxima. Therefore, there is no hope in finding systematically the global optima of (9). The MVSA algorithm, we introduce below aims at “good” suboptimal solutions of optimization problem (9).

Our first step is to simplify the set of constraints $1_p^T QY = 1_N^T$ by noting that every spectral vector y in the data set can be written as a linear combination of p linearly independent vectors taken from the data set, say $Y_p \equiv [y_{i1}, y_{i2}, \dots, y_{ip}]$

, where the weights add to one: i.e., $y = Y_p \beta$, where $1_p^T \beta = 1$. It turns out then, the constraint $1_p^T QY = 1_N^T$ is equivalent to $1_p^T QY_p = 1_N^T$ or else to $1_p^T Q = 1_N^T (Y_p)^{-1}$. Defining $q_m = 1_N^T (Y_p)^{-1}$, we get the equality constraint $1_p^T Q = 1_N^T (Y_p)^{-1}$. Then, the problem (9) simplifies to

$$Q^* = \arg \max \log |\det(Q)| \quad (10)$$

$$\text{s.t.: } QY \geq 0, 1_p^T Q = q_m$$

We solve the optimization problem (10) by finding the solution of the respective Kuhn-Tucker equations using sequential quadratic programming (SQP) methods. This method belongs to the constrained Newton (or quasi-Newton) and guarantee superlinear convergence by accumulating second-order information regarding

The Kuhn-Tucker equations. Each quadratic problem builds a quadratic approximation for the Lagrangian function associated to (10). For this reason, we supply the gradient and the Hessian of \ln each SQP iteration.

Usually, the hyperspectral data sets are huge and, thus, the above maximization is heavy from the computational point of view. To lighten the MVSA algorithm, we initialize it with the set of end-members $M \equiv [m_1, m_2, \dots, m_p]$ generated by the VCA algorithm [6]. We selected VCA because it is the fastest among the state-of-the-art.

Pure pixel based methods. Since the output of VCA is a set of p vectors that are in the data set, then we can discard all vectors belonging to the convex set generated by the columns of M . If the number of endmembers is high, it may happen that the initial simplex provided by VCA contains very few pixels inside and, therefore, most are out-side, violating the non negativity constraints and slowing down the algorithm. In such cases, we expand the initial simplex to increase the number of pixels that are in the convex hull of the identified endmembers, which speeds up the algorithm. The pseudo code for the MVSA method is shown in below. Symbols

$g(Q)_{:,j}$ and $g(Q)_{i,:}$ stand for, respectively, the j th column and the i th line of $g(Q)$, the gradient of $f(Q)$.

III. STATISTICAL APPROACHES

The geometrical based methods give poor results whenever the spectral mixtures are highly mixed. So whenever number of bands gets increased the result of geometrical approaches get reduces. This is also true for increment in number of pixels in the image. As we know that in geometrical approach it always needs at least one pure pixel which is not possible for every image. So we have to move on to the statistical methods, which are powerful alternative, but come with price: higher computational complexity. In this approach we don't need every time a pure pixel as well as often the full additive constraint is also verified.

A. NMF

In the unmixing process of hyperspectral data, the method of NMF can be applied for the minimization of the objective function given by eq. (11). So basic NMF problem can be defined as:

Given a nonnegative matrix $R \in R_{m \times n}$ and a positive integer $k < \min\{m, n\}$, find nonnegative matrices $M \in R_{m \times k}$ and $S \in R_{k \times n}$ to minimize the objective function given in eq. (11).

$$f(M, S) = \frac{1}{2} \|R - MS\|_F^2 \quad (11)$$

The multiplication factor MS is called a NMF of our original data set R . Here data R is not needed equal to the multiplication MS . But the multiplication MS is an approximate factorization term that is having the at most k . Another key characteristic of NMF is the ability of numerical methods that minimize eq. (11) to extract underlying features as basis vectors in M , which can then be subsequently used for identification and classification. By not allowing negative entries in M and S , NMF enables a non-subtractive combination of parts to form a whole [6], [7].

Fundamental Algorithms:

1) Multiplicative update algorithm

The basic multiplicative algorithm was introduced by Lee and Seung (2001) [5], [6]. This multiplicative update rules contained the mean squared error objective function of eq. (11) is given below [5], [6].

Here eq. (12) and eq. (13) are the basic update equation for this algorithm.

$$S \leftarrow S \frac{M^T R}{M^T M S} \quad (11)$$

$$M \leftarrow M \frac{R S^T}{M S S^T} \quad (12)$$

2) ALS Algorithm

This algorithm comes with modification in LS algorithm where one extra least square step with changed fashion is added after the first least square step. ALS algorithms were first introduced by Paatero, in 1994. But this algorithm comes with one limitation, that the problem of eq. (11) cannot convex is both the matrix M and S . It may convex in only any one of them [5], [6].

B. Constrained NMF

In this simple NMF problem our objective function shown in eq. (11) makes the solution nonunique for the factorization of R into M and S matrix so that there is necessity to add different constraints to make the solution unique.

The adaptive potential function given by the eq. (13) is used to represent the characteristic as a piecewise smoothness of spectral data.

$$g(x) = -e^{-x^2/\gamma+1} \quad (13)$$

Here the in this function constant 1 is added to make the results of it nonnegative. And γ is a positive parameter which controls the shape of this potential function.

Hyperspectral images are having high spectral resolution so that they are having strong continuity of spectral signature as compare to

abundance map. So that parameter γ is defined for both spectral correlation as well as spatial correlation as γ_m and γ_s respectively. They both should have different values. The adaptive potential function $g(\mathbf{m}-\mathbf{m}_N)$ represents the piecewise smoothness of the spectral signature \mathbf{m} . this can be generated by observing the spectral signature \mathbf{m} and its neighbor \mathbf{m}_N .

The i^{th} entry in this adaptive potential function is defined as $g(\mathbf{m}_i-\mathbf{m}_{N_i})$ as given in eq. (14).

$$g(\mathbf{m}_i-\mathbf{m}_{N_i}) = \sum_{i' \in N_i} g(\mathbf{m}_i-\mathbf{m}_{i'}) \quad (14)$$

Here $N_i = \{i-1, i+1\}$.

Same concept is defined for the piecewise smoothness of endmember abundances that can be given by $g(\mathbf{S}-\mathbf{S}_N)$. The entry at position (p, k) is derived by eq. (15).

$$g(\mathbf{S}_{pk}-\mathbf{S}_{N_{pk}}) = g\left(\frac{\mathbf{S}_{ijp}}{\mathbf{S}_{N_{ijp}}}\right) = \sum_{i'j' \in N_{ijp}} g\left(\frac{\mathbf{S}_{ijp}}{\mathbf{S}_{ijp}} - \frac{\mathbf{S}_{i'j'p}}{\mathbf{S}_{i'j'p}}\right) \quad (15)$$

Here $\mathbf{S}_{pk} = \mathbf{S}_{ijp}$ and N_{ijp} is the neighborhood of \mathbf{S}_{ijp} . The assumption is taken as,

$$N_{ijp} = \{(i-1)j, (i+1)j, i(j-1), i(j+1)\}.$$

So our objective function that is only based on Euclidian distance given in eq. (3.1) will now added with extra constraints. It will be as follow.

$$D(\mathbf{M}, \mathbf{S}) = \text{Euc}(\mathbf{M}, \mathbf{S}) + \alpha \langle g(\mathbf{M}-\mathbf{M}_N) \rangle + \beta \langle g(\mathbf{S}-\mathbf{S}_N) \rangle \quad (16)$$

Here $\langle \cdot \rangle$ defines the total sum of the matrix elements, such as

$$\langle g(\mathbf{M}-\mathbf{M}_N) \rangle = \sum_{l,p=1}^{L,P} g(\mathbf{M}_{lp}-\mathbf{M}_{N_{lp}}) \quad (17)$$

Same rule can be applied to matrix \mathbf{S} .

So now for this objective function our updating rules are also changed as follows.

$$\mathbf{M} \leftarrow \mathbf{M} \cdot \frac{(\mathbf{R}\mathbf{S}^T + \alpha (\mathbf{M} \cdot \mathbf{h}(\mathbf{M}-\mathbf{M}_N)) - \mathbf{g}'(\mathbf{M}-\mathbf{M}_N))}{(\mathbf{M}\mathbf{S}\mathbf{S}^T + \alpha \mathbf{M} \cdot \mathbf{h}(\mathbf{M}-\mathbf{M}_N))} \quad (18)$$

$$\mathbf{S} \leftarrow \mathbf{S} \cdot \frac{(\mathbf{M}^T \mathbf{R} + \beta (\mathbf{S} \cdot \mathbf{h}(\mathbf{S}-\mathbf{S}_N)) - \mathbf{g}'(\mathbf{S}-\mathbf{S}_N))}{\mathbf{M}^T \mathbf{M} \mathbf{S} + \beta \mathbf{S} \cdot \mathbf{h}(\mathbf{S}-\mathbf{S}_N)} \quad (19)$$

Here \cdot and \cdot^* represents element wise division and multiplication respectively and $(\cdot)^T$ defines the transposition of the any matrix. And,

$$\mathbf{h}(\mathbf{m}_i-\mathbf{m}_{N_i}) = \frac{2}{\gamma_m} \sum_{i' \in N_i} e^{-\frac{(\mathbf{m}_i-\mathbf{m}_{i'})^2}{\gamma_m}} \quad (20)$$

$$\mathbf{g}'(\mathbf{m}_i-\mathbf{m}_{N_i}) = \frac{2}{\gamma_m} \sum_{i' \in N_i} (\mathbf{m}_i-\mathbf{m}_{i'}) e^{-\frac{(\mathbf{m}_i-\mathbf{m}_{i'})^2}{\gamma_m}} \quad (21)$$

1) Piecewise Smoothness Constraint (nsNMF)

The smoothness of the image is very important parameter for unmixing process. Here in this algorithm one smoothness matrix \mathbf{C} is included into our objective function given by eq. (11) will now changed to eq. (22)

$$f(\mathbf{M}, \mathbf{S}) = \frac{1}{2} \|\mathbf{R}-\mathbf{MCS}\|_F^2 \quad (22)$$

Here $\mathbf{C} \in \mathbb{R}_{p \times p}$ is positive symmetric matrix which is defined by eq. (23)

$$\mathbf{C} = (1-\theta) \mathbf{I} + \frac{\theta}{p} \mathbf{1}\mathbf{1}^T \quad (23)$$

Here \mathbf{I} is the identity matrix and $\mathbf{1}$ is the vector of ones. Smoothness of \mathbf{C} is controls by parameter θ ($0 < \theta < 1$). after adding this parameter to our objective function the algorithm of constraint NMF will be implemented. But here now update equation for matrix \mathbf{S} given by eq. (19) is now changed to eq. (24).

$$\mathbf{S} \leftarrow \mathbf{S} \cdot \frac{(\mathbf{M}\mathbf{C}^T \mathbf{R} + \beta (\mathbf{S} \cdot \mathbf{h}(\mathbf{S}-\mathbf{S}_N)) - \mathbf{g}'(\mathbf{S}-\mathbf{S}_N))}{\mathbf{M}\mathbf{C}^T \mathbf{M}\mathbf{C}\mathbf{S} + \beta \mathbf{S} \cdot \mathbf{h}(\mathbf{S}-\mathbf{S}_N)} \quad (24)$$

The smoothness constraint may or may not give the unique solution for our objective function

given in eq. (11) so that more constraints will be used to get the unique solution.

2) NMF with Sparseness Constraint (NMFSC)

This criterion is based on the relationship between L1 and L2 norm of the measured data. The sparseness of the image is a measured energy of any vector contained into a small number of components. This algorithm only changes the update equations for the matrix S by setting the L1 and L2 norm as well as the nonnegativity constraint.

For NMFSC the same algorithm of constraint NMF is implemented but only 1 step is added that after updating matrix by eq. (19) and then for achieving the desired sparseness project each row of S.

IV. CONCLUSION

Today spectral unmixing is a very active and interesting research topic in the remote sensing technologies. By using the spectral sensor the captured image is a mixture of various signatures of different materials and their fractional available in that scene. But in many applications we need to identify this material and their relative fractions. So this paper represents the recent developments in the unmixing field as well as the various approaches of unmixing problem.

REFERENCES

[1] G. A. Shaw and H.-H. K. Burke, "Spectral imaging for remote sensing", *Linc. Lab. J.*, vol. 14, no. 1, pp. 3–28, 2003.

[2] N. Keshava and J. F. Mustard, "Spectral unmixing", *IEEE Signal Process. Mag.*, vol. 19, no. 1, pp. 44–57, Jan 2002.

[3] Bioucas-Dias J.M., Plaza A., Dobigeon N., Parente M., Qian Du, Gader, P., Chanussot J., "Hyperspectral Unmixing Overview: Geometrical, Statistical, and Sparse Regression-Based Approaches", *IEEE Journal of Selected Topics in Applied Earth Observations and Remote Sensing*, vol.5, no.2, pp.354, April 2012.

[4] M. Parente and A. Plaza, "Survey of geometric and statistical unmixing algorithms for hyperspectral images", in

Proc. IEEE GRSS Workshop Hyperspectral Image Signal Process.: Evolution in Remote Sens. (WHISPERS), pp. 1–4, 2010.

[5] Mehul S Raval, "Hyperspectral Imaging: A Paradigm in Remote Sensing", *CSI communication*, pp.7-9, Jan 2014.

[6] M. W. Berry, M. Browne, A. N. Langville, V. P. Pauca, and R. J. Plemmons, "Algorithms and applications for approximate nonnegative matrix factorization", *Computational Statistics & Data Analysis.*, vol. 52, no. 1, pp. 155–173, Elsevier, Sep 2007.

[7] D. D. Lee and H. S. Seung, "Algorithms for non-negative matrix factorization", in *Adv. Neural Inform. Processing System*, vol. 13. Cambridge, MA:MIT Press, pp. 556–562, 2000.

[8] SenJia, YuntaoQian, "Constrained Nonnegative Matrix Factorization for Hyperspectral Unmixing", *IEEE Transactions on Geoscience and Remote Sensing*, vol.47, no.1, pp.161, Jan 2009.

[9] A. Pascual-Montano, J. M. Carazo, K. Kochi, D. Lehmann, and R. D. Pascual-Marqui, "Nonsmooth nonnegative matrix factorization (nsNMF)", *IEEE Trans. Pattern Anal. Mach. Intell.*, vol. 28, no. 3, pp. 403–415, Mar 2006.

[10] Jose M. P.Nascimento, José M. Bioucas-Dias, "Vertex component analysis: a fast algorithm to unmix hyperspectral data", *IEEE Transactions on Geoscience and Remote Sensing*, vol.43 (no.4), pp.898, 910, April 2005.

[11] Jun Li and Jose M. Bioucas-Dias, "Minimum Volume Simplex Analysis: A Fast Algorithm To Unmix Hyperspectral Data", *IEEE International on Geoscience and Remote Sensing Symposium (IGARSS)*, vol.3, pp.250, 253, July 2008.

[12] USGS Digital Spectral Library: <http://speclab.cr.usgs.gov/spectral-lib.htm>



DENOISING USING FRAMELET TRANSFORM

Swati D. Khandare¹, Vandana Shah²

PG Student , Assistant professor Dept. of ECE, , Sarvajanic College of Engineering, Surat, Gujarat., India¹

ABSTRACT: Images are produced to record or display useful information or details. Due to flaws in the imaging and capturing process or transmission and compression process, the recorded image always represents noisy version of the original one. The undoing of these imperfections is critical to many of the successive image processing tasks. The visual quality of images plays an important role in accuracy of diagnosis which can be seriously degraded by existing noise. The noise affects both the diagnostic tasks and the ability of automatic computerized analysis, like segmentation, classification, image reconstructions and registration. There are two typical ways for noise reduction in the image processing. One way is that acquiring the data several times and averages them. However this processes is time consuming. Another way for denoise the images by post processing methods. For this purpose construction of efficient, less time consuming and high Quality technique need to be introduce. There are many techniques exist for denoising using wavelet transform but having drawbacks of losing high frequency component containing fine details. Wavelet transform has proved to be effective noise removal technique and also reduce computational complexity with better noise reduction performance. This paper describe the difference between image denoising using DWT and Framelet transform. Framelet transform provide shift invariance property. So using Framelet transform which is nearly similar to wavelet transform only with the difference is that framelet transform contains two or more high frequency filter bank which is used to produce more subband in decomposition.

KEYWORDS: DWT, Framelet Transform, AWGN Noise, Image denoising

I. INTRODUCTION:

Image denoising is preprocessing step in image processing. In day to day life too many images are captured in so many fields. Those images are transferred to many different locations. Like in MRI center and also Astronomical application, images are taken and transferred to different locations for analysis but during acquisition or transmission images are corrupted by some noise. Noise modeling in images which are greatly affects images because of instruments used in capturing, data transmission media, image quantization. Depending on noise models different algorithms are used. Most of the natural images are assumed to have additive random noise which is modeled as a Gaussian. In ultrasound images Speckle noise is observed whereas Rician noise affects MRI images[2]. Due to the presence of noise, the information which needs to analyse should be hidden. So that proper prediction is not possible in that case. Some of the standard algorithms use to remove noise from images and perform filtering process but the image is either over smoothen or blur due to loss of edges. Algorithm which remove noise from the image without loss of edges and reconstruct the Image nearer to original is needed. The common assumption during image denoising is that the image is contaminated with Additive White Gaussian noise with zero mean and known variance. It is also assume that the noise in image is stationary and uncorrelated among pixels. An ideal image x is measured when additive white Gaussian noise with zero mean and constant variance is present in the image. We can formulate the observed image as:

$$y = x + n \quad (1)$$

Where y is the observed noisy image, x is the original image and n is the noise added in an image. So many transforms like FFT, STFT, (DWT)wavelet transform, etc. are available for removing noise from images with each have its own advantages and limitations. Images contain the low frequency component and high frequency component. Noise in the low frequency component can be removed easily with certain available techniques. But noise present in high frequency component which contains fine details of image cannot be removed easily. Because when we try to remove noise from high frequency component then there is possibility for losing fine details of the image. Transforms like wavelet transforms are used for image denoising using sub-band decomposition. Wavelet transform [6] is effective technique in noise removal and also reduce computational complexity, better noise reduction performance. But shift invariance property is absent in DWT. Shift variance exist due to critical sub sampling in DWT. Due to this property every second wavelet at each decomposition level is discarded automatically. So there is a need for enhancement of image quality.

In this paper, we discuss about Framelet Transform for noise reduction from noisy image. The organization of this paper is as follows: section II contains the types of noise and Methodes of Elliminating noise, Section III contains Frmalet Trnsform and requirements, Section IV contains Image denoising using Framelet Transform and Section V contain the Results and Discussion. Last section contains the conclusion and references

II. NOISE MODELS AND ASSUMPTION

Additive Noise^[1]: Additive white Gaussian noise is evenly distributed over the signal which is added in each pixel evenly and it is also called as Gaussian noise. Each pixel in the noisy image is equal to the sum of the original pixel value and randomly distributed Gaussian noise value.

Substitutive Noise^[1]: Substitutive noise like salt and pepper noise. Due to data transmission error, white and black dots are added in the output image.

Multiplicative Noise: This type of noise is occurred in all coherent imaging systems like laser and synthetic aperture radar imagery ^[1].

Speckle noise is multiplicative noise. In MRI images, noise like speckle noise is observed due to thermal effect^[2].

Methods of Eliminating Noise:

Two areas of operations are available for removal of noise i.e. Space field and Transformation field. In space field ^[3], the data operation is carried on the original image, and processes the image grey value, like neighborhood average method, wiener filter, center value filter and so on. Transformation field has the operational area in the transformation domain of images, and the coefficients after transformation are processed for denoising.

III. FRAMELET TRANSFORM AND REQUIREMENT

From Fourier theory signal can be expressed as the summation of a possibly infinite series of sine and cosine waves. The disadvantage of the Fourier extension is that it has only frequency resolution and no time resolution. So to get both at a time, both Time-Frequency joint representations is the solution to the problem i.e. cut the signal of interest into several part and then analyze the part separately. But problem of cutting the signal has been arises i.e. How to cut? Short time window gives the solution to the this problem. We can cut the signal using short time window which gives us the time frequency representation of the interest. Short term Fourier transform gives spectrum of frequency band at specific time interval. Again the problem here is cutting the signal resultant to a convolution among the signal and the cutting window as convolution in time domain is one and the same as multiplication in frequency domain and frequency components are smeared out all over the frequency axis. In fact this condition is the opposite of the standard Fourier transform since here is time resolution but no frequency resolution at all. The wavelet analysis is possibly the most current solution to overcome the shortcoming of the Short time Fourier transform. The use of fully scalable modulated window resolves the signal cutting problem. The window is shifted next to the signal and for every spot spectrum is calculated. Then this process is repeated numerous times with slightly shorter or longer window for each new cycle then the result is time frequency collection of the signal all with

different resolution. By using varying window, one can deal resolution in time for resolution in frequency. In order to separate discontinuity in signal requires short basis function and for fine frequency analysis requires long low frequency basis function. This is realized by wavelet transforms where the basis functions are obtained from a single model wavelet by shift and extraction/ contraction^[8]

Discrete wavelet transform which transforms the discrete data from time field into frequency field. The value of the transformed data in time frequency field are called the coefficients where large coefficients correspond to the signal and small one corresponds to usually noise [1]. The noise free data is obtained by inverse transforming the proper threshold coefficients.

Orthonormal wavelets have many applications such as in image processing and image denoising. We are interested in tight wavelet frames that are derived from refinable function through a multiresolution analysis. A tight wavelet frame is an overview of an orthonormal wavelet basis by introducing redundancy into a wavelet system. Tight wavelet frames also called as framelet have advantageous features like shift invariant wavelet frame transforms and it may be helpful in recognize patterns in a redundant/repeatable transforms. In order to get fast wavelet frame transform also called framelet transform, tight wavelet frames are generally derived from refinable function through MRA^[9].

IV. IMAGE DENOISING USING FRAMELET TRANSFORM

Tight frame is generated by B-spline scaling function and two framelets with vanishing moment of order 2 and 1 respectively. It means that the unvarying signal cannot pass through the high pass filter h_2 and neither unvarying nor linear signal can pass through the h_1 . For large numbers of images these two framelets are capable of capturing the crucial texture information since the natural images are often piecewise smooth and locally uncorrelated. Lifting factorization of this tight frame provides the sparse approximation. If we are combining the lifting factorization of tight frame that is polyphase matrix with the directional lifting structure then we are getting specific translation

invariant directional framelet transform. TIDFT is considered as one of the effective sparse approximation tools with edge preserving property for analysis of images.

TIDFT will be used for noise reduction which is based on the MAP estimator. First of all images are transfer into transform domain, and then the denoising algorithm is applied on the framelet coefficient. Since distribution of framelet coefficients take over the behavior like peaked long tail Gaussian like distribution, SCE and ECE distributions^[4] are used. Algorithm for noise reduction using TIDFT is as follows:

- After applying Translation invariant directional framelet transform on the noisy signal, at the output noisy framelet coefficients are obtained.
- Maximum A Posteriori estimation criteria based shrinkage rules like SCE and ECE distribution will be applied on the framelet coefficient.
- Calculation of variance of noise and signal is necessary to estimate standard deviation of signal

For checking sparse representation potential of TIDFT, Spherically contour exponential distribution is used and for checking noise suppression capability, elliptically contour exponential distribution is used. This will give us denoised output image.

IV. RESULT AND DISCUSSION

Noise level of 10dB and 20 dB is added to the original image which is removed by Framelet transform as shown below. Noise such as AWGN noise, Salt and pepper noise and Speckle noise is added in original image and analyze the Framelet output. Framelet can remove AWGN noise from the original image and give denoised output. But Salt and pepper noise and Speckle noise cannot be removed totally by the Framelet because Framelet is additive which can not remove multiplicative noise and the salt and pepper noises which are shown below:

a. For AWGN Noise



Figure 1 Image Denoising usings Framelet (AWGN Noise)

Figure 1 shows image denoising using framelet transform for AWGN noise, left hand side figure shows original image, figure in middle shows noisy image and right side figure shows denoised image.

b. For Salt and Pepper Noise

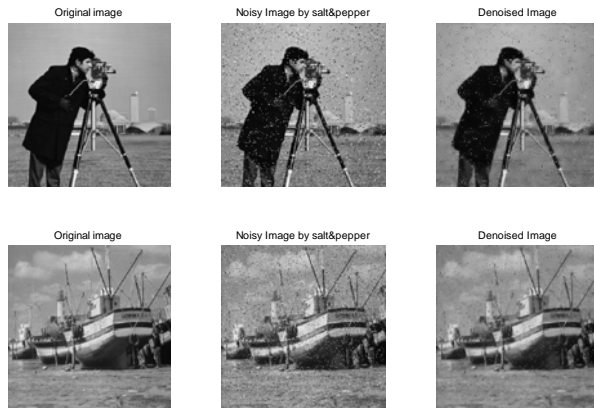


Figure 2 Image Denoising using Framelet (Salt and Pepper)

Figure 2 shows image denoising using framelet transform for Salt and pepper noise, left hand side figure shows original image, figure in middle shows noisy image and right side figure shows denoised image.

c. For Speckle Noise



Figure 3 Image Denoising using Framelet (Speckle Noise)

Figure 3 shows image denoising using framelet transform for Speckle noise, left hand side figure shows original image, figure in middle shows noisy image and right side figure shows denoised image.

PSNR Comparison of Framelet Transform for different Noises and for Different Images

Noise Type	Noise Level	Image (Size)	PSNR
Gaussian Noise	$\sigma=10$	Barbara (512*512)	38.9166
	$\sigma=20$	Barbara (512*512)	34.9317
	$\sigma=10$	Boat (512)	39.1966
	$\sigma=20$	Boat (512)	35.8367
	$\sigma=10$	Lena (512)	40.3816
	$\sigma=20$	Lena (512)	37.2659
	$\sigma=10$	Cameraman (256*256)	32.3110
	$\sigma=20$	Cameraman (256*256)	28.4591
Speckle Noise	$v=0.04$	Barbara (512*512)	31.4797
	$v=0.1$	Barbara (512*512)	27.2388
	$v=0.04$	Boat (512)	31.9199
	$v=0.1$	Boat (512)	26.7032
	$v=0.04$	Lena (512)	32.9565
	$v=0.1$	Lena (512)	27.5127
	$v=0.04$	Cameraman (256*256)	25.3606
	$v=0.1$	Cameraman (256*256)	20.5166
Salt and Pepper Noise	$d=0.05$	Barbara (512*512)	28.5246
	$d=0.1$	Barbara (512*512)	25.4921
	$d=0.05$	Boat (512)	29.3226
	$d=0.1$	Boat (512)	26.0635
	$d=0.05$	Lena (512)	29.5559
	$d=0.1$	Lena (512)	26.1100
	$d=0.05$	Cameraman (256*256)	22.1859
	$d=0.1$	Cameraman (256*256)	19.1493

IV. CONCLUSION

Image Denoising Using Framelet Transform is implemented and improved PSNR value and recover the corrupted image with high visual quality. Compared PSNR value using Framelet transform for different types of noise such as AWGN, Salt and pepper noise and speckle noise. Framelet Transform have the capability of Noise reduction with edge preserving. Framelet Transform removes the AWGN noise and achieved good PSNR value but can not remove salt and pepper noise and speckle noise completely because Framelet transform is additive and can not remove multiplicative noise.

REFERENCES

- [1] S. Sulochana, R. Vidhya, "Image Denoising using Adaptive Thresholding in Framelet Transform Domain", (IJACSA) International Journal of Advanced Computer Science and Applications, Vol. 3, 2012
- [2] J. Mohan, V. Krishnaveni, Yanhui Guo, "A survey on the magnetic resonance image denoising methods", *Biomedical Signal Processing and Control*, Vol. 9, pp. 56-69, Elsevier, 2014
- [3] Sachin D Ruikar, Dharmal D Doye, "Wavelet Based Image Denoising Technique", (IJACSA) International Journal of Advanced Computer Science and Applications, Vol. 2, pp. 49-53, March 2011
- [4] Yan Shi, Xiaoyuan Yang, and Yuhua Guo, "Translation Invariant Directional Framelet Transform Combined With Gabor Filters for Image Denoising", *IEEE Transactions On Image Processing*, Vol. 23, pp. 44-55, January 2014
- [5] Kostadin Dabov, Alessandro Foi, Vladimir Katkovnik, and Karen Egiazarian, "Image denoising by sparse 3-D transform-domain collaborative filtering," *IEEE Transactions On Image Processing*, vol. 16, no. 8, pp. 2080-2095, Aug. 2007.
- [6] Xiaoyuan Yang, Yan Shi, Liuhe Chen, and Zongfeng Quan, "The Lifting Scheme for Wavelet Bi-Frames: Theory, Structure, and Algorithm", *IEEE Transactions On Image Processing*, Vol. 19, pp. 612 -624, March 2010
- [7] A. Ben Hamza and Hamid Krim, "Image Denoising: A Nonlinear Robust Statistical Approach", *IEEE Transactions on Signal Processing*, Vol. 49, No. 12, pp.3045-3054, December 2001
- [8] Martin Vetterli and Cormac Herley, "Wavelets and Filter Banks: Theory and Design", *IEEE Transactions On Signal Processing*, Vol. 40, No 9, pp. 2207-2232, September 1992
- [9] Bin Han, QunMo, "Symmetric MRA tight wavelet frames with three generators and high vanishing moments", *Applied and computational Harmonic analysis*, Vol. 18, pp. 67-93, Elsevier, December 2005
- [10] Pengliang Yang; Jinghui Gao; Wenchao Chen, "Noise attenuation of the geophysical data using the framelet transform," *IEEE International Geoscience and Remote Sensing Symposium (IGARSS)*, pp.2300-2303, July 2012
- [11] Lixin Shen, Papadakis, M. Kakadiaris, I.A. Konstantinidis, I. Kouri, D. Hoffman, "Image denoising using a tight frame," *IEEE Transactions on Image Processing*, vol.15, no.5, pp.1254-1263, May 2006
- [12] X. Wang, G. Shi, and L. Liang, "Image denoising based on translation invariant directional lifting", *IEEE conference on ICASSP*, pp. 1446-1449, July 2010.
- [13] Zhou Dengwen, "An Image Denoising Algorithm With An Adaptive Window", *IEEE conference on ICIP*, pp. 333-336, 2007.
- [14] Claude Knaus, Matthias Zwicker, "Progressive Image Denoising", *IEEE Transactions On Image Processing*, Vol. 23, No. 7, pp. 3114-3125, July 2014
- [15] K.P. Soman, K.I. Ramachandran, N.G.Resmi, "Insight into Wavelets", 3rd Edition, Asoke K. Ghosh, PHI Learning Private Limited, New Delhi, pp.278-289, March 2010.



MACHINE TRANSLATION SYSTEM IN INDIAN PERSPECTIVE

¹Dr. Sushil Kumar, ²Kiran Soni

Principal, PCEM Raipur, M.Tech Scholar, CVRU Bilaspur
Email: ¹sk1_bit@rediffmail.com, ²kiransoni.soni21@gmail.com

Abstract—This paper gives a survey of the work done on various Indian machine translation systems either developed or under the development. Some systems are of general domain, but most of the systems have their own particular domains like parliamentary documents translation, news readings, children stories, web based information retrieval etc.

Index Terms— Machine translation, computational linguistics, language processing

I. INTRODUCTION

Indian is the largest democratic country in the world and there are more than 30 languages and approximately 2000 dialects used for the communication by the Indian peoples and out of these languages Hindi and English are taken as language for of cial work and there are 22 scheduled languages used by the different states for their administrative work and communication purposes. These 22 languages includes Assamese, Bengali, Bodo, Dogri, Gujrati, Hindi, Malayalam, Manipuri, Marathi, Nepali, Oriya, Punjabi, Sanskrit, Kannada, Kashmiri, Konkani, Maithili, Santali, Sindhi, Tamil, Telugu, Urdu. Because of different culture and multilingual environment in India there is a big requirement for inter-language translation for the transfer of information and sharing of the ideas. Peoples of different states perform their work in their respective regional languages whereas the work at the Union Government of ces is performed in English language which is assumed to be one of the most speaking languages in the world or Hindi Language. So to synchronize between state government and the central / Union

government there is a need for translation from regional languages to English language and vice versa. In India because of different culture there is different news papers published locally as well as globally. From the above discussion it is clear that there is large scope of translation of text from English to Indian Languages and vice versa. The initial work on Indian Machine Translation (in the beginning of 90's) was performed at various locations by different persons like IIT Kanpur, Computer and Information Science department of Hyderabad, NCST Mumbai, CDAC Pune, department of IT, Ministry of Communication and IT Government of India. In the mid 90's and late 90's some more machine translation projects also started at IIT Bombay, IIT Hyderabad, department of computer science and Engineering Jadavpur University, Kolkata, JNU New Delhi etc. The next part of the paper gives a brief introduction of the various machine translation works done so far although there are some advancement is going on some projects so the latest information may be taken from the respective websites. The next section is divided into ve sub-sections A to E for the different languages.

II. MACHINE TRANSLATION SYSTEM

The development of the Indian Machine Translation system can be divided into different categories. The scope of this paper is restricted to Hindi, Punjabi, Sanskrit, Bengali and English Language as a source language.

A. *Anusaaraka*

A project named “ANUSAARAKAA” for machine translation from one Indian Language to another Language in 1995. It has been used for translation from Telugu, Kannada, Bengali,

Punjabi and Marathi to Hindi language translation and vice versa. The ANUSAARAKA system is a language accessor cum Machine Translation system that works on principles of Paninian Grammar (PG)". The system provides both the robustness incase of failure and no loss of information while translating the text. The output of the system follows the grammar of the source language. The approach for the translation in this system is divided in two parts: 1) The ANUSAARAKA system which is based on language knowledge 2) the domain specific knowledge based on world knowledge, statistical knowledge etc. It was started at IIT Kanpur and now shifted to IIIT Hyderabad Currently ANUSAARAKA is working for Telugu, Kannada, Marathi, Bengali, and Punjabi to Hindi language translation and in near future reverse translation will also be feasible.

B. The Mantra(Machine assisted Translation Tool)

A machine translating system named "MANTRA" which translates the text from English to Hindi language with a precise domain in Office order, administrative work texts etc.in1999. The basis of this system was the Tree Adjoining Grammar(TAG) formalism from the University of Pennsylvania. It uses Lexicalized Tree Adjoining Grammar (LTAG) for representing the English and the Hindi Language. It uses the TAG for parsing as well as Generation purposes. Now this system is also used in the nance, agriculture, health care, information technology, education and the general purpose activities of the government domains. The system named 'MANTRA-RAJYASABHA' is developed for the RAJYASABHA purposes. Currently the work for the language pairs English-Bengali, English-Telugu, EnglishGujarati, Hindi-English, Hindi-Marathi, Hindi-Bengali is also going on.

C. Anubharti-II Technology

A system with an approach for machine aided translation having the combination of example-based and corpus based approaches and some elementary grammatical analysis. In ANUBHARTI the traditional EBMT approach has been modified to reduce the requirement of a large example base. ANUBHARTI-II in 2004 uses Hindi as a source language for translation to other Indian language [8].

D. Hindi Generation from Interlingua

Prof. Pushpak Bhattacharyya and Prof. Om. P. Damani reported a work on Hindi generation (Hindi Deconverter) from UNL graphs with the satisfactory results. The linguistic concerns have been clearly separated from the computational tasks which results in the possibility of the generation of the other languages also [31].

E. Punjabi to Hindi Machine Translation System

In 2007 a system based on direct word-word translation for machine translation between Punjabi as source language and Hindi as target Language was proposed .The system has reported 92.8% accuracy [24].

F. Sanskrit-Hindi Anusaarka

In 2009 a language accessor cum machine translation system for Sanskrit -Hindi language pair by following the Anusaarka approach was proposed and it allows the user to access the source language text and give the rough output in the target language. The translation mechanism was transparent to the end user [27].

G. Constrained Based Parser for Sanskrit Language

In 2010, Dr. Amba Kulkarni, Sheetal Pokar, Devanand Shukl designed A Constrained Based Parser for Sanskrit Language at University of Hyderabad in the department of Sanskrit Studies. Based on the designing principles obtained from the generative grammars the parser was modeled for nding the directed tress, from the graph with the nodes as words and edges showing the relations between the words. To rule out the non-solutions they used Mimamsa constraints of Akanksa and Sannidhi to give the priority the solutions. The current system allows only the limited and simple sentences to be parsed [32]. ANGLABHARTI: A machine translation system at IIT Kanpur in 1991 was developed which translates from English to Indian Languages. The concept of pseudo- Interlingua has been used for the development of the machine aided translation system named" ANGLABHARTI "in 1991. This concept exploits the commonality in the Indian Languages. ANLGABHARTI is based on Rule Based Translation System (RBTS) with context free grammar structure of the English language as a source language and produces a pseudo Interlingua code which is applicable to a Group of Indian Languages. The movement rules are obtained by the corpus analysis and the target

constituents are obtained from this analysis. The aim of the ANGLABHARTI was to provide a translation system in which 90% work will be done by the machine and the 10% post editing work will be done by the human [1].

H. Angla Bharti Technology

The AnglaBharti project was launched by Sinha et al. (2001) at the Indian Institute of Technology; Kanpur in 1991 for Machine aided Translation from English to Indian languages. Professor Sinha et al. (2001) has pioneered Machine Translation research in India. The approach and lexicon of the system is general-purpose with provision for domain customization. A machine aided translation system specifically designed for translating English to Indian languages. English is a SVO language while Indian languages are SOV and are relatively offered word-order. Instead of designing translators for English to each Indian language, Angla Bharti uses a (Dave et al., 2001) pseudo-interlingua approach. It analyses English only once and creates an intermediate structure called Pseudo Lingua for Indian Languages.

In Angla Bharti they use rule based system with context free grammar like structure for English, A set of rules obtained through corpus analysis which is used to distinguish conceivable constituents. Overall, the Angla Hindi (Sinha and Jain, 2003) system attempts to generalizing the constituents and replacing them with abstracted form from the raw examples. The abstraction integrate example-based approach with rule-based and human engineered post-editing.

AnglaBharti is a pattern directed rule based system with context free grammar (Sinha and Jain, 2003) like structure for English (source language) which generates a ‘pseudo-target’ (PLIL) applicable to a group of Indian languages (target languages). A set of rules obtained through corpus analysis is used to identify plausible constituents with respect to which movement rules for the PLIL is constructed. The idea of using PLIL is primarily to exploit structural similarity to obtain advantages similar to that of using Interlingua approach. It also uses some example-base to identify noun and verb phrasal’s and resolve their ambiguities.

Sr no	Name of the system	Langua ges for Translati on	Approach es Used	Domain	Year
1	ANGLABHARTI-I (IIT K)	ENG-IL	Pseudo-interlingua	General	1991
2	ANUSAARAKA (U H)	IL-IL	PG	General	1195
3	MANTRA (C-DAC- P)	ENG-IL4 HINDI-EMB	TAG	Administration, of ce orders	1991
4	VAASAANUBAADA (A U)	BENGALI-ASSAMESE	EBMT	NEWS	2002
5	ANGLABHARTI-II (IIT-K)	ENGLISH-IL	GEBMT	General	2004
6	ANUBHARTI-II (IIT-K)	HINDI-IL	GEBMT	General	2004
7	MATRA CDAC-M	ENGLISH-HINDI	Transfer based	General	2004
8	SHIVA & SHAKTI (IIIT-H. II S - B)	ENG- IL3	EBMT & RBMT	General	2004
9	UNL MTS (IIT-B)	ENGHINDI	Interlingua	General	2003
10	ANUBAD (J U)	ENG-BENGALI	RBMT AND SMT	NEWS	2004
11	HINGLISH (IIT -K)	HINDI-ENG	Pseudo interlingua	General	2004
12	ANUVAADAK (SUPER INFOSOFT)	ENG-IL	Not-Available	Not-Availab l e	
13	PUNJABI-HINDI (P U)	PUNJABI-HINDI	Direct word to word	General	2007
14	SAMPARK (IIIT-H, CDAC-N .IIT-KGP, ANNA-U	IL-IL IL5	CPG	Not-Available	2009
15	IBM MTS	ENG-HINDI	EBMT & SMT	Not-Available	2006

IL4	Hindi, Bengali, Telugu, Gujarati
IIT-B	Indian Institute of Technology
Bombay	
IIT-KGP	Indian Institute of Technology
	Kharagpur
IIT-K	Indian Institute of Technology
Kanpur	
UH	University of Hyderabad
PU	Punjabi University
CDAC-N	CDAC Noida
IL	Indian Language
JU	Jadavpur University
ANNA-U	Anna University
IIS-B	Indian Institute of Sciences
Bangalore	
EBMT	Example Based Machine Translation
ENG	English
SMT	Statistical Machine Translation
IL3	Hindi, Marathi, Telugu
IL5	Punjabi, Urdu, Tamil, Marathi,
Hindi	
CPG	Computational Paninian Grammar
EMB	ENG, MARATHI, BENGALI
CDAC-P	CDAC Pune

III. CONCLUSION

Machine translation is relatively new in India-about two decades of research and development efforts. the goal of TDIL project and the various resource centres under the TDIL project works on developing machine translation systems for Indian languages. There are governmental as well as voluntary efforts under way to develop common lexical resources and tools for Indian languages like pos tagger, semantically rich lexicons and word nets.

REFERENCES

- [1] Sitender, Seema Bawa, "Survey of Indian Machine Translation System". Dept of Computer science and Engineering.IJCST Vol. 3 ISSUE 1, JAN- MARCH 2012.
- [2] Sanjay Kumar Dwivedi, Pramod Premdas sukhadeve "Machine Translation system in Indian Perspective". Dept of Computer Science and engineering. ISN 1549-3636 ,2010
- [3] Sudhir K Mishra "Sanskrit karaka analyzer for Machine Translation" a Ph.D thesis , SCS JNU New Delhi, 2007.
- [4] G.S.Josam, G. S. lehal "A Punjabi to Hindi Machine Translation system", Coling 2008. Companiono volume Posters an Demonstrations, Manchester, UK , pp 15160, 2008
- [5] Tejinder Singh Saini, Gurpreet singh , lehal "Shahmukhi to Gumukhi Transliteration System", A Corpus based Approach , Advanced in natural Languages Processing Application Research in computing Science 33, pp.151 162,2008.
- [6] Akashar Bharti, Amba Kulkarni, "Anusaarka: An Accessor cum Machine Translator", Department of Sanskrit Studies, University of Hyderabad, Hyderabad, 2009.
- [7] G.S. Josan G.S. Lehal "A Punjabi to Hindi Machine Translation System ", Coling 2008: Companion volume: Postersand Demonstrations, Manchester , UK pp. 157-160, 2008.
- [8] Saha Gautam Kumar, "The EB-ANUBAD translator- A Hybride Scheme", Journal of Zhejjang University Science, pp. 1047-1050, 2005.
- [9] Vishal Goyal, Gurpreet Singh Lehal, "Web Based Hindi to Punjabi Machine Translation System", journal of emerging technologies in web intelligence, Vol. 2, May 2010.
- [10] EnConverter Speci cation Version 2.1UNU/IAS/UNL Centre, Tokyo 150-8304, Japan, 2000



AUTOMATED WHEELCHAIR

Rupali Deshmukh¹, Y. V. Chavan²

^{1,2}Padmabhooshan Vasantdada Patil Institute of Technology, Pune, MS-India

Email: ¹rajvi.deshmukh@gmail.com , ²chavan.yashwant@gmail.com

Abstract— Project includes ARM7 at the core, which is used as a control system to control the entire wheelchair. The persons who are paralyzed dependent on others due to loss of self-mobility. The main objective was to design and build a cheap, intuitive and practical powered wheelchair. The proposed system presents a user-friendly human machine interface (HMI) for hands-free control of an electric powered wheelchair (EPW). Its two operation modes are based on Mode 1 four head movement through accelerometer, and Mode 2 voice command through speech recognition in MATLAB. Proposed Wheelchair can also detect the slope and accordingly control the speed which helps to avoid the accidents. To provide safety IR sensors are used which gives feedback whenever there is any obstacle.

Keywords-: Electric power wheelchair (EPW); speech recognition, Micro-electromechanical systems (MEMS), Accelerometer, DC motors.

I. INTRODUCTION

The ability to moving independently is essential for the full development of our lives, for that reason it is necessary to carry out work aimed at helping people with a motor disability as quadriplegic or tetraplegic to have adequate tools for mobility. The physically challenged people who use a normal wheelchair for navigation, usually requires an external person to move around. In this busy world, the elderly people may be left alone at home and also may not find any person for external help. Here comes the need of an automated home navigation system, which consists of a wheelchair which can be used by the elderly and the physically challenged

people without the help of an external person. The wheelchair automation system can be operated using voices which is recorded into it. Some elderly or physically challenged people may find problems in talking while others may find problems in their body parts or find disability in moving their body parts. These problems are also taken into consideration, as there is an option in wheelchair automation system to customize it with accelerometer which is mounted on head or hand. Another important feature is that the personal security of the person who is using the wheelchair is also taken care. If the person feels uncomfortable or insecure, he can call the emergency service like police or hospital by making use of messaging facility provided by GSM module. Also accident avoidance system includes IR sensor. If any patient is using the wheelchair it is monitoring by temperature sensor and pulse rate sensor.

II. PROPOSED SYSTEM

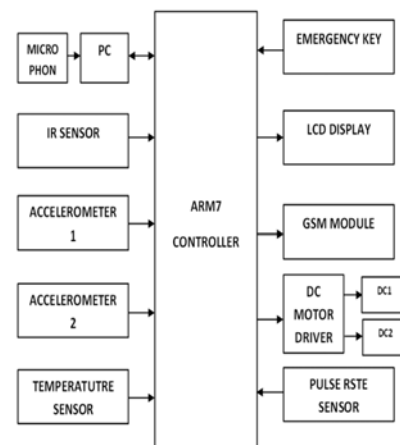


Fig 1: Block Diagram

The block diagram of the system is shown in Fig 1 and each of the modules is explained in brief in the following sections.

A. ARM Controller:

ARM architecture is designed to allow very small, with high performance implementation. This simplicity leads to very small implementations which allow devices with very low power consumption. Now a day's most industries are using this controller to develop their product. One of the examples includes the I-phone 5 mobile which uses ARM 7 processor.

ARM is a RISC architecture which has the following features:

- A large uniform register file.
- A load-store architecture, where data processing operations only operate on register content, not directly on memory contents.
- Simple addressing modes.
- Uniform and fixed length instruction fields.
- High performance, low code size.
- Low power consumption and silicon area.
- ARM based embedded system has good performance and portability; therefore it has been widely used in various industries. Different operating systems can be ported easily on this controller.
- Directly on memory contents.
- Simple addressing modes.
- Uniform and fixed length instruction fields.
- High performance, low code size.
- Low power consumption and silicon area.
- ARM based embedded system has good performance and portability; therefore it has been widely used in various industries. Different operating systems can be ported easily on this controller

B. Accelerometer:

The ADXL335 is a small, thin, low power, complete 3-axis accelerometer with signal conditioned voltage outputs. The product measures acceleration with a minimum full-scale range of ± 3 g. It can measure the static acceleration of gravity in tilt-sensing applications, as well as dynamic acceleration resulting from motion, shock, or vibration.

The user selects the bandwidth of the accelerometer using the CX, CY, and CZ capacitors at the XOUT, YOUT, and ZOUT pins. Bandwidths can be selected to suit the application, with a range of 0.5 Hz to 1600 Hz for the X and Y axes, and a range of 0.5 Hz to 550 Hz for the Z axis.

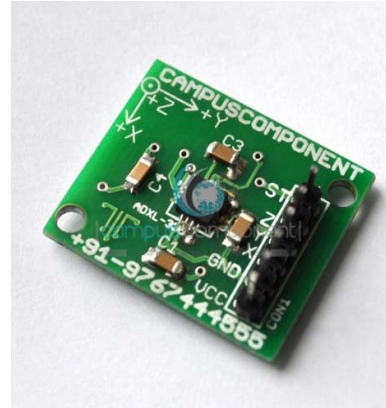


Fig 2: Accelerometer

C. DC MOTOR:

DC motors are used to physically drive the application as per the requirement provided in software. The dc motor works on 12v. To drive a dc motor, we need a dc motor driver called L293D. This dc motor driver is capable of driving 2 dc motors at a time. In order to protect the dc motor from a back EMF generated by the dc motor while changing the direction of rotation, the dc motor driver have an internal protection suit. We can also provide the back EMF protection suit by connecting 4 diode configurations across each dc motor.

D. DC Motor Driver IC:

The module contains L293D at the core. The L293D is a 16 pin IC, with eight pins, on each side, dedicated to the controlling of a motor. There are 2 INPUT pins, 2 OUTPUT pins and 1 ENABLE pin for each motor. L293D consist of two H-bridge. H-bridge is the simplest circuit for controlling a low current rated motor.

The module contains L293D at the core. The L293D is a 16 pin IC, with eight pins, on each side, dedicated to the controlling of a motor. There are 2 INPUT pins, 2 OUTPUT pins and 1 ENABLE pin for each motor. L293D consist of two H-bridge. H-bridge is the simplest circuit for controlling a low current rated motor.

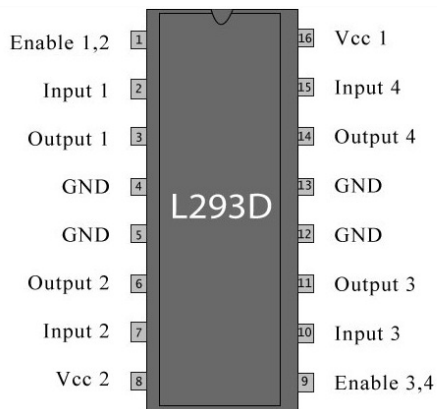


Fig 3: Pin Diagram of L293D

E. GSM Module:

GSM (Global System for Mobile communication) is a digital mobile telephony system. With the help of GSM module interfaced, we can send short text messages to the required authorities as per the application. GSM module is provided by SIM uses the mobile service provider and send SMS to the respective authorities as per programmed. It operates at either the 900 MHz or 1800 MHz frequency band.

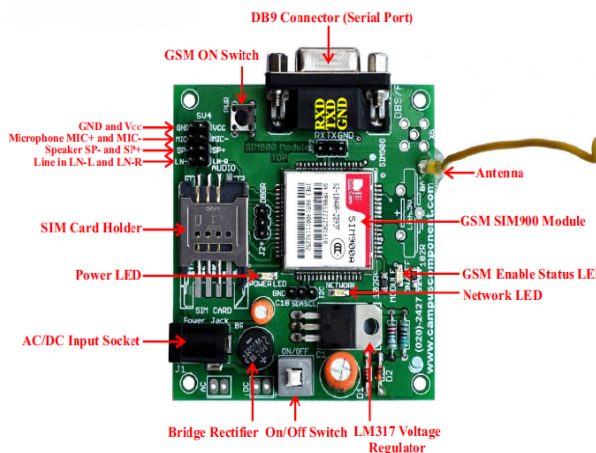


Fig 4: SIM900A GSM Module

F. Temperature Sensor:

Temperature sensor is used to sense the temperature [6]. We have used a Temperature sensor called LM35. This temperature sensor can sense the temperature of the atmosphere around it or the temperature of any machine to which it is connected or even can give the temperature of the human body in case if used. So, irrespective of the application to which it is used, it gives the

reading of the temperature. The LM35 series are precision integrated-circuit temperature sensors, whose output voltage is linearly proportional to the Celsius (Centigrade) temperature. Temperature sensor is an analog sensor and gives the output into form of analog signal. This signal is feed to ADC which will convert it into digital form. Once converted into analog form, the microcontroller can process the digital temperature signal as per the application.

G. IR Sensor:

Here we are connecting an IR based obstacle sensor to detect the obstacle in the way. But to increase the range of the obstacle sensor we are using a lower range resistor (50 ohm). On the receiver side we have connected the IR receiver in reverse bias. So as soon as the light falls in the IR receiver, the anode voltage increases and when the anode voltage is more than the cathode voltage then the LED are in forward bias mode and start conducting.

H. Emergency key:

Emergency key is provided for the wheelchair user. By pressing the key user can send the emergency message to the respective authority.

I. Pulse Rate Sensor:

This is the design of a very low-cost device which measures the heart rate of the subject by clipping sensors on one of the fingers and then displaying the result on a text based LCD. The device has the advantage that it is microcontroller based and thus can be programmed to display various quantities, such as the average, maximum and minimum rates over a period of time and so on. Another advantage of such a design is that it can be expanded and can easily be connected to a recording device or a PC to collect and analyze the data for over a period of time.

J. Microphone:

It is used for the voice command input to the pc in which speech recognition algorithm is used to detect the command that is left, right, forward and backward. And according to command the controller give controlling signal to the wheelchair motor.

K. LCD Display:

LCD is used in a project to visualize the output of the application. We have used 16x2 LCD which indicates 16 columns and 2 rows. So, we can write 16 characters in each line. So, total 32 characters we can display on 16x2 LCD.

These are the overall parts of the system explained here. The algorithm of the system flow is explained in the next section in the form of flow chart. Flow charts for both, that is wheelchair control by accelerometer and by voice command is given.

III. System Flow Charts

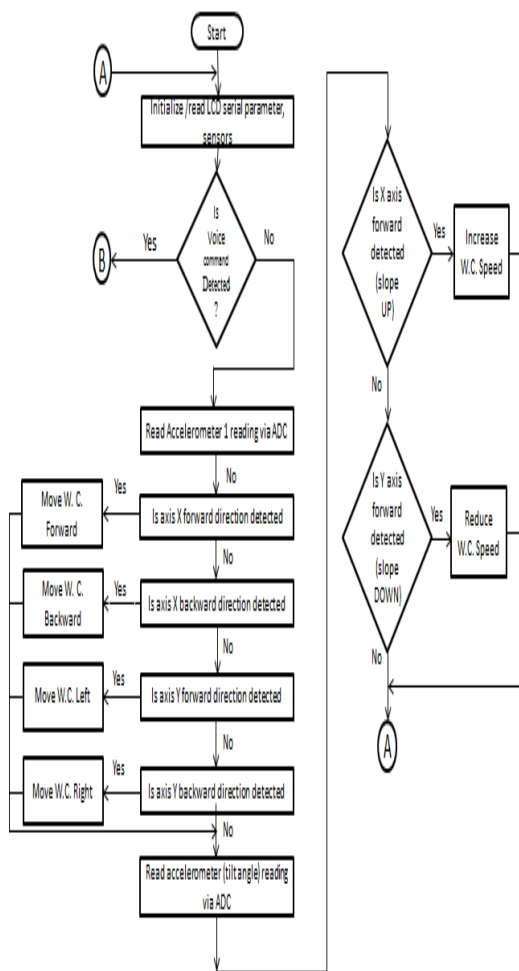


Fig 5: Flow Chart for Accelerometer

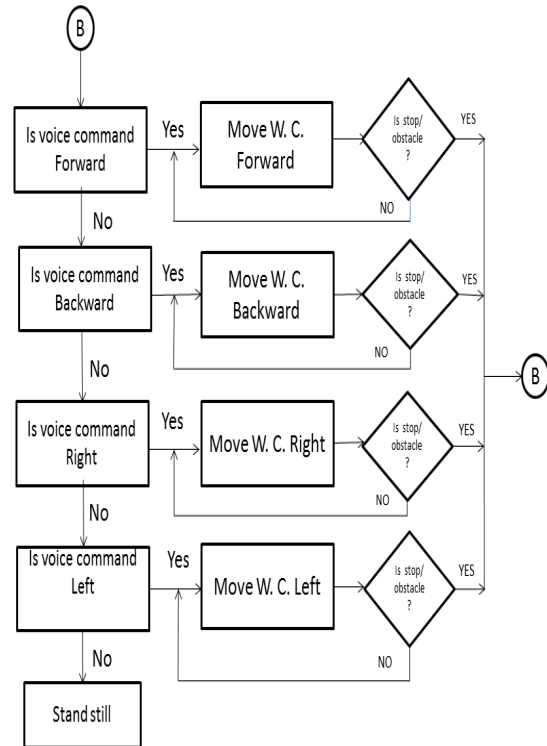


Fig 6: Flow Chart for Voice Command

IV. SOFTWARE USED

MATLAB is used for the voice command detection. And the code is develop using C language which controls the wheelchair movement.



Fig 7: Experimental setup

V. RESULT

1. It Is The Flexibility Of Person Who Is Operating The Wheelchair, to Move It Forward, Backward, Left & Right & this is achieved here, Otherwise the Wheelchair move for 2 Seconds By Default.
2. Temperature & pulse rate sensor measurement on wheelchair are additional features provided on wheelchair for person monitoring is achieved.
3. The emergency message as well as temperature and pulse rate message of person (if any patient) are provided to the respective authority through GSM is effectively achieved.
4. Accident avoidance is done by using IR sensor and by reducing the speed of wheelchair on slope.

VI. CONCLUSION

The wheelchair system was earlier in existence has only one type of control i.e. speech or accelerometer but, proposed system comprised of smart controlling modes [accelerometer + speech recognition] with environment awareness [collision detector & also slope detection] by stopping vehicle when obstacle detected and reduce speed on slope detection, also patient monitoring using sensors and if any emergency sending message to respective authority. So this will help in achieving a smart wheelchair control system.

This system uses voice driven principle which improves human machine interaction and makes the control of the system simple.

VII. REFERENCES

- [1] A. Ruíz-Serrano, R. Posada-Gómez, A. Martínez Sibaj, G. Aguila Rodríguez, B.E. Gonzalez-Sanchez, O.O. Sandoval-Gonzalez. "Development of a dual control system applied to a smart wheelchair, using magnetic and speech control." Science Direct 2013.
- [2] S. Manogna1, Sree Vaishnavi, B.Geethanjali. "Head Movement Based Assist System For Physically Challenged" 2010 IEEE.
- [3] Prof. Vishal V. Pande, Nikita S.Ubale, Darshana P. Masurkar, Nikita R. Ingole, Pragati P. Mane. "Hand Gesture Based Wheelchair Movement Control for Disabled Person Using MEMS." IJERA 2014.
- [4] M. M.A. Hashem, Rushdi Shams, Md. Abdul Kader, and Md. Abu Sayed. "Design and Development of a Heart Rate Measuring Device using Fingertip.
- [5] National semiconductor, "LM35 Precision Centigrade Temperature sensors datasheet", National Semiconductors Corporation, November 2000.
- [6] LPC2131/32/34/36/38 Single-chip 16/32-bit microcontrollers; 32/64/128/256/512 Kb ISP/IAP flash with 10-bit ADC and DAC Rev. 04 — 16 October 2007 Product datasheet
- [7] www.analog.com ©2009 Analog Devices, Inc. Small, Low Power, 3-Axis ± 3 g Accelerometer ADXL335 datasheet
- [8] SIM300 Hardware Specification, www.DataSheet4U.com.



INCREASING EFFICIENCY OF TRANSMISSION LINES BY SIMULTANEOUS AC-DC POWER TRANSMISSION SCHEME AND THEIR PERFORMANCE AT FAULT OPERATION

¹Dr. Sushil Kumar, ²Kiran Soni, ³Prakash Soni

¹Principal, PCEM, Raipur, ²PG Scholar, CVRU Bilaspur, ³Ph.D. Scholar, Kalinga Raipur

Email: ¹Sk1_bit@rediffmail.com, ²kiransoni.soni21@gmail.com, ³praksoni@gmail.com

Abstract –This paper presents the method and operation of simultaneous ac-dc power transmission system. We know that in Transmission system if long extra high voltage (EHV) ac lines loaded to their thermal limits so large amount of power loading results large instability occurs in transmission system that affects the whole power system. It is very difficult operation to load transmission lines to their sufficient margin of thermal limits. By using this method of proposed in this paper, it will be possible to load transmission lines to maximum values of their thermal limits. In this method transmission lines are allowed to carry ac along with dc supply superimposed on it. The conductors' bears ac along with the dc supply. This system gives conversion of double line ac transmission into composite parallel ac-dc transmission system thus having the advantage to transient ability, dynamic stability and damp out oscillation. In this paper the Simulation operation perform in MATLAB software package having Simulink software.

Keywords— EHVAC Transmission, EHVDC Transmission, Facts Power System Stability, Transmission Efficiency, Alternating Current and Direct Current Calculation, MATLAB, Simultaneous ac-dc Power Transmission.

I. INTRODUCTION

We know that whole world require the large amount of power with low loss because year by year the

growth of all industries, commercial and residential part of the world demanding power for their growth. The demand of electric power having steady growth power is but the availability of power often not available at the increasing load centers and remote locations. On the environmental acceptability, and the economic concerns also giving the availability of energy are the factors which determining all these locations. Here because of stability considerations, the transmission having available energy through its existing ac lines having in upper limit. So it is very difficult to load long extra high voltage (EHV) ac lines to their thermal limits as given proper margin which kept against transient instability. The modern world having the situations that is full utilization of available energy which applying the new concepts to the old power transmission theory with a view the system availability and their security.

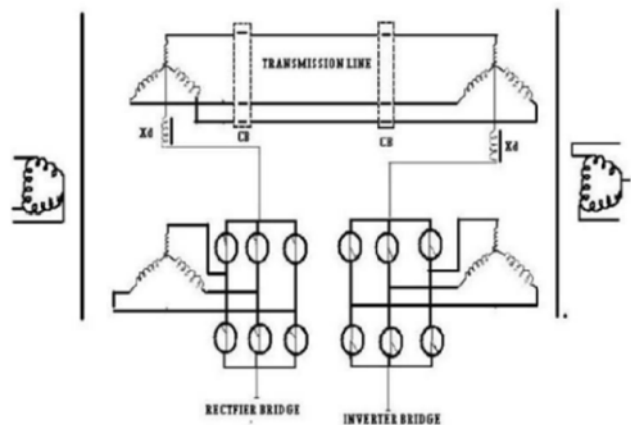


Fig.1.Basic Circuit of AC-DC transmission

The flexible ac transmission system has based on the application of power electronic technology which existing ac transmission system, the role of power electronics improves stability and efficiency to reach power transmission close to its thermal limit. Here we are talking about Simultaneous ac-dc power transmission which was earlier proposed through a single circuit ac transmission line with uni-polar dc link with ground as return path was used for their transmission operation. The Major limitations of ground as return path is due to the fact that the use of ground may corrode any metallic material if it comes in its path. The conductor voltage with respect to ground Three becomes higher due to addition of dc voltage on ac line, hence more insulator discs have to be added with each insulator string so that it can withstand this increased voltage. But condition is that the conductor separation distance was kept constant, as the line-to-line voltage must be unchanged [1]. This paper gives us the method of converting a double circuit ac line into composite ac-dc power transmission line without altering the original line conductors, insulator strings and tower structure. Economic factors such as the high cost of long lines and revenue from the delivery of additional power provide strong incentives to explore all economically and technically feasible means of raising the stability limit. The development of effective ways [3].

Basic proof justifying the feasibility of simultaneous AC-DC transmission has been reported in these papers. In this paper, the improvement of transient stability by utilization of the inherent built-in short-term overloads capacity Of the DC system and rapidly modulating the DC power converted into simultaneous AC-DC line. A single machine infinite bus connected by a double circuit AC line, converted for simultaneous AC-DC power transmission has been studied. The transmission angle is varied up to case of simultaneous AC-DC power transmission system. So that cause the effective performance and increasing the efficiency of power transmission capability of power system.

II. TRANSMISSION SCHEME AND THEIR TRENDS

We know that the world require a large amount of energy of which electrical energy used by whole world. We have already consumed major portion of

its natural resources like coal, fuels, petroleum and we are looking for renewable sources like solar and wind energy other than Hydro and Thermal to cater for the rapid rate of consumption. It will not slow down with year and therefore there exists a need to reduce the rate of annual increase in energy consumption by any intelligent society if resources have to be preserved for posterity. It requires very high voltages for transmission. The very rapid stride taken by development of dc transmission since 1950 is playing a major role in extra-long-distance transmission, complementing E.H.V. ac transmission. They have roles to play and a country must make intelligent assessment of both in order to decide which is best suited for the country's economy. The high voltage ac transmission gives the large amount of corona loss, skin effect and use of bundled conductor and compensation require for power transmission.

ADVANTAGES OF HVDC

- (1) No corona loss.
- (2) No necessary use of bundled conductors.
- (3) No surface voltage gradient on conductors.
- (4) It does not having the problem of Audible Noise, Radio Interference, Carrier Interference, and TV Interference. High electrostatic field under the line.
- (6). It prevents by Increased Short-Circuit currents and possibility of Ferro resonance conditions.
- (8). It does not require any compensation or use of any capacitive circuit.

III. METHODOLOGY

Here for the operation of simultaneous ac-dc power flow through a dual circuit ac transmission line we want to add the dc supply with ac supply.

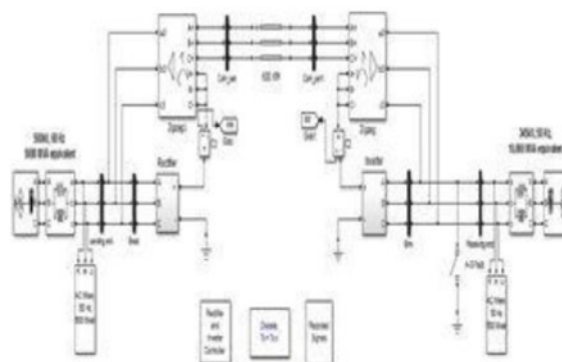


Fig.2.Simulation Model of Simultaneous AC-DC Power Transmission

In these method we are using Line commutated 12-pulse rectifier bridge for HVDC and the dc power is connected to the neutral point of the zigzag transformer of sending end and we get the recovered back to ac again by using the line commutated 12-pulse bridge inverter on the receiving end side hence we get the both part of the power ac as well as dc on the receiving end side that means the same supply on sending end side the inverter bridge is also connected to the neutral of zigzag connected winding of the receiving end transformer to recover the dc current by using the inverter. The dc current on the neutral point is dividing on all the three phases and then each conductor of each transmission line carries one third of the total dc current with ac current superimposed on transmission conductor [8].

The division of current in all phases depends upon the resistance of conductor and then the value of dc current depends upon resistance of conductor. Since the resistance is equal in all the three phases of secondary winding of zigzag transformer and the three conductors of the line, the dc current is divided in all the three phases.

The conductor of the second transmission line provides return path for the dc current to flow. If we are talking about the saturation of transformer then the saturation of transformer due to dc current can be removed by using zigzag connected winding at both ends of transformer.

So the production of fluxes by the dc current ($I_d / 3$) flowing through each winding of the core of a zigzag transformer gives equal magnitude and give opposite in direction and hence cancels.

At any instant of time the total dc flux becomes zero. Thus, dc saturation of core is removed. Here higher value of reactor used to harmonics in dc current. In the absence of harmonics (3^{rd}) or **it's** multiple and zero sequence, under normal operating conditions, the ac current flowing in each transmission line gets restricted between the zigzag connected windings and the

conductors of the transmission line [9].

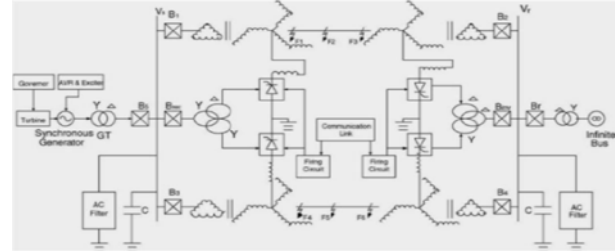


Fig.3. Basic Scheme for Combine AC-DC Transmission [2]

The presence of these components are producing negligible current through the ground due to higher value of X_d . Here if we are assuming constant current control of rectifier and constant extinction angle control of inverter, the equivalent circuit of the model considering single ac line under steady-state operating condition. The ac current return path is denoted by risk lines.

The second transmission line acts as the return path for dc current, and each conductor of the line carries ($I_d / 3$) along with the ac current per phase and the maximum values of rectifier and inverter side dc voltages are V_{dro} and V_{dio} respectively. So these are useful values to analyse the increasing of efficiency on transmission lines.

IV. MATHEMATICAL REPRESENTATION OF SCHEME

Here the strategy to resolve the equations area unit given below that we tend to area unit neglecting the resistive voltage drops and therefore the role of dc currents giving a collection of algebraically expressions for ac voltage and current, and conjointly giving for active and reactive powers in terms of A, B, C, D parameters of every line. These is also given by:

$$E_s = A E_r + B I_r \text{----- (1)}$$

$$I_s = E_r + D I_r \text{----- (2)}$$

$$P_s + j Q_s = -E_s * E_r^* / B^* + D^* E_s^2 / B^* \text{----- (3)}$$

$$P_r + j Q_r = E_s * E_r / B^* - A^* E_r^2 / B^* \text{----- (4)}$$

Hence neglect the resistive voltage drops within the zigzag transformers and therefore the tie lines, the dc current I_d , dc power P_{dr} and P_{di} of every rectifier and electrical converter is also expressed as:

$$I_d = [V_{dro} \cos \phi - V_{dio} \cos \phi] / [R_{cr} + R_{eq} - R_{ci}] \text{---- (5)}$$

$$P_{dr} = V_{dr} * I_d \text{ ----- (6)}$$

$$P_{di} = V_{di} * I_d \text{ ----- (7)}$$

Reactive powers needed by the converters are:

$$Q_{dr} = P_{dr} * \tan \phi_r \text{ ----- (8)}$$

$$Q_{di} = P_{di} * \tan \phi_i \text{ ----- (9)}$$

$$\cos \phi_r = [\cos \phi + \cos(\phi + \mu_r)] / 2 \text{ ----- (10)}$$

$$\cos \phi_i = [\cos \phi + \cos(\phi + \mu_i)] / 2 \text{ ----- (11)}$$

μ_i denotes the commutation angles of electrical converter and μ_r denotes the commutation angle of rectifier and therefore the total active and reactive powers at each the ends are:

$$P_{st} = P_{dr} + P_{di} \text{ and } P_{rt} = P_r + P_{di} \text{ ----- (12)}$$

$$Q_{st} = Q_s + Q_{dr} \text{ and } Q_{rt} = Q_r + Q_{di} \text{ ----- (13)}$$

Here transmission loss for every line is:

$$P_l = (P_s + P_{dr}) - (P_r + P_{di}) \text{ ----- (14)}$$

I_a is the RMS AC current through the conductor at any part of the road, the RMS current per conductor of the road becomes:

$$I = [I_a^2 + (I_d/3)^2]^{1/2};$$

Power loss for every line = $P_L = 3I^2R$.

The total current I in any of the conductors is offset from zero. Currently by setting Infobahn current through the conductor the same as its thermal limit (I_{th}):

$$I_{th} = [I_a^2 + (I_d/3)^2]^{1/2} \text{ ----- (15)}$$

Let V_p be per part RMS voltage of the initial ac line. conjointly allow us to think about V_a be the per part voltage of the ac a part of synchronic ac-dc tie line with constant dc voltage Cupid's itch composed thereon. Because the insulators area unit unchanged, the height voltage within the 2 cases should be equal. If the rated conductor current with relation to its allowable temperature increase is I_{th} and $I_{wa} = X * I_{th}$; X (too but unity) therefore the dc current becomes:

$$I_d = 3 * \sqrt{1 - X^2} * I_{th} \text{ ----- (16)}$$

The worth of voltage in conductor that's section to ground voltage can written because the dc voltage contagion with a composition of sinusoidal varied ac voltages that has RMS worth E_{ph} and also the peak value being:

$$E_{max} = V + 1.414 E_{ph}$$

Electric field that of the composite AC-DC line that consists of the sphere made by the dc line that feeding power and also the ac line that making a superimposed result of electrical fields. This will

be simply see that the sharp changes in field polarity happens which changes its sign doubly in a very single cycle if $(V_d/E_{ph}) < 1.414$. Here we have a tendency to see that the gap for nonconductor discs employed in HVDC lines. every conductor has got to be insulated for the utmost E_{max} however the very fact is line to line voltage has no element of dc voltages and $E_{LL(max)} = 1.414 E_{ph}$. Therefore, we have a tendency to come back to the conclusion that conductor to conductor separated distance is observed solely by ac voltage of the road in place of the entire superimposed one.

Detailed analysis of the filter and instrumentation networking that square measure needed for the planned theme and conjointly short current ac style for protecting theme is out the scope of gift work, however preliminary analysis qualitatively bestowed below says that usually used techniques in HVDC and AC composite system may be adopted exclusively for this purpose. completely different values of ac filters and dc filters square measure employed in HVDC system and also these could also be connected to the delta facet of the electrical device and zigzag neutral severally to separate out higher harmonics **fourteen that's** $(n*p+1)$ st order and the $(n*p)$ th order from dc and ac provides. Moreover, filters conjointly could also be omitted for terribly low values of contagion and I_d . within the neutral terminals of zigzag electrical device winding dc current and dc voltages may be observed by incorporating common ways that square measure employed in HVDC system.

Standard CVTS or electrical phenomenon voltage electrical device as employed in EHV ac lines to live stepped down AC element of line voltage. The composite ac-dc voltage within the line does the operating of covets. Linear couplers that has high air-gap core could also be used for activity ac element of line current because the dc element of line current cannot saturate high air-gap cores.

V. UNDER FAULTY CONDITION WHEN LINE TO GROUND FAULT OCCURRENCE IN SYSTEM

Under fault conditions the causation of sending side voltage and receiving side voltage suddenly

dips of original wave form when fault is cleared. The causation and receiving finish currents rises to a precise spike then recovers step by step. Normally the voltage of across the rectifier and electrical converter dips on the prevalence of fault whereas this level spikes beneath fault conditions. The on top of results square measure obtained by employing a single line to ground fault within the distributed parameters for the one circuit line model.

The results stay nearly similar beneath dc fault. Beneath fault conditions the reactive power demand will increase as is inferred from the graph. Because the reactive power is employed within the circuit thus the reactive power at the receiving finish aspect is lowered to a negative value. The one line circuit model uses ground as return path. Hence use of unipolar dc link for simultaneous ac-dc transmission can pose threats to the equipment located nearby in the ground since using ground as return path can corrode the metallic material if it is in its path.[7] Another thing is that the sluggishness in the system is removed, if we consider an EHV line and on occurrence of a fault the transient response of the system for example the voltage profile or the current or the sudden surge in the reactive power requirement has inherent sluggishness, the system requires a long time to recover. But by using the simultaneous ac-dc model the transient response is increased and hence the transient stability.

The stability is additional increased owing to faster current management mechanism of HVDC blocks that's the rectifier and electrical converter blocks. Within the management mechanism there's a master management and on an individual basis there's electrical converter and rectifier protection that works on VDCOL management procedures. Whenever the voltage dips on prevalence of a fault this is restricted therefore the fault current is additionally diminished and also the most vital factor is that it's terribly little time constant that's it works in time.

VI. SIMULATION RESULTS

We see the simulation result for the simultaneous AC-DC power transmission the overall result for sending end voltages, receiving end voltages that shows the combined supply graph for AC with DC supply.

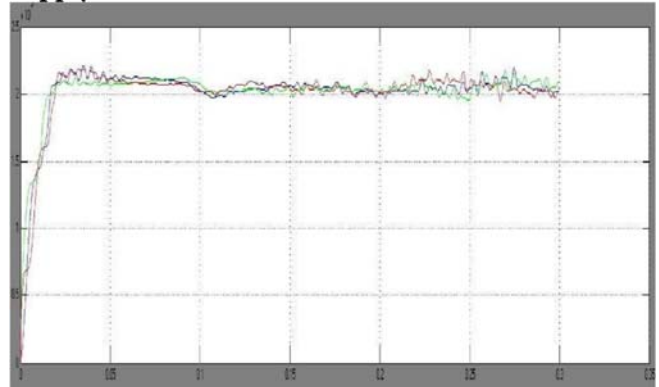


Fig.4.Receiving End Voltage at No fault condition

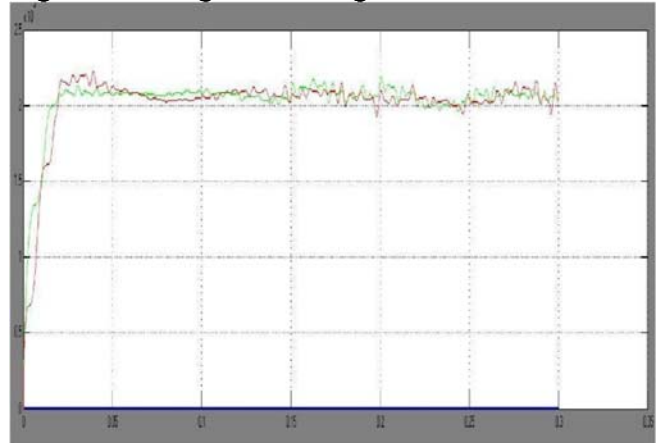


Fig.5. Receiving End Voltage at Fault condition

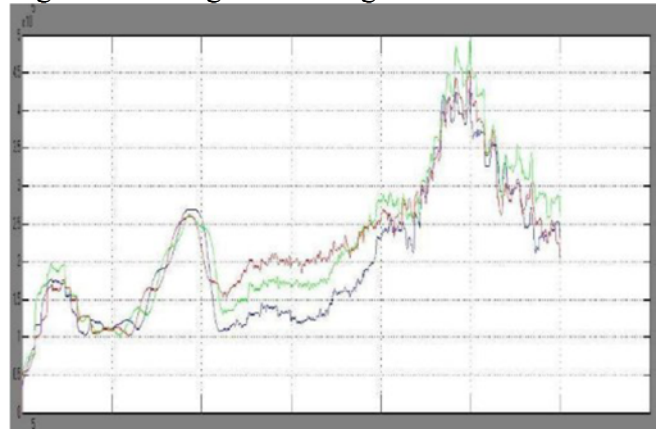


Fig.6.Receiving End Current in case of no Fault

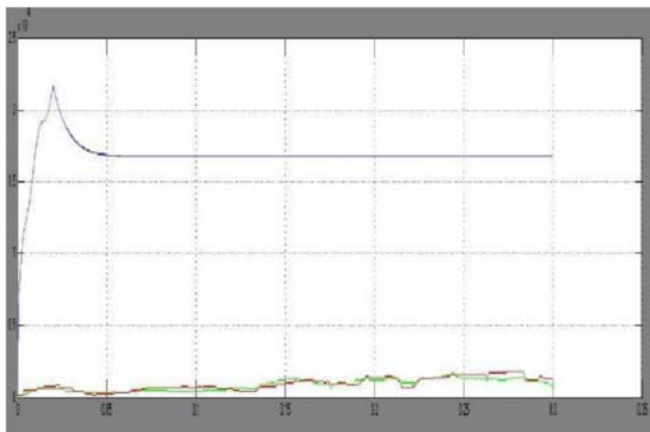


Fig.7. Receiving End Current in case of Fault

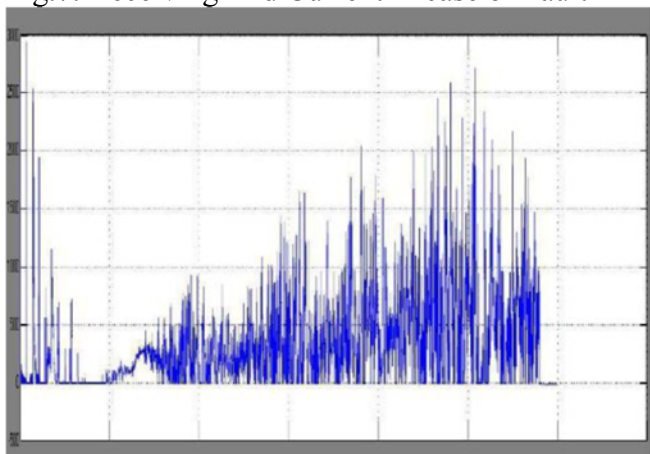


Fig.8. Sending End Line Voltage in case of No Fault

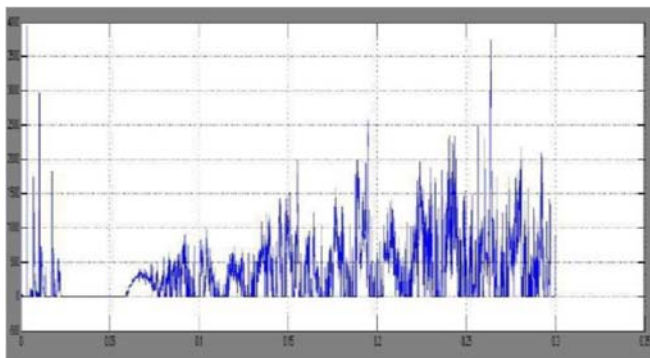


Fig.9. Sending End Line Voltage in case of Fault

REFERENCES

[1] H. Rahman, B.H. Khan, Enhanced power transfer by simultaneous transmission of AC-DC: a new FACTS concept, in: IEE Conference on Power Electronics, Machines and Drives (PEMD 2004), vol. 1, 31 March, 2 April 2004, Edinburgh, 2004, pp. 186–191

[2] H. Rahman, B.H. Khan, Power upgrading of double circuit ac transmission line by simultaneous ac-dc power transmission, in: Proceedings the IEEE, PES, PowerIndia, 2006, doi:10.1109/POWERI.2006.163262.

[3] H. Rahman, B.H. Khan, Power upgrading of transmission line by combining ac-dc transmission, IEEE Trans. Power Syst. 22 (1) (2007) 459–466, doi:10.1109/TPWRS.2006.887895 (Paper ID No. TPWRS-0864-2005)

[4] T. Vijay Muni, T. Vinoditha and D. Kumar Swamy, “Improvement of Power System Stability by Simultaneous AC-DC Power Transmission” International Journal of Scientific & Engineering Research Volume 2, Issue 4, April-2011.

[5] N.G. Hingorani, L.K. Gyugyi, Understanding FACTS—Concept and Technology of Flexible A.C. Transmission Systems, IEEE Press, 2000.

[6] L.K. Gyugyi, Unified power flow control on flexible A.C. transmission system, in: IEEE Proceedings, July 1992, p. 323.

[7] A. Clerici, L. Paris, and P. Danfors, —HVDC conversion of HVAC line to provide substantial power upgrading, IEEE Trans. Power Del., vol. 6, no. 1, pp. 324–333, Jan. 1991.

[8] Prabha Kundur-power system stability and control Tata Mcgraw Hill edition, New Delhi 1993, 11th reprint 2011

[9] N.A. Vovos, G.D. Galanos, Transient stability of ac-dc system, IEEE Trans. Power Apparatus Syst. PAS-98(4)(1979) 1375–1383.

[10] K.P. Basu and B. H. Khan, “Simultaneous ac-dc power transmission,” Inst. Eng. (India) J. -E L, vol. 82, pp. 32–35, Jun. 2001.

[11] Sriram Kondiparthi, M. Pravee, Ramu M., I.E.S Naidu, “Power Transfer Enhancement in Transmission Line by Combining AC – DC Transmission”, International Journal of Engineering Research and Applications (IJERA), ISSN: 2248-9622, Vol. 1, Issue 2, pp.194-201, July 2011. [12] Alok Kumar Mohanty, Amar Kumar Barik, “Power System Stability Improvement

Using FACTS Devices”,International Journal of Modern Engineering Research(IJMER), ISSN: 2249-6645, Vol.1, Issue 2, pp-666-672,November 2011.

[13] Vikash Choudhary, Abdul Kadir, Prathibha Gupta, “ANovel Idea: Simultaneous AC-DC Power Transmission”,International Journal of Advanced Engineering Technology, ISSN: 0976-3945, Vol. 2, Issue 4, December 2011.

[14] Baljit Singh, Gagandeep Sharma, “Power upgrading of Transmission Line by converting EHVAC into EHVDC”,International Journal for Science and Emerging Technologies with Latest Trends, ISSN: 2250-3641, Vol. 4, Issue 1, pp. 20-24, 201